

Light-Cone Sum Rules for $B \rightarrow K\pi$ Form Factors and Applications to Rare Decays

Sébastien Descotes-Genon^a, Alexander Khodjamirian^b and Javier Virto^{c,d}

^a *Laboratoire de Physique Théorique (UMR 8627), CNRS, Univ. Paris-Sud,
Université Paris-Saclay, 91405 Orsay, France*

^b *Theoretische Physik 1, Naturwissenschaftlich-Technische Fakultät,
Universität Siegen, Walter-Flex-Straße 3, D-57068 Siegen, Germany*

^c *Center for Theoretical Physics, Massachusetts Institute of Technology,
77 Mass. Ave., Cambridge, MA 02139, USA*

^d *Physics Department T31, Technische Universität München,
James Frank-Straße 1, D-85748 Garching, Germany*

Abstract

We derive a set of light-cone sum rules relating the hadronic form factors relevant for $B \rightarrow K\pi\ell^+\ell^-$ decays to the B -meson light-cone distribution amplitudes (LCDAs). We obtain the sum rule relations for all $B \rightarrow K\pi$ form factors of (axial)vector and (pseudo)tensor $b \rightarrow s$ currents with a P -wave $K\pi$ system. Our results reduce to the known light-cone sum rules for $B \rightarrow K^*$ form factors in the limit of a single narrow-width resonance. We update the operator-product expansion for the underlying correlation function by including a more complete set of B -meson LCDAs with higher twists, and produce numerical results for all $B \rightarrow K^*$ form factors in the narrow-width limit. We then use the new sum rules to estimate the effect of a non-vanishing K^* width in $B \rightarrow K^*$ transitions, and find that this effect is universal and increases the factorizable part of the rate of $B \rightarrow K^*X$ decays by a factor of 20%. This effect, by itself, goes in the direction of increasing the current tension in the differential $B \rightarrow K^*\mu\mu$ branching fractions. We also discuss $B \rightarrow K\pi$ transitions outside the K^* window, and explain how measurements of $B \rightarrow K\pi\ell\ell$ observables above the K^* region can be used to further constrain the $B \rightarrow K^*$ form factors.

Contents

1	Introduction	3
2	$B \rightarrow K\pi$ Form Factors: Definitions, Kinematics and Partial Waves	6
3	LCSRs with B-meson Distribution Amplitudes	8
3.1	General framework	8
3.2	Sum Rules for P -wave $B \rightarrow K\pi$ Form Factors	9
4	Parametrization of $B \rightarrow K\pi$ Form Factors	12
4.1	Resonance models for $B \rightarrow K\pi$ form factors	13
4.2	Narrow-width limit	16
4.3	z -parametrization and q^2 dependence	18
4.4	Phenomenological formula for $B \rightarrow K\pi$ form factors	19
5	Numerical Analysis	20
5.1	Numerical input and strategy	20
5.2	The vector $K\pi$ form factor from τ data	22
5.3	Effective threshold from a two-point QCD sum rule	25
5.4	Fitting the OPE to the z -expansion	28
5.5	$B \rightarrow K^*$ form factors in the narrow-width limit	30
5.6	Finite-width effects in $B \rightarrow K^*$ form factors	32
5.7	Beyond the K^* window and the $K^*(1410)$ contribution	35
6	Applications to rare decays	38
6.1	A toy example	38
6.2	Angular distribution of the non-resonant $B \rightarrow K\pi \ell\ell$ decay	39
6.3	Finite-width effects in $B \rightarrow K^* \ell\ell$	42
6.4	High $K\pi$ -mass moments of the $B \rightarrow K\pi \ell\ell$ angular distribution	43
7	Conclusions and Perspectives	46
A	Light-Cone Sum Rules for $B \rightarrow V$ Form Factors	50
B	B-meson distribution amplitudes up to twist 4	51
B.1	Definition of B -meson distribution amplitudes	51
B.2	Models and numerics for LCDAs	53
C	Calculation of Correlation Functions	55
C.1	Two-particle contributions	57

C.2	Three-particle contributions	59
C.3	Explicit derivation of Eq. (C.18)	60
D	OPE expressions	61
E	Results for OPE coefficients in different models	62
F	Beyond the narrow-width approximation	65
F.1	Breit-Wigner model with fixed widths	65
F.2	The case of s -dependent widths	67
G	Kinematics for $B \rightarrow K\pi\ell\ell$	67

1 Introduction

Exclusive $b \rightarrow s$ decay modes have been under intense experimental and theoretical scrutiny since the era of the B -factories and the Tevatron, and have had a recent revival with the new data from the LHC. Compared to the corresponding inclusive decay modes they have smaller branching ratios, but they are easier to measure, and with the much larger numbers of B mesons produced at the LHC experiments and the larger number of observables they provide, the exclusive modes lead the quest for indirect searches for New Physics [1, 2].

On the theory side, predictions for the exclusive $b \rightarrow s$ observables – and thus our ability to interpret the experimental data – require the knowledge of hadronic form factors, defined as the matrix elements of flavour-changing quark currents between an initial B meson and a final exclusive mesonic state:

$$F_i^{B \rightarrow M}(q^2) = \langle M(k) | \bar{s} \Gamma_i b | B(q+k) \rangle.$$

A very substantial effort has been devoted in the past to the study of form factors where M is a single pseudoscalar ($P = K, \pi, \eta$) or vector ($V = K^*, \rho, \phi, \omega$) meson. In the attempt to calculate these form factors directly from QCD, two largely complementary approaches stand out. Lattice QCD (see Ref. [3] and references therein) applies to the region of small momenta of the final meson M , where the momentum transfer q^2 is such that $0 \ll q^2 \lesssim (m_B - m_M)^2$, typically $q^2 \gtrsim 20 \text{ GeV}^2$. The method of QCD Light-Cone Sum Rules (LCSRs) [4–6] applied to the form factors is on the other hand limited to the region of large and intermediate recoil of M , or $0 < q^2 \ll (m_B - m_M)^2$, usually $q^2 \lesssim 10 \text{ GeV}^2$. In addition, two versions of the LCSRs exist, depending on whether they relate the form factors to the light-cone distribution amplitudes (LCDAs) of the light meson (see e.g. Refs. [7, 8] and [9, 10] for the LCSRs with P -meson and V -meson LCDAs, respectively), or to the B -meson LCDAs [11, 12] (for more recent applications see e.g. Refs. [13–16]). We will use the latter approach in this article.

Our main focus here is on the $B \rightarrow K^*$ form factors. Current state-of-the-art calculations of $B \rightarrow K^*$ form factors from lattice QCD [17] and LCSRs [18] are compatible with each other and have estimated uncertainties at the level of 5% – 20%. While systematic improvement in the lattice calculations will eventually render the LCSRs not competitive, the latter will remain an important alternative and a complementary method.

As we shall discuss below, the sum rules with B -meson LCDAs help to assess the following limitation of the current calculations of $B \rightarrow V$ form factors. Both approaches, lattice QCD and LCSRs work under the assumption that the vector mesons are stable. This is certainly a reasonable approximation if one assumes that corrections to the narrow-width limit are suppressed by the width-to-mass ratio, which is $\sim 5\%$ for the K^* and below the percent for the ϕ . However, once the uncertainties of the calculated form factors get below the ten-percent level (specially for the $B \rightarrow K^*$ form factors), a proper estimation of the finite-width effects becomes mandatory. In addition, other non-resonant backgrounds such as the interference among P and S waves in the $K\pi$ system are known to be important. While these are disentangled at the level of the experimental analysis, a fully consistent match between experimental measurements and theoretical predictions requires addressing all effects beyond the narrow-width approximation from the theory point of view, too.

Thus, ideally one needs to consider the form factors with two stable mesons in the final state, e.g. $\langle K\pi|\bar{s}\Gamma b|B\rangle$ instead of $\langle K^*|\bar{s}\Gamma b|B\rangle$. As discussed originally in Ref. [19], the LCSRs with B -meson LCDAs provide a natural framework to perform this generalization, making also the relationship with the narrow-width limit completely transparent. This method was used in Ref. [19] to study the $B \rightarrow \pi\pi$ form factors and their relation to $B \rightarrow \rho$ transitions. The purpose of the present article is to derive the corresponding LCSRs for $B \rightarrow K\pi$ form factors, and to study some of the phenomenological implications, with a focus on the semileptonic decay $B \rightarrow K\pi\ell\ell$ both on and off resonance.

The LCSRs derived here are valid for small and intermediate momentum transfer squared $0 < q^2 \lesssim 10 \text{ GeV}^2$ and, simultaneously, small invariant mass of the $K\pi$ system, typically up to the mass of the second radial excitation of K^* , $k^2 \equiv m_{K\pi}^2 \lesssim m(K^*(1680))^2$. In other regions of phase space different calculational tools apply [20]. For example, for large invariant masses of the $K\pi$ system the $B \rightarrow K\pi$ form factors can be factorized into $B \rightarrow K$ form factors and convolutions of perturbative kernels with pion light-cone distribution amplitudes [21]. In the same region of small q^2 and k^2 , one may use LCSRs with $K\pi$ distribution amplitudes analogous to the ones derived in Refs. [22, 23] for the $B \rightarrow \pi\pi$ case. The drawback of these sum rules is our currently limited knowledge of the generalized dimeson LCDAs.

A summary of the main points and novelties of this article is the following:

- We derive the LCSRs with B -meson LCDAs for the P -wave $B \rightarrow M_1 M_2$ form factors, with $M_{1,2}$ pseudoscalar mesons. This generalizes the results of Ref. [19] to the case where the two mesons have different masses. We also include the tensor form factors that were

not considered in that reference. The focus is put on $B \rightarrow K\pi$ form factors but the analytic results are general to other two-body final states. The LCSRs are summarized in Eq. (31).

- We recalculate the Operator Product Expansion (OPE) side of the sum rules including two- and three-particle contributions up to twist four, within a new parametrization of B -meson LCDAs with definite conformal twist, proposed recently in Ref. [24]. This in turn updates the results for $B \rightarrow V$ form factors in Refs. [12, 25]. These results are collected in Appendices A and D. A brief review of the new parametrization and of the OPE calculation is given in Appendix B. This update has also been done recently in Refs. [15, 16].
- We use our sum rules to constrain a resonance model for the form factors, and demonstrate explicitly how the narrow-width limit of the LCSRs leads analytically to the known $B \rightarrow K^*$ sum rules. The models for all form factors are summarized in Eqs. (42) and (69). We use these models with the correct narrow-width limit to estimate the finite-width effects. We find that this correction is universal and encoded in a multiplicative factor $\mathcal{W}_{K^*} \simeq 1.1$. Thus the finite width effects are a 20% correction at the level of the decay rate.
- We use the data from the Belle collaboration on the $\tau \rightarrow K\pi\nu$ spectrum to determine the decay constants f_{K^*} and $f_{K^*(1410)}$, and update the hadronic part of the two-point QCD sum rule to determine the threshold parameter s_0 . We find that the threshold parameter is lower than the one used in the literature for $B \rightarrow K^*$ form factors in the narrow-width limit.
- We apply our results to the rare decay $B \rightarrow K\pi\ell\ell$ on and off resonance. We rederive the angular distribution and we demonstrate that in the narrow-width limit we recover the angular coefficients of the $B \rightarrow K^*\ell\ell$ decay. With this generalization at hand, we show how to use the LHCb data on the angular moments around the $K^*(1410)$ region to improve our control on the $B \rightarrow K^*$ form factors.

The $B \rightarrow K\pi\ell\ell$ decay off resonance has also been discussed in Refs. [26, 27], focusing on the other end of the physical kinematic region, that is, at large dilepton masses. In this case the form factors can be parametrized using Heavy Hadron Chiral Perturbation Theory. In addition, the $B \rightarrow K\pi\ell\ell$ decay at large recoil with a soft pion has been discussed in Ref. [28]. These analyses are complementary to the one presented here.

While we will focus on the application to the semileptonic flavour-changing neutral-current decays, this is not the only case to which the results of this article apply. Analogously to non-leptonic decays of the type $B \rightarrow K^*M$ where factorization in the heavy-quark limit reduces the amplitudes to simpler objects including $B \rightarrow K^*$ form factors [29, 30], the three body

non-leptonic decays such as $B \rightarrow K\pi\pi$ are also reducible to $B \rightarrow K\pi$ form factors in certain regions of phase space [31–33]. Thus the results presented here are also needed to compute predictions for non-leptonic three-body decays. Our results can be generalized to form factors of charged currents, such as those appearing in $B_s \rightarrow K\pi\ell\nu$. In this case naive factorization is exact and the form factors are the only non-perturbative input, allowing for a simultaneous study of V_{ub} and right-handed currents [34].

The plan of this article is the following. We begin in Section 2 reviewing the basic definitions, kinematics and partial-wave expansions of the form factors. In Section 3 we derive the light-cone sum rules for vector, timelike-helicity and tensor form factors. In Section 4 we construct a phenomenological model for the $B \rightarrow K\pi$ form factors and rewrite the LCSRs in the context of this model. Using this model we demonstrate that the narrow-width limit leads to the well-known LCSRs for $B \rightarrow K^*$ form factors. Section 5 contains a comprehensive numerical analysis. Applications of the results derived in this are discussed in Section 6, with a focus on the rare $B \rightarrow K\pi\ell\ell$ decay. Section 7 contains a summary and a brief discussion on future directions. The various appendices include further material that complements the main part of the article: Appendix A contains a collection of the LCSRs with B -meson LCDAs for the $B \rightarrow V$ form factors in the narrow-width limit. In Appendix B we give the definitions for the B -meson LCDAs and a discussion of the models used in the article. In Appendix C we review our calculation of the correlation functions in the OPE, and the results are collected in Appendix D. Appendix E contains some numerical results that complement the numerical analysis of Section 5. Finally, in Appendix F we review the formalism for corrections to the narrow-width limit in Breit-Wigner models. Appendix G contains some details on the kinematics of the $B \rightarrow K\pi\ell\ell$ decay.

2 $B \rightarrow K\pi$ Form Factors: Definitions, Kinematics and Partial Waves

A general Lorentz decomposition of the $\bar{B}^0 \rightarrow K^-\pi^+$ hadronic matrix elements of the $b \rightarrow s$ currents consistent with parity invariance is given by¹:

$$i\langle K^-(k_1)\pi^+(k_2)|\bar{s}\gamma^\mu b|\bar{B}^0(q+k)\rangle = F_\perp k_\perp^\mu, \quad (1)$$

$$-i\langle K^-(k_1)\pi^+(k_2)|\bar{s}\gamma^\mu\gamma_5 b|\bar{B}^0(q+k)\rangle = F_t k_t^\mu + F_0 k_0^\mu + F_\parallel k_\parallel^\mu, \quad (2)$$

$$\langle K^-(k_1)\pi^+(k_2)|\bar{s}\sigma^{\mu\nu} q_\nu b|\bar{B}^0(q+k)\rangle = F_\perp^T k_\perp^\mu, \quad (3)$$

$$\langle K^-(k_1)\pi^+(k_2)|\bar{s}\sigma^{\mu\nu} q_\nu\gamma_5 b|\bar{B}^0(q+k)\rangle = F_0^T k_0^\mu + F_\parallel^T k_\parallel^\mu, \quad (4)$$

¹ Our conventions are $\epsilon_{0123} = -\epsilon^{0123} = +1$ and $\gamma_5 \equiv (i/4!) \epsilon^{\mu\nu\rho\sigma} \gamma_\mu \gamma_\nu \gamma_\rho \gamma_\sigma$.

where $k \equiv k_1 + k_2$ is the total dimeson momentum and q is the momentum transfer. The $B \rightarrow K\pi$ form factors $F_i^{(T)}$ ($i = \perp, t, 0, \parallel$) are Lorentz-invariant scalar functions of three kinematic invariants, $F_i^{(T)} = F_i^{(T)}(k^2, q^2, q \cdot \bar{k})$, with

$$\bar{k}^\mu = \left(1 - \frac{\Delta m^2}{k^2}\right) k_1^\mu - \left(1 + \frac{\Delta m^2}{k^2}\right) k_2^\mu, \quad (5)$$

and $\Delta m^2 \equiv k_1^2 - k_2^2 = m_K^2 - m_\pi^2$, such that $k \cdot \bar{k} = 0$. In the Lorentz decomposition (1–4) defining the form factors $F_i^{(T)}$ we use the following set of orthogonal Lorentz vectors:

$$\begin{aligned} k_\perp^\mu &= \frac{2}{\sqrt{k^2}\sqrt{\lambda}} i\epsilon^{\mu\alpha\beta\gamma} q_\alpha k_\beta \bar{k}_\gamma, & k_t^\mu &= \frac{q^\mu}{\sqrt{q^2}}, \\ k_0^\mu &= \frac{2\sqrt{q^2}}{\sqrt{\lambda}} \left(k^\mu - \frac{k \cdot q}{q^2} q^\mu\right), & k_\parallel^\mu &= \frac{1}{\sqrt{k^2}} \left(\bar{k}^\mu - \frac{4(q \cdot k)(q \cdot \bar{k})}{\lambda} k_\mu + \frac{4k^2(q \cdot \bar{k})}{\lambda} q_\mu\right), \end{aligned} \quad (6)$$

where $\lambda \equiv \lambda(m_B^2, q^2, k^2) = m_B^4 + q^4 + k^4 - 2(m_B^2 q^2 + m_B^2 k^2 + q^2 k^2)$ is the kinematic Källén function. Some useful relations are:

$$\begin{aligned} q \cdot k &= \frac{1}{2}(m_B^2 - q^2 - k^2), & q \cdot \bar{k} &= \frac{\sqrt{\lambda} \lambda_{K\pi} \cos \theta_K}{2k^2}, \\ \lambda &= 4(q \cdot k)^2 - 4q^2 k^2, & k^2 \bar{k}^2 &= -\lambda_{K\pi}, \end{aligned} \quad (7)$$

where $\lambda_{K\pi} \equiv \lambda(k^2, m_K^2, m_\pi^2)$, and θ_K is the angle between the 3-momenta of the pion and the B -meson in the $(K\pi)$ rest frame. Occasionally, for example in the sum rules, the functions λ and $\lambda_{K\pi}$ will depend on a variable s or m_R^2 instead of k^2 . In these cases we will use the notation $\lambda(x) \equiv \lambda(m_B^2, q^2, x)$ and $\lambda_{K\pi}(x) \equiv \lambda(x, m_K^2, m_\pi^2)$.

Other $B \rightarrow K\pi$ form factors with different flavour quantum numbers such as $\langle \bar{K}^0 \pi^0 | \bar{s}\Gamma b | \bar{B}^0 \rangle$ or $\langle K^- \pi^0 | \bar{s}\Gamma b | B^- \rangle$ are related to $\langle K^- \pi^+ | \bar{s}\Gamma b | \bar{B}^0 \rangle$ by isospin. Since the $b \rightarrow s$ current is an isosinglet, in the isospin symmetry limit the $I = 3/2$ component of the final $K\pi$ state does not contribute to the form factor. In the case of the neutral $K\pi$ state, the isospin decomposition is given by

$$|K^- \pi^+\rangle = \sqrt{1/3}|K\pi\rangle_{3/2} + \sqrt{2/3}|K\pi\rangle_{1/2}, \quad |\bar{K}^0 \pi^0\rangle = \sqrt{2/3}|K\pi\rangle_{3/2} - \sqrt{1/3}|K\pi\rangle_{1/2}, \quad (8)$$

which implies the isospin relation

$$\langle \bar{K}^0(k_1) \pi^0(k_2) | \bar{s}\Gamma b | \bar{B}^0(p) \rangle = -\frac{1}{\sqrt{2}} \langle K^-(k_1) \pi^+(k_2) | \bar{s}\Gamma b | \bar{B}^0(p) \rangle. \quad (9)$$

From Eq. (2) also follows that

$$-i \langle K^-(k_1) \pi^+(k_2) | \bar{s} \not{q} \gamma_5 b | \bar{B}^0(p) \rangle = \langle K^-(k_1) \pi^+(k_2) | i(m_b + m_s) \bar{s} \gamma_5 b | \bar{B}^0(p) \rangle = \sqrt{q^2} F_t, \quad (10)$$

so that the timelike-helicity form factor F_t is simply related to the matrix element of the pseudoscalar current, which is not independent.

The form factors $F_i^{(T)}(k^2, q^2, q \cdot \bar{k})$ can be expanded in partial waves, by expressing the invariant $q \cdot \bar{k}$ in terms of the polar angle θ_K by virtue of Eq. (7) :

$$F_{0,t}(k^2, q^2, q \cdot \bar{k}) = \sum_{\ell=0}^{\infty} \sqrt{2\ell+1} F_{0,t}^{(\ell)}(k^2, q^2) P_{\ell}^{(0)}(\cos \theta_K), \quad (11)$$

$$F_{\perp,\parallel}(k^2, q^2, q \cdot \bar{k}) = \sum_{\ell=1}^{\infty} \sqrt{2\ell+1} F_{\perp,\parallel}^{(\ell)}(k^2, q^2) \frac{P_{\ell}^{(1)}(\cos \theta_K)}{\sin \theta_K}, \quad (12)$$

and similarly for the tensor form factors $F_{\perp,0,\parallel}^T$. Our conventions for the Legendre polynomials are such that $P_0^{(0)}(\cos \theta) = 1$, $P_1^{(0)}(\cos \theta) = \cos \theta$, $P_1^{(1)}(\cos \theta) = -\sin \theta$, etc. The sum rules derived below will project out the P -wave components $F_i^{(\ell=1)}$. Starting from different correlation functions one may derive analogous sum rules for other partial waves. These other sum rules will be discussed in a forthcoming publication [35].

We will also need the definition of the $K\pi$ form factors:

$$\langle K^-(k_1)\pi^+(k_2)|\bar{s}\gamma_{\mu}d|0\rangle = f_+(k^2) \bar{k}_{\mu} + \frac{m_K^2 - m_{\pi}^2}{k^2} f_0(k^2) k_{\mu}. \quad (13)$$

In the isospin limit, $f_{+,0}(k^2)$ can be related to the vector and scalar form factors $F_{V,S}$ accessible from τ decays, which have been measured e.g. by Belle [36] (see Section 5.2 for details).

We end this section by noting that the definitions for the form factors $F_i^{(\ell)}$ depend on the choice of the polar angle θ_K . In Ref. [19] (which focused on $B \rightarrow \pi\pi$ form factors) the partial-wave expansion was performed with respect to the angle θ_{π} between the B -meson and the particle with momentum k_2 , and corresponds to θ_K here. Thus the definitions for $F_{0,t}^{(\ell=1)}$ in Ref. [19] agree with the ones used here. One can derive the results in Ref. [19] from the results in this article by taking $m_K \rightarrow m_{\pi}$, and including an isospin factor as discussed below.

3 LCSRs with B -meson Distribution Amplitudes

3.1 General framework

We follow the method used in Refs. [12, 19], which we review here very briefly. We consider correlation functions of the type:

$$\mathcal{P}_{ab}(k, q) = i \int d^4x e^{ik \cdot x} \langle 0 | T \{ j_a(x), j_b(0) \} | \bar{B}^0(q+k) \rangle, \quad (14)$$

where j_a is the current interpolating the final state and j_b is the quark transition current. Within a kinematic region where both invariant variables k^2 and q^2 are far below the hadronic

thresholds in the channels of interpolating and transition currents, respectively, these correlation functions can be calculated by means of a light-cone OPE in terms of B -meson LCDAs:

$$\mathcal{P}_{ab}(k, q) = \mathcal{P}_{ab}^{\text{OPE}}(k, q).$$

A dispersion relation in the variable k^2 relates this object to the spectral density of the correlation function:

$$\mathcal{P}_{ab}^{\text{OPE}}(k^2, q^2) = \frac{1}{\pi} \int_{s_{\text{th}}}^{\infty} ds \frac{\text{Im}\mathcal{P}_{ab}(s, q^2)}{s - k^2}. \quad (15)$$

The imaginary part of the correlation function can be obtained from unitarity by inserting a full set of states between the two currents in the T-product:

$$2 \text{Im}\mathcal{P}_{ab}(k, q) = \sum_h \int d\tau_h \langle 0 | j_a | h(k) \rangle \langle h(k) | j_b | \bar{B}^0(q + k) \rangle. \quad (16)$$

The interpolating current j_a is chosen such that the desired quantum numbers of the states h are projected out. In our case this will be a vector current with the flavour of a $K\pi$ state. The standard assumption when deriving $B \rightarrow K^*$ form factors is that the K^* state is stable and thus contributes as a one-particle state in Eq. (16), and as a simple pole at $k^2 = m_{K^*}^2$ in the correlation function $\mathcal{P}_{ab}(k^2, q^2)$. The hadronic representation with $h = K\pi, \dots$ goes beyond the single-pole approximation. This is the generalization proposed in Ref. [19], and the representation that we will use in this article.

One then performs a Borel transformation in the variable k^2 and uses the quark-hadron duality approximation to equate the hadronic integral above the effective threshold s_0 with its OPE expression. The sum rule becomes:

$$\frac{1}{\pi} \int_{s_{\text{th}}}^{s_0} ds e^{-s/M^2} \text{Im}\mathcal{P}_{ab}(s, q^2) = \mathcal{P}_{ab}^{\text{OPE}}(q^2, \sigma_0, M^2), \quad (17)$$

where $\mathcal{P}_{ab}^{\text{OPE}}(q^2, \sigma_0, M^2)$ is the Borel-transformed OPE expression after subtracting the contribution from the dispersion integral above the effective threshold, with σ_0 depending on s_0 . The choice of the effective threshold s_0 is made such that the main contribution to $\text{Im}\mathcal{P}_{ab}(s, q^2)$ in the integral comes from $h = K\pi$, and other higher states (e.g. $h = K\pi\pi\pi$) are suppressed. The Borel transformation makes the sum rule less sensitive to the duality approximation, and improves the convergence of the OPE. One typically checks that the integral from s_0 to infinity in the OPE side is a small fraction of the total integral, thus minimizing the dependence on the duality ansatz. The specific values of the effective threshold s_0 in the numerical analysis will be taken by fitting the corresponding QCD (SVZ) sum rule for the vacuum-to-vacuum correlation function of two interpolating currents (see Section 5.3).

3.2 Sum Rules for P -wave $B \rightarrow K\pi$ Form Factors

In order to project out the specific P -wave $K^-\pi^+$ state in the sum rules, we need to take as an interpolating current the vector current with strangeness, $j_a = \bar{d}\gamma_\mu s$. The choice for the

transition current j_b depends on the type of the form factor. We consider first the form factors of the V–A current $\bar{s}\gamma^\nu(1 - \gamma_5)b$, and start from the correlation function:

$$\begin{aligned} \mathcal{P}_{\mu\nu}(k, q) &= i \int d^4x e^{ik \cdot x} \langle 0 | T \{ \bar{d}(x) \gamma_\mu s(x), \bar{s}(0) \gamma_\nu (1 - \gamma_5) b(0) \} | \bar{B}^0(q+k) \rangle \\ &= \varepsilon_{\mu\nu\rho\sigma} q^\rho k^\sigma \mathcal{P}_\perp(k^2, q^2) + i g_{\mu\nu} \mathcal{P}_\parallel(k^2, q^2) + i q_\mu k_\nu \mathcal{P}_-(k^2, q^2) \\ &\quad + i k_\mu k_\nu \mathcal{P}_{(kk)}(k^2, q^2) + i q_\mu q_\nu \mathcal{P}_{(qq)}(k^2, q^2) + i k_\mu q_\nu \mathcal{P}_{(kq)}(k^2, q^2), \end{aligned} \quad (18)$$

where the notation used for the invariant amplitudes $\mathcal{P}_{\perp, \parallel, -}$ indicates the form factors that will be extracted from them. The hadronic spectral function of the correlation function is obtained from unitarity, i.e. inserting the complete set of states with the quantum numbers of the interpolating current between the two currents in Eq. (18):

$$2 \text{Im} \mathcal{P}_{\mu\nu}(k, q) = \sum_{\{K\pi\}} \int d\tau_{K\pi} \langle 0 | \bar{d}\gamma_\mu s | K\pi \rangle \langle K\pi | \bar{s}\gamma_\nu (1 - \gamma_5) b | \bar{B}^0(q+k) \rangle + \dots \quad (19)$$

Here the lightest intermediate states $\{K\pi\} = \{K^- \pi^+, \bar{K}^0 \pi^0\}$ are included explicitly and the ellipsis denotes the contributions from other intermediate states with higher thresholds, such as $K\pi\pi, K\pi\pi\pi, K\pi\bar{K}K$, etc.

As mentioned above, the interpolating $\bar{d}\gamma_\mu s$ current in Eq. (19) projects out the $I = 1/2$ components of the $K\pi$ states – given by Eq. (8) – and this allows us to relate the two contributions:

$$\sum_{\{K\pi\}} \langle 0 | \bar{d}\gamma_\mu s | K\pi \rangle \langle K\pi | = \langle 0 | \bar{d}\gamma_\mu s | K\pi \rangle_{1/2} \langle K\pi |_{1/2} = \frac{3}{2} \langle 0 | \bar{d}\gamma_\mu s | K^- \pi^+ \rangle \langle K^- \pi^+ |, \quad (20)$$

such that

$$2 \text{Im} \mathcal{P}_{\mu\nu}(k, q) = \frac{3}{2} \int d\tau_{K\pi} \langle 0 | \bar{d}\gamma_\mu s | K^- \pi^+ \rangle \langle K^- \pi^+ | \bar{s}\gamma_\nu (1 - \gamma_5) b | \bar{B}^0(q+k) \rangle + \dots \quad (21)$$

This factor $3/2$ must be taken into account when comparing the sum rules in this article with the ones derived in Ref. [19] for $\bar{B} \rightarrow \pi^+ \pi^0$ form factors.

We consider now the invariant functions $\mathcal{P}_\perp, \mathcal{P}_\parallel$ and \mathcal{P}_- in Eq. (18). Using the definition for the $K\pi$ form factors in Eq. (13) and the ones for the $B \rightarrow K\pi$ form factors in Eqs.(1) and (2), and following closely the derivation in Ref. [19] (recalled in Section 3.1), we find the sum rules:

$$\int_{s_{\text{th}}}^{s_0} ds e^{-s/M^2} \omega_i(s, q^2) f_+^*(s) F_i^{(\ell=1)}(s, q^2) = \mathcal{P}_i^{\text{OPE}}(q^2, \sigma_0, M^2), \quad (22)$$

for $i = \{\perp, \parallel, -\}$, where we have defined the combination of form factors:

$$F_-^{(\ell=1)}(s, q^2) \equiv (m_B^2 - q^2 - s) F_\parallel^{(\ell=1)}(s, q^2) + \frac{2s^{3/2} \sqrt{q^2}}{\sqrt{\lambda_{K\pi}(s)}} F_0^{(\ell=1)}(s, q^2), \quad (23)$$

and the functions:

$$2\omega_{\parallel}(s, q^2) = \sqrt{\lambda(s)}\omega_{\perp}(s, q^2) = -\lambda(s)\omega_{-}(s, q^2) = -\frac{\sqrt{3}\lambda_{K\pi}^{3/2}(s)}{16\pi^2 s^{5/2}}. \quad (24)$$

These sum rules contain implicitly the factor 3/2 that accounts for the two intermediate $K\pi$ states in the isospin limit. The functions $\mathcal{P}_i^{\text{OPE}}(q^2, \sigma_0, M^2)$ are given explicitly in Appendix D and can be compared to Ref. [12].

In the limit $m_K \rightarrow m_{\pi}$ the expressions in Ref. [19] are recovered². The relative sign difference in the F_0 term with respect to Ref. [19] has been discussed at the end of Section 2. We also note that due to the chosen Lorentz structures, the scalar $K\pi$ form factor $f_0(s)$ does not contribute.

For the timelike-helicity form factor we start from the correlation function with a pseudoscalar transition current $j_b = i(m_b + m_s)\bar{s}\gamma_5 b$:

$$\begin{aligned} \mathcal{P}_{\mu}(k, q) &= i \int d^4x e^{ik \cdot x} \langle 0 | T \{ \bar{d}(x) \gamma_{\mu} s(x), i(m_b + m_s) \bar{s}(0) \gamma_5 b(0) \} | \bar{B}^0(q+k) \rangle \\ &= q_{\mu} \mathcal{P}_t(k^2, q^2) + k_{\mu} \mathcal{P}_{(k)}(k^2, q^2). \end{aligned} \quad (25)$$

Focusing on the invariant amplitude \mathcal{P}_t , and following the same procedure as before we find the sum rule

$$\int_{s_{\text{th}}}^{s_0} ds e^{-s/M^2} \omega_t(s, q^2) f_{+}^*(s) F_t^{(\ell=1)}(s, q^2) = \mathcal{P}_t^{\text{OPE}}(q^2, \sigma_0, M^2), \quad (26)$$

where

$$\omega_t(s, q^2) = -\frac{\sqrt{3q^2} \lambda_{K\pi}(s)}{16\pi^2 s \sqrt{\lambda(s)}}. \quad (27)$$

The function $\mathcal{P}_t^{\text{OPE}}$, also given in Appendix D, was not derived in Ref. [12]. It was, however, considered in Ref. [19] for the $B \rightarrow \pi\pi$ case. As before, the result in Ref. [19] is recovered when $\lambda_{K\pi}(s) \rightarrow s^2[\beta_{\pi}(s)]^2$ and the proper isospin factors are included. Also in this case the scalar $K\pi$ form factor does not contribute.

For the tensor form factors we start from the correlation function with a tensor transition current $j_b = \bar{s}\sigma_{\nu\rho}q^{\rho}(1 + \gamma_5)b$:

$$\begin{aligned} \mathcal{P}_{\mu\nu}^T(k, q) &= i \int d^4x e^{ik \cdot x} \langle 0 | T \{ \bar{d}(x) \gamma_{\mu} s(x), \bar{s}(0) \sigma_{\nu\rho} q^{\rho} (1 + \gamma_5) b(0) \} | \bar{B}^0(q+k) \rangle \\ &= i \varepsilon_{\mu\nu\rho\sigma} q^{\rho} k^{\sigma} \mathcal{P}_{\perp}^T(k^2, q^2) + [q_{\mu} q_{\nu} - q^2 g_{\mu\nu}] \mathcal{P}_{(qq)}^T(k^2, q^2) \\ &\quad + [q^2 k_{\mu} k_{\nu} - (k \cdot q) k_{\mu} q_{\nu}] \mathcal{P}_{(kk)}^T(k^2, q^2) + [q_{\mu} k_{\nu} - (k \cdot q) g_{\mu\nu}] \mathcal{P}_{(qk)}^T(k^2, q^2). \end{aligned} \quad (28)$$

²In this limit, $\lambda_{K\pi}(s) \rightarrow s^2[\beta_{\pi}(s)]^2 = s(s - 4m_{\pi}^2)$, and $f_{+}^*(s) F_i^{(\ell=1)}(s, q^2) \rightarrow -\frac{2\sqrt{2}}{3} F_{\pi}^*(s) F_i^{(\ell=1)}(s, q^2)$, which takes into account the various isospin factors.

Proceeding analogously to the vector form factors, but focusing on the three invariant functions \mathcal{P}_\perp^T , $\mathcal{P}_\parallel^T \equiv q^2 \mathcal{P}_{(qq)}^T + (k \cdot q) \mathcal{P}_{(qk)}^T$ and $\mathcal{P}_-^T \equiv 2\mathcal{P}_{(qq)}^T - \mathcal{P}_{(qk)}^T$ we find

$$\int_{s_{\text{th}}}^{s_0} ds e^{-s/M^2} \omega_i(s, q^2) f_+^*(s) F_i^{T(\ell=1)}(s, q^2) = \mathcal{P}_i^{T, \text{OPE}}(q^2, \sigma_0, M^2), \quad (29)$$

where the functions $\omega_i(s, q^2)$ are given in Eq. (24), and we have defined

$$F_-^{T(\ell=1)}(s, q^2) \equiv \frac{2s^{3/2}(m_B^2 - s)}{\sqrt{q^2} \sqrt{\lambda_{K\pi}(s)}} F_0^{T(\ell=1)}(s, q^2) + (m_B^2 - q^2 + 3s) F_\parallel^{T(\ell=1)}(s, q^2). \quad (30)$$

As before, the scalar $K\pi$ form factor does not contribute. While the tensor $B \rightarrow \pi\pi$ form factors were not considered in Ref. [19], these can be derived by performing the replacement indicated in footnote 2 in the results given here. The functions $\mathcal{P}_{\perp, \parallel, -}^{T, \text{OPE}}$ can be found in Appendix D ($\mathcal{P}_{\parallel, -}^{T, \text{OPE}}$ are new with respect to Ref. [12]).

The sum rules in Eqs. (22), (26) and (29) can be written compactly as:

$$\int_{s_{\text{th}}}^{s_0} ds e^{-s/M^2} \omega_i(s, q^2) f_+^*(s) F_i^{(T)(\ell=1)}(s, q^2) = \mathcal{P}_i^{(T), \text{OPE}}(q^2, \sigma_0, M^2) \quad (31)$$

for³ $i = \{\perp, \parallel, -, t\}$, with the functions $\omega_i(s, q^2)$ given in Eqs. (24) and (27).

The functions $\mathcal{P}_i^{(T), \text{OPE}}(q^2, \sigma_0, M^2)$ are all collected in Appendix D. The set of sum rules given by Eq. (31) together with the OPE functions collected in Appendix D are the main results of this article. They generalize and update the results in Refs. [12, 19] in four directions: 1) going beyond the single-pole (narrow-width) approximation considered in Ref. [12], 2) allowing the two mesons in the final state to have different masses (thus generalizing the $B \rightarrow \pi\pi$ case of Ref. [19]), 3) including the tensor form factors, and 4) using the new parametrization of the B -meson LCDAs from Ref. [24]. In the rest of the article we will discuss how to exploit these sum rules, how to interpret the narrow-width limit and how to go beyond it, and we will present a few applications of these results.

4 Parametrization of $B \rightarrow K\pi$ Form Factors

The sum rules derived in the previous section and summarized in compact form in Eq. (31) relate the OPE functions $\mathcal{P}_i^{(T), \text{OPE}}$ depending on the B -meson LCDAs to the P -wave form factors $F_i^{(T)(\ell=1)}(s, q^2)$ weighted by the timelike $K\pi$ form factor $f_+(s)$ and integrated over the duality interval $s_{\text{th}} < s < s_0$. As such, these sum rules do not provide closed-form expressions for the $B \rightarrow K\pi$ form factors. The dominance of the K^* resonance in $f_+(s)$ and the choice

³For the tensor form factors F_i^T we only have $i = \{\perp, \parallel, -\}$, since there is no timelike-helicity form factor for the tensor current F_i^T . For simplicity, we will not remind this difference between the vector-axial and tensor cases whenever we quote the form factors $F_i^{(T)}$ generically.

of the Borel exponent makes the integral over the hadronic spectral density in the sum rules dominated by the region $s \sim m_{K^*}^2$. As will be shown below, in the narrow-width limit the product $F_i^{(T)(\ell=1)}(s, q^2) f_+(s) \sim \delta(s - m_{K^*}^2)$ removes the integral on the l.h.s. of the sum rules and reduces them to a set of equations for the $B \rightarrow K^*$ form factors, which coincide with the $B \rightarrow K^*$ sum rules in Ref. [12].

The fact that the sum rules (31) only provide weighted integrals of the form factors means that no “local” information on the s dependence can be obtained. One needs to start from an ansatz or model for the form factors, using the sum rules to constrain its parameters [19]. In this section we consider one particular set of models for the form factors, and show how their free parameters can be constrained using the sum rules.

4.1 Resonance models for $B \rightarrow K\pi$ form factors

For all P -wave form factors we will consider a resonance model similar to the one considered in Ref. [19]. The starting point is to assume that the P -wave $K\pi$ state couples to its interpolating current $\bar{s}\Gamma d$ resonantly, through a set of Breit-Wigner-type vector resonances.

Consider first the $K\pi$ vector form factor. The resonance ansatz then implies that

$$\langle K(k_1)\pi(k_2)|\bar{s}\gamma^\mu d|0\rangle = \sum_{R,\eta} BW_R(k^2)\langle K(k_1)\pi(k_2)|R(k,\eta)\rangle\langle R(k,\eta)|\bar{s}\gamma^\mu d|0\rangle \quad (32)$$

where the sum runs over $R = \{K^*(892), K^*(1410)\}$ and the vector-meson polarization states η . The third factor in the right-hand side is related to the R decay constants f_R :

$$\langle R(k,\eta)|\bar{s}\gamma^\mu d|0\rangle = \epsilon_\eta^{*\mu} m_R f_R \quad (33)$$

which are defined to be real and positive by definition of the phases of the states $\langle R(k,\eta)|$. Here $\epsilon_\eta^{*\mu}$ is the polarization vector of R with polarization η . The second factor in (32) is related to the strong coupling of the resonances to the $K^-\pi^+$ state:

$$g_{RK\pi} e^{i\varphi_R} \bar{k} \cdot \epsilon_\eta = \langle K^-\pi^+|R(k,\eta)\rangle = -\sqrt{2} \langle \bar{K}^0\pi^0|R(k,\eta)\rangle, \quad (34)$$

where we include a phase φ_R related to the normalization of the hadronic state. This phase will be merged later on with the relative phases between the separate resonance contributions to the form factors. The first factor in (32) is a Breit-Wigner function with an energy-dependent width, which is assumed in our simple model to describe well the line shapes of the K^* resonances:

$$BW_R(s) = \frac{1}{m_R^2 - s - i\sqrt{s}\Gamma_R(s)}, \quad (35)$$

with

$$\Gamma_R(s) = \Gamma_R^{\text{tot}} \left[\frac{\lambda_{K\pi}(s)}{\lambda_{K\pi}(m_R^2)} \right]^{3/2} \frac{m_R^5}{s^{5/2}} \theta(s - s_{\text{th}}). \quad (36)$$

The strong coupling $g_{RK\pi}$ is determined by the total width of the resonance R by

$$\Gamma_R^{\text{tot}} = \frac{g_{RK\pi}^2 \lambda_{K\pi}^{3/2}(m_R^2)}{48\pi m_R^5} \frac{1}{\mathcal{B}(R \rightarrow K^-\pi^+)}, \quad (37)$$

where $\mathcal{B}(K^*(892) \rightarrow K^-\pi^+) = 2/3$ is the isospin-limit prediction (assuming a 100% branching ratio to $K\pi$ [37]), and $\mathcal{B}(K^*(1410) \rightarrow K^-\pi^+) \simeq 2/3 \times 0.06 = 0.04$ [37]. In our computations, it proves useful to write the strong coupling in terms of the energy-dependent width:

$$g_{RK\pi}^2 = \frac{48\pi s^{5/2} \Gamma_R(s)}{\lambda_{K\pi}^{3/2}(s)} \mathcal{B}(R \rightarrow K^-\pi^+), \quad (38)$$

which follows from Eqs. (36) and (37), and where the s dependence in the r.h.s. cancels out.

Plugging Eqs. (34) and (33) into Eq. (32), and summing over the three polarizations of the vector resonance: $\sum_{\eta} \epsilon_{\eta}^{*\mu} \epsilon_{\eta}^{\nu} = -g^{\mu\nu} + k^{\mu} k^{\nu} / k^2$, we obtain

$$\langle K^-(k_1) \pi^+(k_2) | \bar{s} \gamma^{\mu} d | 0 \rangle = -\bar{k}^{\mu} \sum_R g_{RK\pi} m_R f_R B W_R(k^2) e^{i\phi_R(k^2)} \quad (39)$$

and comparing to Eq. (13) we get

$$f_+(s) = - \sum_R \frac{m_R f_R g_{RK\pi} e^{i\phi_R(s)}}{m_R^2 - s - i\sqrt{s} \Gamma_R(s)}. \quad (40)$$

The relative s -dependent phases between the R -resonance terms emerge due to the admixture with other resonances via $R \rightarrow K\pi \rightarrow R'$ strong transitions. This effect complements the diagonal $R \rightarrow K\pi \rightarrow R$ transitions which, after resummation, generate the energy-dependent width of the resonance R ⁴.

The model in Eq. (40) for the vector $K\pi$ form factor is equivalent to the one used by Belle in Ref. [36], which fits well the data for the $\tau \rightarrow K\pi\nu$ decay for the relevant energy range. This model is thus phenomenologically justified (see Section 5.2).

In the case of the $B \rightarrow K\pi$ form factors and along the same lines we have:

$$\langle K(k_1) \pi(k_2) | \bar{s} \Gamma b | B(q+k) \rangle = \sum_{R,\eta} B W_R(k^2) \langle K(k_1) \pi(k_2) | R(k,\eta) \rangle \langle R(k,\eta) | \bar{s} \Gamma b | B(q+k) \rangle, \quad (41)$$

for a generic Dirac structure Γ . The third factor in the right-hand side is related to $B \rightarrow R$ form factors $\mathcal{F}_{R,i}^{(T)}(q^2)$ (as defined in Table 1 and Appendix A). Plugging Eq. (34) and the definition of the various form factors from Appendix A into Eq. (41), and summing over the three polarizations we obtain the following compact expression for all P -wave $B \rightarrow K\pi$ form factors:

$$F_i^{(T),(\ell=1)}(s, q^2) = \sum_R \frac{Y_{R,i}^{(T)}(s, q^2) g_{RK\pi} \mathcal{F}_{R,i}^{(T)}(q^2) e^{i\phi_R(s)}}{m_R^2 - s - i\sqrt{s} \Gamma_R(s)} \quad (42)$$

⁴A more detailed analysis of the mixing between resonances and meson loops demands a coupled channel approach, which is beyond our scope here.

Traditional Notation [12]	V^{BR}	A_1^{BR}	A_2^{BR}	A_0^{BR}	T_1^{BR}	T_2^{BR}	T_3^{BR}
This work	$\mathcal{F}_{R,\perp}$	$\mathcal{F}_{R,\parallel}$	$\mathcal{F}_{R,-}$	$\mathcal{F}_{R,t}$	$\mathcal{F}_{R,\perp}^T$	$\mathcal{F}_{R,\parallel}^T$	$\mathcal{F}_{R,-}^T$

Table 1: *Notation for the various $B \rightarrow R$ form factors used in this article (for R a vector resonance), as compared to the “traditional” notation (see e.g. Ref. [12]). The notation used in this article has a closer correspondence to the notation for the “parent” $B \rightarrow P_1 P_2$ form factors.*

with $i = \{\perp, \parallel, -, t\}$ and

$$\begin{aligned}
Y_{R,\perp}^T &= (m_B + m_R) Y_{R,\perp} = \frac{m_R \sqrt{\lambda}}{\sqrt{3}}, & Y_{R,\parallel}^T &= (m_B - m_R) Y_{R,\parallel} = \frac{(m_B^2 - m_R^2) m_R}{\sqrt{3}}, \\
Y_{R,-}^T &= (m_B + m_R) Y_{R,-} = \frac{m_R \lambda}{\sqrt{3}}, & Y_{R,t}^T &= -\frac{\sqrt{\lambda} \lambda_{K\pi}}{m_R \sqrt{3} q^2},
\end{aligned} \tag{43}$$

where $Y_{R,i}^{(T)}(s, q^2)$ depend on s and q^2 also implicitly through the functions $\lambda \equiv \lambda(m_B, q^2, s)$ and $\lambda_{K\pi} \equiv \lambda(s, m_K^2, m_\pi^2)$. In Eq. (42) we are assuming that the relative phase $\phi_R(s)$ is a genuine characteristic of the resonance R – such as the width – and thus independent of the process where R is produced (interpolating current or B -meson decay).

It is now useful to rewrite the LCSRs of Eq. (31) in the framework of this resonance model. Putting Eq. (42) into (31), we find:

$$\sum_R \mathcal{F}_{R,i}^{(T)}(q^2) d_{R,i}^{(T)} I_R(s_0, M^2) = \mathcal{P}_i^{(T), \text{OPE}}(q^2, \sigma_0, M^2), \tag{44}$$

with

$$I_R(s_0, M^2) = \frac{m_R}{16 \pi^2} \int_{s_{\text{th}}}^{s_0} ds e^{-s/M^2} \frac{g_{RK\pi} \lambda_{K\pi}^{3/2}(s) |f_+(s)|}{s^{5/2} \sqrt{(m_R^2 - s)^2 + s \Gamma_R^2(s)}}, \tag{45}$$

and

$$\begin{aligned}
d_{R,\perp} &= -d_{R,-} = (m_B + m_R)^{-1}, & d_{R,\parallel} &= \frac{(m_B + m_R)}{2}, & d_{R,t} &= -m_R, \\
d_{R,\perp}^T &= -d_{R,-}^T = 1, & d_{R,\parallel}^T &= \frac{(m_B^2 - m_R^2)}{2}.
\end{aligned} \tag{46}$$

We refrain from replacing $f_+(s)$ by its model expression (40), since one may choose to use another model or a direct experimental determination of $f_+(s)$ inside the integral in Eq. (45). In deriving Eq. (44) we have also adopted the ansatz that the phase cancellation between f_+ and the form factors $\mathcal{F}_{R,i}^{(T)}$ that follows from unitarity happens at the level of the individual resonances [19]. This is enforced by imposing that the phases $\phi_R(s)$ in Eq. (42) are such that

$$\tan [\delta_{K\pi}(s) - \phi_R(s)] = \frac{\sqrt{s} \Gamma_R(s)}{m_R^2 - s}, \tag{47}$$

which follows from the more general unitarity condition $\text{Im}[F_i^{(\ell=1)}(s, q^2)f_+^*(s)] = 0$ [19]. Here we have defined $\delta_{K\pi}(s)$ as the phase of the $K\pi$ form factor:

$$f_+(s) = |f_+(s)|e^{i\delta_{K\pi}(s)}. \quad (48)$$

Note that this assumption also implies that the phases $\phi_R(s)$ are q^2 -independent. One can see that the model for $f_+(s)$ in Eq. (40) satisfies the condition (47) trivially. This is also true for the models used by Belle [36] (see Section 5.2), which are equivalent to that in Eq. (40).

4.2 Narrow-width limit

The narrow-width limit is model-independent as long as the model used leads to a resonance pole at the right position (mass). Inserting the model in Eq. (40) for $f_+(s)$ into the integrand in Eq. (45) and considering for the moment the case of a single resonance, we have

$$I_R(s_0, M^2) = 3 m_R f_R \mathcal{B}(R \rightarrow K^+\pi^-) \int_{s_{\text{th}}}^{s_0} ds e^{-s/M^2} \frac{m_R}{\sqrt{s}} \left[\frac{1}{\pi} \frac{\sqrt{s} \Gamma_R(s)}{(m_R^2 - s)^2 + s \Gamma_R^2(s)} \right]. \quad (49)$$

Here we have used Eq. (38) in order to write $g_{RK\pi}$ in terms of $\Gamma(s)$. The expression inside square brackets becomes a delta function $\delta(s - m_R^2)$ in the narrow-width limit, $\Gamma_R^{\text{tot}} \rightarrow 0$. Thus, the narrow-width limit is simply recovered by the substitution

$$I_R(s_0, M^2) \xrightarrow{\Gamma_R^{\text{tot}} \rightarrow 0} 3 m_R f_R \mathcal{B}(R \rightarrow K^+\pi^-) e^{-m_R^2/M^2}. \quad (50)$$

Implementing this limit in Eq. (44) leads to the LCSRs in the narrow-width limit:

$$3 m_R f_R d_{R,i}^{(T)} \mathcal{F}_{R,i}^{(T)}(q^2) e^{-m_R^2/M^2} \mathcal{B}(R \rightarrow K^+\pi^-) = \mathcal{P}_i^{(T), \text{OPE}}(q^2, \sigma_0, M^2). \quad (51)$$

This agrees with the LCSRs for $B \rightarrow V$ form factors collected in Appendix A. For example, in the case of $\mathcal{F}_{R,\perp} \equiv V^{BR}$, we have $d_\perp = (m_B + m_R)^{-1}$ and

$$e^{-m_R^2/M^2} \frac{3 f_R m_R \mathcal{F}_{R,\perp}(q^2)}{(m_B + m_R)} \mathcal{B}(R \rightarrow K^+\pi^-) = \mathcal{P}_\perp^{\text{OPE}}(q^2, \sigma_0, M^2), \quad (52)$$

which agrees exactly with Eq. (A.3) when $\mathcal{B}(R \rightarrow K^+\pi^-) = 2/3$. In the narrow-width limit all sum rules for $B \rightarrow V$ form factors in Appendix A are reproduced in the same way.

The same exercise goes through if we keep the various resonances and send all widths to zero (all of them scaling with the same factor $\Gamma \rightarrow 0$). In this case the cross-terms in the sum have a vanishing contribution in the narrow-width limit:

$$\frac{g_{RK\pi} g_{R'K\pi}}{[m_R^2 - s + i\sqrt{s} \Gamma_R(s)][m_{R'}^2 - s - i\sqrt{s} \Gamma_{R'}(s)]} + c.c. \xrightarrow{\Gamma_{R,R'}^{\text{tot}} \rightarrow 0} 0, \quad (53)$$

so that the limit produces one simple pole for each resonance, *e.g.*

$$\sum_R 3 m_R f_R d_{R,i}^{(T)} \mathcal{F}_{R,i}^{(T)}(q^2) e^{-m_R^2/M^2} \mathcal{B}(R \rightarrow K^+ \pi^-) = \mathcal{P}_i^{(T),\text{OPE}}(q^2, \sigma_0, M^2) . \quad (54)$$

This is exactly what is expected from the LCSRs with several stable vector resonances.

The $\mathcal{O}(\Gamma)$ corrections to Eq. (54) can also be calculated. The arguments given in Eq. (53) indicate that the overlap of two different resonances from the $K\pi$ form factor and the $B \rightarrow K\pi$ form factor yield a contribution of order $\mathcal{O}(\Gamma^2)$, so we can focus to the contributions coming from the same resonance in both cases, i.e. the $\mathcal{O}(\Gamma)$ correction to the integral defined in Eq. (49). Using the formalism reviewed in Appendix F and denoting $\tilde{I}_R(s_0, M^2)$ as the value of I_R in the limit $\Gamma_R^{\text{tot}} \rightarrow 0$, we have

$$\frac{I_R(s_0, M^2) - \tilde{I}_R(s_0, M^2)}{\tilde{I}_R(s_0, M^2)} = \frac{\Gamma_R^{\text{tot}}}{m_R} \Delta_R(s_0, M^2) + \mathcal{O}(\Gamma^2) , \quad (55)$$

with

$$\Delta_R(s_0, M^2) = \frac{1}{\pi} \left[-\frac{m_R^2(s_0 - s_{\text{th}})}{(s_0 - m_R^2)(m_R^2 - s_{\text{th}})} + m_R^2 [\phi'(m_R^2) + \rho'(m_R^2)] \log \frac{s_0 - m_R^2}{m_R^2 - s_{\text{th}}} + \tilde{F}(s_0, m_R) - \tilde{F}(s_{\text{th}}, m_R) \right] , \quad (56)$$

$$\tilde{F}(s, m_R) = \int_1^{s/m_R^2} \frac{d\tau}{(\tau - 1)^2} \left[\phi(m_R^2 \tau) \rho(m_R^2 \tau) - 1 - (\tau - 1) m_R^2 [\phi'(m_R^2) + \rho'(m_R^2)] \right] , \quad (57)$$

and with

$$\rho(m_R^2 \tau) = \gamma(m_R^2 \tau) \sqrt{\tau} , \quad \gamma(m_R^2 \tau) = \left[\frac{\lambda_{K\pi}(m_R^2 \tau)}{\lambda_{K\pi}(m_R^2)} \right]^{3/2} \frac{1}{\tau^{5/2}} \theta(m_R^2 \tau - s_{\text{th}}) , \quad (58)$$

$$\rho'(m_R^2) = \frac{-2(m_K^2 - m_\pi^2)^2 + m_R^2(m_R^2 + m_\pi^2 + m_K^2)}{m_R^2 \lambda_{K\pi}(m_R^2)} , \quad (59)$$

$$\phi(m_R^2 \tau) = \frac{1}{\sqrt{\tau}} e^{-\frac{m_R^2}{M^2}(\tau-1)} , \quad \phi'(m_R^2) = -\frac{1}{M^2} - \frac{1}{2m_R^2} . \quad (60)$$

Up to order $\mathcal{O}(\Gamma)$, the l.h.s. of Eq. (54) then reads

$$\sum_R 3 m_R f_R d_{R,i}^{(T)} \mathcal{F}_{R,i}^{(T)}(q^2) e^{-m_R^2/M^2} \left[1 + \frac{\Gamma_R^{\text{tot}}}{m_R} \Delta_R(s_0, M^2) + \dots \right] \mathcal{B}(R \rightarrow K^+ \pi^-) . \quad (61)$$

We see, in particular, that the generalization of the LCSRs formulae for the $B \rightarrow K^*$ form factors (in the one-resonance approximation) to include $\mathcal{O}(\Gamma_{K^*})$ corrections is rather simple: one must multiply all form factors in Eqs. (A.3)-(A.9) by $(1 - \Delta_{K^*} \Gamma_{K^*}/m_{K^*})$. The numerical impact of this correction will be discussed in Section 5.6.

4.3 z -parametrization and q^2 dependence

Following Ref. [19], we parametrize the q^2 -dependence of the $B \rightarrow R$ form factors $\mathcal{F}_{R,i}^{(T)}(q^2)$ entering Eq. (42) with the standard z -series expansion [38], as adopted in Ref. [25]. One defines the following function in the complex plane:

$$z(q^2) = \frac{\sqrt{t_+ - q^2} - \sqrt{t_+ - t_0}}{\sqrt{t_+ - q^2} + \sqrt{t_+ - t_0}}, \quad (62)$$

with $t_{\pm} \equiv (m_B \pm m_{K^*})^2$ and $t_0 = t_+(1 - \sqrt{1 - t_-/t_+})$. This function maps the segment $t_+ \leq q^2 < \infty$ onto the unit circle $|z| = 1$, and the rest of the complex q^2 plane onto the interior of the disc $|z| < 1$. The form factors $\mathcal{F}_{K^*,i}^{(T)}(q^2)$ are meromorphic in the first Riemann sheet and have a branch cut for $q^2 \geq t_+$, so they admit a Padé representation as a function of z for $|z| < 1$. In practice one only needs to subtract the subthreshold $B_s^{(*)}$ poles, and the remainder can be Taylor expanded. In the case of $K^*(1410)$ form factors, one would normally choose a different form for $z(q^2)$ where m_{K^*} is replaced by $m_{K^*(1410)}$, since in this case the branch cut starts at the higher threshold $(m_B \pm m_{K^*(1410)})^2$. However, keeping the same form of $z(q^2)$ for both sets of form factors will prove advantageous, and this choice does not invalidate any of the properties of the z -expansion for the $B \rightarrow K^*(1410)$ form factors.

Thus, for a generic form factor $\mathcal{F}_{R,i}^{(T)}(q^2)$, with $i = \{\perp, \parallel, -, t\}$ and $R = \{K^*(892), K^*(1410)\}$, we write⁵:

$$\mathcal{F}_{R,i}^{(T)}(q^2) = \frac{1}{1 - q^2/m_i^2} \left\{ \mathcal{F}_{R,i}^{(T)}(0) + b_{R,i}^{(T)} \zeta(q^2) + \dots \right\}, \quad (63)$$

where

$$\zeta(q^2) = z(q^2) - z(0) + \frac{1}{2}[z(q^2)^2 - z(0)^2], \quad (64)$$

and m_i is the lowest heavy-light pole mass in the q^2 channel with a spin-parity depending on the type of the form factor [37]:

$$\begin{aligned} m_{\perp} &= m_{B_s^*} = 5.415 \text{ GeV} \quad (J^P = 1^-), \\ m_{\parallel,-} &= m_{B_{s1}} = 5.829 \text{ GeV} \quad (J^P = 1^+), \\ m_t &= m_{B_s} = 5.366 \text{ GeV} \quad (J^P = 0^-). \end{aligned} \quad (65)$$

The sum rules in Eq. (44) can then be written in the form of the z -parametrization:

$$\sum_R \frac{\mathcal{F}_{R,i}^{(T)}(0) + b_{R,i}^{(T)} \zeta(q^2)}{1 - q^2/m_i^2} d_{R,i}^{(T)} I_R(s_0, M^2) = \mathcal{P}_i^{(T),\text{OPE}}(q^2, \sigma_0, M^2). \quad (66)$$

⁵We use a slightly different notation compared to Ref. [25] as we do not normalize the slope parameters $b_{R,i}^{(T)}$ to the form factors at $q^2 = 0$. In this way the slope parameters are well behaved when any of the $\mathcal{F}_{R,i}^{(T)}(0)$ assume very small values in the scans, with the errors not blowing up. In addition, the coefficients $b_{R,i}$ coincide then with the parameters $\alpha_1^{(i)}$ in Refs. [15, 18].

It is now useful (and advantageous from the point of view of the z -expansion) to write the r.h.s. of the sum rules in the same z -expanded form:

$$\mathcal{P}_i^{(T),\text{OPE}}(q^2, \sigma_0, M^2) = \frac{\kappa_i^{(T),\text{OPE}} + \eta_i^{(T),\text{OPE}} \zeta(q^2)}{1 - q^2/m_i^2}, \quad (67)$$

where $\kappa_i^{(T),\text{OPE}}(\sigma_0, M^2)$ and $\eta_i^{(T),\text{OPE}}(\sigma_0, M^2)$ both depend on the effective threshold and the Borel parameter. Note that this is merely a convenient reparametrization, and does not imply that the OPE functions depend on the resonance masses m_i^2 in any way. Thus, one arrives to the final form of the sum rules in the resonance model with z -expansion:

$$\begin{aligned} \sum_R \mathcal{F}_{R,i}^{(T)}(0) d_{R,i}^{(T)} I_R(s_0, M^2) &= \kappa_i^{(T),\text{OPE}}(\sigma_0, M^2), \\ \sum_R b_{R,i}^{(T)} d_{R,i}^{(T)} I_R(s_0, M^2) &= \eta_i^{(T),\text{OPE}}(\sigma_0, M^2), \end{aligned} \quad (68)$$

with I_R and $d_{R,i}^{(T)}$ given in Eqs. (45) and (46).

This form of the sum rules can be used to fit the parameters $\mathcal{F}_{R,i}^{(T)}(0)$ and $b_{R,i}^{(T)}$ which determine the P -wave $B \rightarrow K\pi$ form factors through Eqs. (42) and (63). These equations can also be compared to Eq. (36) of Ref. [19], to which they reduce in the limit $m_K \rightarrow m_\pi$, up to the appropriate isospin factors. In this form, it becomes clear that the sum rules can only be used to determine the combination of resonant contributions in Eq. (68). This illustrates explicitly the point made at the beginning of this section, i.e. the sum rules only give information on a weighted integral over the $K\pi$ invariant mass. Thus, in the context of the resonance model, some information on the relative importance of each resonance is necessary.

4.4 Phenomenological formula for $B \rightarrow K\pi$ form factors

We summarize here the main points in this section. We use a two-resonance model for the P -wave $B \rightarrow K\pi$ form factors which matches the model for the form factor $f_+(s)$ used by Belle and which fits well the τ -decay data (see Section 5.2). This model reproduces in the narrow-width limit the $B \rightarrow K^*$ form factors derived in Ref. [12], calculated in Ref. [25], and rederived in Appendix A. Putting together Eqs. (42), (63) and (47), the $B \rightarrow K\pi$ form factors take the following form:

$$F_i^{(T),(\ell=1)}(s, q^2) = \sum_R \frac{g_{RK\pi} Y_{R,i}^{(T)}(s, q^2) [\mathcal{F}_{R,i}^{(T)}(0) + b_{R,i}^{(T)} \zeta(q^2)] e^{i\delta_{K\pi}(s)}}{(1 - q^2/m_i^2) \sqrt{(m_R^2 - s)^2 + s \Gamma_R^2(s)}} \quad (69)$$

for $i = \{\perp, \parallel, -, t\}$, where the sum runs over $R = \{K^*(892), K^*(1410)\}$, the functions $Y_{R,i}^{(T)}(s, q^2)$ are given in Eq. (43), the function $\zeta(q^2)$ is given in Eq. (64), $\delta_{K\pi}(s)$ is the phase of the $K\pi$ form factor $f_+(s)$ (see Eq. (47)), and all the numerical parameters are collected

in Table 2. The form factors $F_0^{T,(\ell=1)}$ can in turn be obtained from $F_{\parallel,-}^{(T),(\ell=1)}$ by means of Eqs. (23) and (30). Note that the phase $\delta_{K\pi}(s)$ could in principle be extracted directly from data.

The sum rules in the form of Eq. (68) together with the OPE expressions in Appendix D (or the numerical values collected in Table 4) and the Belle determination of $|f_+(s)|$ from Ref. [36] (see Section 5.2) can be used to fit for the parameters $\mathcal{F}_{R,i}^{(T)}(0)$, $b_{R,i}^{(T)}$. This is discussed further in Section 5 below.

For phenomenological applications, one can take the form factor models in Eq. (69) together with the parameters in Table 2. Alternatively, one may use the sum rules Eq. (68) to refit the parameters of the models under different assumptions, or for more specific analyses one can write new motivated models for the form factors and use the sum rules in Eq. (31) to fit their free parameters.

5 Numerical Analysis

5.1 Numerical input and strategy

In this section we perform a numerical study of the $B \rightarrow K\pi$ form factors employing the LCSRs that we have derived. For this purpose, we start discussing the numerical input in the sum rules, both in the hadronic and OPE sides. All input parameters are collected in Table 2. Meson and quark masses are taken from the PDG review [37]. For m_b and m_s we use the running $\overline{\text{MS}}$ masses. We neglect uncertainties on the masses since they are negligible with respect to other sources of uncertainty. For the mass and width of the $K^* \equiv K^*(892)$ we take the central values and uncertainties obtained in the fit of Ref. [36]. Since this reference does not provide fit results for the $K^*(1410)$, we take its mass and width (with uncertainties) from the PDG review.

The B -meson decay constant is taken from the 2-point QCD sum rule determination in Ref. [39]. This determination is consistent with lattice QCD computations, e.g. $f_B^{2+1+1} = 190.0(1.3)$ MeV [40–44]. Probably the most important parameter regarding the OPE determination of the correlation functions in this article is λ_B , the inverse moment of the 2-particle B -meson LCDA. Unfortunately this quantity is still known rather poorly. As in Ref. [19], we use the following interval:

$$\lambda_B \equiv \lambda_B(1 \text{ GeV}) = 460 \pm 110 \text{ MeV}, \quad (70)$$

derived from QCD sum rules [45]. This determination satisfies the lower limit $\lambda_B > 238$ MeV (at 90% C.L.) obtained by the Belle collaboration [46], which combines the search for $B \rightarrow \gamma \ell \nu_\ell$ with the theory prediction for its branching ratio [47, 48]. It is worth recalling that this limit is a challenge for the lower values ($\lambda_B \sim 200 - 250$ MeV) preferred by the QCD factorization

Parameter	Value	Ref	Parameter	Value	Ref
m_{π^\pm}	140 MeV	[37]	m_{K^\pm}	494 MeV	[37]
m_\perp	5.415 GeV	[37]	m_{B^0}	5.28 GeV	[37]
$m_{\parallel,-}$	5.829 GeV	[37]	f_B	207_{-9}^{+17} MeV	[39]
m_t	5.366 GeV	[37]	$\bar{m}_b(m_b)$	4.2 GeV	[37]
$m_{K^*(892)}$	895.4(2) MeV	[36]	$\Gamma_{K^*(892)}$	46.1(6) MeV	[36]
$m_{K^*(1410)}$	1421(9) MeV	[37]	$\Gamma_{K^*(1410)}$	236(18) MeV	[37]
λ_B	460 ± 110 MeV	[45]	R	$0.4_{-0.3}^{+0.5}$	[24]
	$\{1.00, 1.26(18)\}$ GeV ²				
$\{M^2, s_0\}$	$\{1.25, 1.31(12)\}$ GeV ²	Sec.5.3	$m_s(1 \text{ GeV})$	123(14) MeV	[37]
	$\{1.50, 1.35(09)\}$ GeV ²				

Table 2: *Compendium of numerical inputs used in the analysis.*

analysis of $B \rightarrow \pi\pi$ decays (see e.g. Refs. [49, 50]). The estimate $\lambda_B = 358_{-30}^{+38}$ MeV [51] has been obtained by comparing the LCSRs with pion [52] and B -meson LCDAs for the $B \rightarrow \pi$ form factor and using a similar model for the B -meson DA as the Model I used here (see Appendix B.2). Since we are not including next-to-leading-order (NLO) corrections in the correlation functions, we do not take into account the renormalization of λ_B . Concerning the 3-particle B -meson LCDAs, the models that we will consider depend on one single parameter R corresponding to a ratio of LCDA moments. As discussed in more detail at the end of Appendix B.2, the value adopted for this parameter is $R = 0.4_{-0.3}^{+0.5}$.

The $K\pi$ form factor $f_+(s)$ is a key input to the sum rule, which can be extracted from data. This is done in Section 5.2 employing two models used by Belle which fit well the $\tau \rightarrow K\pi\bar{\nu}_\tau$ data: the first one (Model 1) contains only a $K^*(892)$ vector resonance plus two scalar ones, and the second one (Model 2) contains the $K^*(892)$ and the $K^*(1410)$, plus one scalar resonance. We will consider the impact of both models in the LCSRs for the $B \rightarrow K\pi$ form factors.

Another key input to the sum rules is the effective threshold s_0 . In order to fix this input we follow Ref. [19] and use the SVZ QCD sum rules to relate an integral of the $K\pi$ form factor to the vacuum correlation function of two K^* interpolating currents. In this way, the duality interval that satisfies the SVZ sum rule correlates the effective threshold s_0 to the Borel parameter M^2 . This analysis is carried out in Section 5.3.

For the Borel parameter M^2 we take values inside the interval $M^2 = 1.0 - 1.5$ GeV², in

all the sum rules, following Ref. [19]. This is slightly narrower than the one used in Ref. [11]. Within this interval, the convergence of the OPE is manifested by relatively small three-particle DA contributions:

$$\frac{\mathcal{P}_{i,[3\text{-particle}] }^{(T),\text{OPE}}}{\mathcal{P}_{i,[2\text{-particle}] }^{(T),\text{OPE}}} \lesssim 15\% \quad \text{for } q^2 \in [0, 5] \text{ GeV}^2, \quad (71)$$

for all form factors and all three models for the LCDAs considered. Simultaneously, the duality-subtracted part of the integral over the spectral density of the correlation function (l.h.s. of Eq. (17) with the integral above $s = s_0$) does not exceed $\sim 40\%$ of the total integral, making the result weakly sensitive to the quark-hadron duality approximation.

Once the numerical input has been fixed, we produce numerical results for the OPE side of the sum rules, in the context of the z -expansion. This is done in Section 5.4. With these results at hand, we put the LCSRs to work and study the $B \rightarrow K\pi$ form factors in three steps: the $B \rightarrow K^*$ form factors in the narrow-width limit (Section 5.5), the finite-width corrections to $B \rightarrow K^*$ form factors (Section 5.6), and discuss the $B \rightarrow K\pi$ form factors beyond the K^* window (Section 5.7).

5.2 The vector $K\pi$ form factor from τ data

The $K\pi$ form factors in the time-like region can be extracted from the measurement of the $\tau \rightarrow K_S \pi^- \nu_\tau$ spectrum by Belle [36]. This spectrum provides the scalar and vector form factors $f_{+,0}^{K_S \pi^-}(s)$ – actually, one particular combination – which are related to the ones in the $K^- \pi^+$ channel by isospin symmetry:

$$f_{+,0}(s) \equiv f_{+,0}^{K^- \pi^+}(s) = -f_{+,0}^{\bar{K}^0 \pi^-}(s) = -\sqrt{2} f_{+,0}^{K_S \pi^-}(s). \quad (72)$$

CP invariance is assumed and the K_S , which is the mass eigenstate of the neutral kaon system with shorter lifetime, is identified through its decay into two pions.

Belle measures the binned spectrum of events in $\tau \rightarrow K_S \pi^- \nu_\tau$ as a function of the invariant mass of the $K_S \pi^-$ pair $\sqrt{s} = \sqrt{(p_K + p_\pi)^2}$, which is related to the differential decay rate by:

$$\frac{N_{\text{events}}^{\text{bin}}}{N_{\text{events}}^{\text{total}}} = \frac{1}{\Gamma} \int_{\text{bin}} d\sqrt{s} \frac{d\Gamma}{d\sqrt{s}} \simeq \frac{\Delta_{\text{bin}}}{\Gamma} \frac{d\Gamma}{d\sqrt{s}} \Big|_{\text{bin}} = \frac{\Delta_{\text{bin}}}{\Gamma} 2\sqrt{s} \frac{d\Gamma}{ds} \Big|_{\text{bin}}, \quad (73)$$

where $\Gamma \equiv \Gamma(\tau \rightarrow K_S \pi^- \nu_\tau)$, Δ_{bin} is the size of the \sqrt{s} -bin, and in the second step we have assumed that the bin is small enough such that the differential rate does not change sensibly within it. In the Belle analysis the bin size is fixed to $\Delta_{\text{bin}} = 11.5$ MeV, and the total number of events is $N_{\text{events}}^{\text{total}} = 53\,113.2$.

On the other hand, the differential decay rate is given by (see Refs. [53, 54]):

$$\frac{d\Gamma}{ds} = \frac{N_\tau}{s^3} \left(1 - \frac{s}{m_\tau^2}\right)^2 \left(1 + 2\frac{s}{m_\tau^2}\right) \lambda_{K\pi}^{3/2} |\tilde{f}_+(s)|^2 \left\{ 1 + \frac{3(\Delta m^2)^2}{(1 + 2s/m_\tau^2) \lambda_{K\pi}} |\tilde{f}_0(s)|^2 \right\}, \quad (74)$$

with the normalization

$$N_\tau = \frac{G_F^2 |V_{us}|^2 |f_+(0)|^2 m_\tau^3}{1536\pi^3} S_{EW}^{\text{had}}. \quad (75)$$

Here $S_{EW}^{\text{had}} = 1.0201 \pm 0.0003$ accounts for the short-distance electroweak corrections [55], and we have included in the normalization the vector form factor at zero momentum transfer to define the “normalized” form factors $\tilde{f}_{+,0}(s)$, such that $\tilde{f}_+(0) = 1$ and $\tilde{f}_0(s) = f_0(s)/f_+(s)$. While the normalization $f_+(0)$ is well known from the lattice [40], we will not assume that the model used here for $f_+(s)$ is very precise at $s = 0$. We will rather fix this normalization from the total $\tau \rightarrow K_S \pi^- \nu_\tau$ decay rate as measured by Belle [36]. The CKM element $|V_{us}|$ is extracted from a global fit to $K_{\ell 3}$ observables [37, 40]: $|V_{us}| = 0.2243 \pm 0.0005$ ⁶. We will neglect all uncertainties in N_τ .

Belle [36] uses the following model for the vector and scalar form factors in their fits (in our notation)⁷:

$$\tilde{f}_+(s) = \sum_R \frac{\xi_R m_R^2}{m_R^2 - s - i\sqrt{s} \Gamma_R(s)}, \quad f_0(s) = f_+(0) \cdot \sum_{R_0} \frac{\xi_{R_0} s}{m_{R_0}^2 - s - i\sqrt{s} \Gamma_{R_0}(s)}, \quad (76)$$

with $R = \{K^*(892), K^*(1410), K^*(1680)\}$ and $R_0 = \{K^*(800), K^*(1430)\}$. For the case of S -wave resonances, the energy-dependent width is modified with respect to Eq. (36):

$$\Gamma_{R_0}(s) = \Gamma_{R_0}^{\text{tot}} \left[\frac{\lambda_{K\pi}(s)}{\lambda_{K\pi}(m_{R_0}^2)} \right]^{1/2} \frac{m_{R_0}^3}{s^{3/2}} \theta(s - s_{\text{th}}). \quad (77)$$

In the notation of Belle, $\xi_{K^*(892)} = 1/(1 + \beta + \chi)$, $\xi_{K^*(1410)} = \beta/(1 + \beta + \chi)$, $\xi_{K^*(1680)} = \chi/(1 + \beta + \chi)$, $\xi_{K_0^*(800)} = \varkappa$ and $\xi_{K_0^*(1430)} = \gamma$.

Belle finds two models that fit well the data, the first one (hereon Model 1) with the $K^*(892)$ plus the two scalar resonances $K_0^*(800)$ and $K_0^*(1430)$, and the second one (hereon Model 2) where the scalar $K_0^*(1430)$ is replaced by the vector $K^*(1410)$. In both fits the mass and width of the $K^*(892)$ are left as free parameters, but in both cases the fits give results which are essentially equal to the numbers given in Table 2. For the other parameters Belle finds: $\varkappa = 1.27$ and $\gamma = 0.954 e^{i0.62}$ (Model 1), and $\varkappa = 1.57$ and $\beta = 0.075 e^{i1.44}$ (Model 2), where we have ignored the uncertainties. In our notation, this implies:

$$\mathbf{Model 1} : \quad \xi_{K^*(892)} = 1, \quad \xi_{K_0^*(800)} = 1.27, \quad \xi_{K_0^*(1430)} = 0.954 e^{i0.62}, \quad (78)$$

$$\mathbf{Model 2} : \quad \xi_{K^*(892)} = 0.988 e^{-i0.07}, \quad \xi_{K^*(1410)} = 0.074 e^{i1.37}, \quad \xi_{K_0^*(800)} = 1.57, \quad (79)$$

⁶We are assuming that there is no physics beyond the Standard Model (BSM) affecting the τ decay, directly or indirectly. This includes any BSM contributions affecting the extraction of G_F or V_{us} , see e.g. Ref. [56].

⁷This model does not fulfill the theoretical constraint $f_+(0) = f_0(0)$, which is however not a concern for us: we are mostly focused on the behaviour of the f_+ form factor at $s > (m_K + m_\pi)^2$, whose fit to the data is unlikely to be altered significantly if we changed the behaviour of the f_0 form factor at zero.

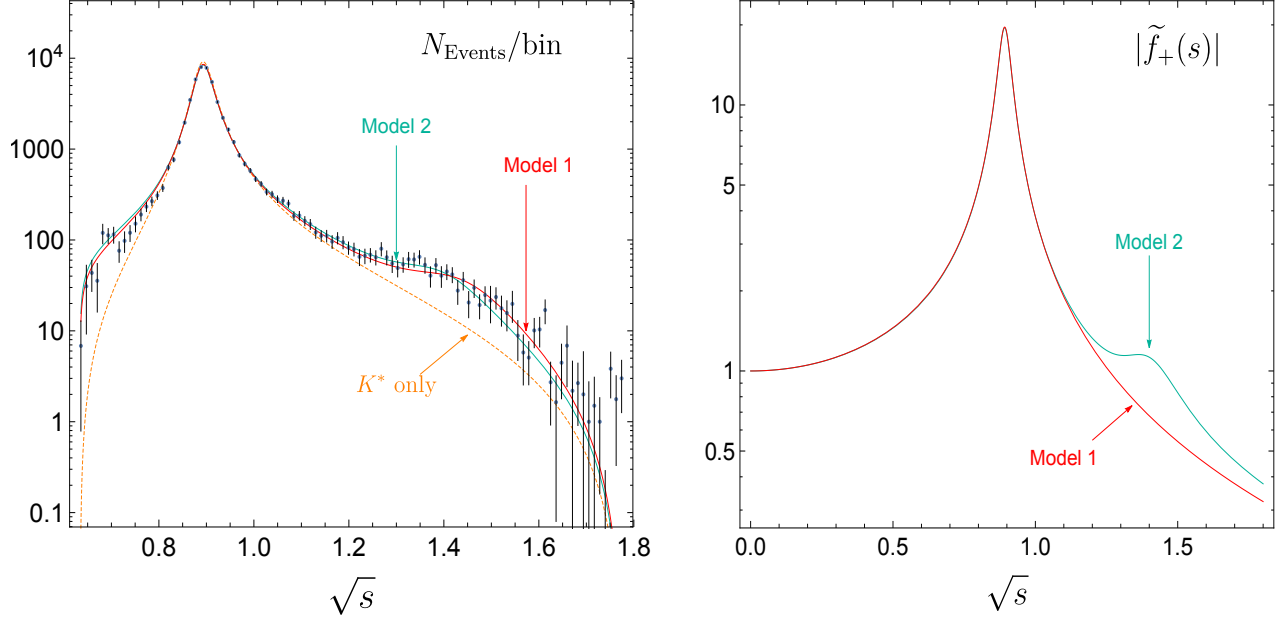


Figure 1: *Left:* $\tau \rightarrow K_S \pi^- \nu_\tau$ spectrum from Belle [36], and the corresponding curves from Model 1 and Model 2 (two solid lines) as well as the isolated contribution from the $K^*(892)$ (dashed). *Right:* Normalized form factor $\tilde{f}_+(s)$ in the two models that fit well the spectrum.

with the omitted parameters set to zero.

The spectrum of events given in Eq. (73) does not depend on the normalization of the rate N_τ . In Figure 1 (left panel) we show the Belle data compared to the curves obtained from Eqs. (73) and (74) in the two models for the form factors, and including a model with only a $K^*(892)$ resonance. The normalized vector form factor $\tilde{f}_+(s)$ is also shown in Figure 1 (right panel), within the two models considered.

In order to fix the normalization of the vector form factor $f_+(s)$ we consider the total branching fraction of $\tau \rightarrow K_S \pi^- \nu_\tau$. Belle gives $\mathcal{B}(\tau \rightarrow K_S \pi^- \nu_\tau)_{\text{Belle}} = 0.404 \pm 0.013\%$ [36]. Integrating Eq. (74), and using $\tau_\tau = 4.41 \cdot 10^{11} \text{ GeV}^{-1}$ for the τ lifetime [37], we find:

$$\mathcal{B}(\tau \rightarrow K_S \pi^- \nu_\tau) = \begin{cases} 0.409 |f_+(0)|^2 \% & \text{(Model 1)} \\ 0.411 |f_+(0)|^2 \% & \text{(Model 2)} \end{cases} . \quad (80)$$

Thus, reproducing the central value of Belle requires $|f_+(0)| = 0.99$ (in both models), very close to unity, and close to the central value of the lattice QCD average [40]: $f_+^{\text{LQCD}}(0) = 0.97$. Keeping in mind the other sources of uncertainties affecting our computation, we find it simpler to approximate this number to unity and fix its phase such that $\phi_{K^*(892)} = 0$ in Eq. (40): $f_+(0) = -1$ in Model 1 and $f_+(0) = -e^{i0.07}$ in Model 2.

All in all, the two models for the vector form factor $f_+(s)$ that we will use are given

by Eq. (40) with the following values for the resonance parameters:

$$f_R = \frac{m_R}{g_{RK\pi}} |\xi_R|, \quad \phi_R = \arg \xi_R - \arg \xi_{K^*(892)}, \quad (81)$$

which implies for each of the two models:

$$\textbf{Model 1 :} \quad f_{K^*(892)} = 206 \text{ MeV}, \quad \phi_{K^*(892)} = 0, \quad (82)$$

$$\textbf{Model 2 :} \quad f_{K^*(892)} = 203 \text{ MeV}, \quad \phi_{K^*(892)} = 0, \quad (83)$$

$$f_{K^*(1410)} = 85 \text{ MeV}, \quad \phi_{K^*(1410)} = 1.44, \quad (84)$$

with $f_{K^*(1410)} = f_{K^*(1680)} = 0$ in Model 1 and $f_{K^*(1680)} = 0$ in Model 2. In order to derive these numbers we have used the values for the strong couplings:

$$g_{K^*(892)K\pi} = 4.36, \quad g_{K^*(1410)K\pi} = 1.24, \quad (85)$$

which can be derived from Eq. (37) and the values in Table 2. We note that these values for $f_{K^*(892)}$ are somewhat lower than the narrow-width estimate $f_{K^*(892)} = 217(5)$ MeV [57] obtained from the two-point QCD sum rule for vector currents with strangeness. The reason for this difference will be discussed in the next subsection.

Having rewritten the models of Belle in the notation of Eq. (40) will be useful in order to check the narrow-width limit. Finally, we point out that in order to be able to distinguish the effects of the vector and scalar resonances $K^*(1410)$ and $K_0^*(1430)$, a dedicated angular analysis of Belle and Belle-II data is necessary.

5.3 Effective threshold from a two-point QCD sum rule

In Ref. [12] the duality interval for the interpolating light-quark current was assumed the same as in the QCD (SVZ) sum rule [58, 59] for the two-point correlation function of these currents. In particular, in the LCSRs for $B \rightarrow K^*$ form factors, the value $s_0 = 1.7 \text{ GeV}^2$ [57] stems from the two-point QCD sum rule for vector currents with strangeness. In this sum rule the hadronic part in the duality interval was approximated by a single narrow K^* . We find it more consistent to adopt for this hadronic part the $K\pi$ spectral density expressed via the measured quantity $|f_+(s)|^2$, which includes the K^* with a finite width. This approach was already used in Ref. [19] to set the effective threshold for the dipion channel in the LCSR for the $B \rightarrow \pi\pi$ form factors.

The QCD sum rule that we need [58, 59] is based on the two-point correlation function:

$$\Pi_{\mu\nu}(k) = i \int d^4x e^{ikx} \langle 0 | T \{ \bar{d}(x) \gamma_\mu s(x), \bar{s}(0) \gamma_\nu d(0) | 0 \rangle = (k_\mu k_\nu - k^2 g_{\mu\nu}) \Pi(k^2) + k_\mu k_\nu \tilde{\Pi}(k^2). \quad (86)$$

We focus specifically on the invariant function $\Pi(k^2)$ multiplying the transverse structure, which receives no contributions from the scalar form factor f_0 . Inserting the $K\pi$ intermediate states and performing the phase-space integrals, one finds

$$\frac{1}{\pi}\text{Im}\Pi(s) = \frac{\lambda_{K\pi}^{3/2}(s)}{32\pi^2 s^3} |f_+(s)|^2. \quad (87)$$

Using in this expression the model (40) for $f_+(s)$ with one K^* resonance and taking the narrow-width limit, $\Gamma_{K^*} \rightarrow 0$, one recovers the known result $\frac{1}{\pi}\text{Im}\Pi(s) = f_{K^*}^2 \delta(s - m_{K^*}^2)$.

Writing the dispersion relation for $\Pi(k^2)$, and performing the Borel transformation, we have

$$\Pi(M^2, s_0) \equiv \frac{1}{\pi} \int_{s_{\text{th}}}^{s_0} ds e^{-s/M^2} \text{Im}\Pi(s) = \int_{s_{\text{th}}}^{s_0} ds e^{-s/M^2} \frac{\lambda_{K\pi}^{3/2}(s)}{32\pi^2 s^3} |f_+(s)|^2. \quad (88)$$

The above integral is equated to the Borel-transformed correlation function calculated in QCD and containing the perturbative loop contribution (to NLO) and the vacuum condensate terms (up to $d = 6$):

$$\begin{aligned} \Pi^{\text{OPE}}(M^2, s_0) &= \frac{1}{8\pi^2} \int_{m_s^2}^{s_0} ds e^{-s/M^2} \frac{(s - m_s^2)^2 (2s + m_s^2)}{s^3} \\ &\quad + \frac{\alpha_s(M)}{\pi} \frac{M^2}{4\pi^2} \left(1 - e^{-s_0/M^2}\right) + \frac{v_4}{M^2} + \frac{v_6}{2M^4}. \end{aligned} \quad (89)$$

Power-suppressed terms in the OPE with the coefficients

$$v_4 = m_d \langle 0 | \bar{s}s | 0 \rangle + m_s \langle 0 | \bar{d}d | 0 \rangle + \frac{1}{12} \langle 0 | \frac{\alpha_s}{\pi} G_{\mu\nu}^a G^{a\mu\nu} | 0 \rangle, \quad v_6 = -\frac{224\pi}{81} \alpha_s \langle 0 | \bar{q}q | 0 \rangle^2, \quad (90)$$

include the contributions from the quark ($d = 3$), gluon ($d = 4$) and four-quark ($d = 6$) condensates, respectively. In the latter contribution, the approximation $\langle 0 | \bar{s}s | 0 \rangle (1 \text{ GeV}) = \langle 0 | \bar{d}d | 0 \rangle$ is adopted and, following Ref. [59], we rely on the vacuum saturation approximation to re-express the four-quark condensates in terms of the quark condensate.

In the numerical analysis of the above expressions, owing to the fact that $m_d \ll m_s$, we neglect the first term in the quark-condensate contribution. The input parameters are: $m_s(1 \text{ GeV}) = 123 \pm 14 \text{ MeV}$ [37], $\langle 0 | \bar{d}d | 0 \rangle (1 \text{ GeV}) = \langle 0 | \bar{q}q | 0 \rangle (1 \text{ GeV}) = (-250 \pm 10 \text{ MeV})^3$ [37, 60] and $\langle 0 | \frac{\alpha_s}{\pi} G_{\mu\nu}^a G^{a\mu\nu} | 0 \rangle = 0.012_{-0.012}^{+0.006} \text{ GeV}^4$ [61]. Note that in the four-quark condensate contribution a low-scale $\alpha_s(1 \text{ GeV}) = 0.46$ [37] is taken.

The QCD sum rule obtained equating $\Pi(M^2, s_0)$ and $\Pi^{\text{OPE}}(M^2, s_0)$ differs from the usual QCD sum rule [59] in which the contribution of a narrow ground state is equated to the OPE result integrated over a duality interval, so that s_0 appears only on the OPE side. The threshold parameter is then usually fixed beforehand and the variation with M^2 is interpreted as an uncertainty of the sum rule prediction for the ground state parameters. Here we do not intend to calculate e.g., the ground state K^* decay constant from the sum rule. On the

Borel parameter M^2	Effective threshold s_0	
1.00 GeV ²	1.28 ± 0.18 GeV ² (Model 1)	1.26 ± 0.18 GeV ² (Average)
	1.25 ± 0.18 GeV ² (Model 2)	
1.25 GeV ²	1.33 ± 0.12 GeV ² (Model 1)	1.31 ± 0.12 GeV ² (Average)
	1.31 ± 0.12 GeV ² (Model 2)	
1.50 GeV ²	1.36 ± 0.09 GeV ² (Model 1)	1.35 ± 0.09 GeV ² (Average)
	1.34 ± 0.09 GeV ² (Model 2)	

Table 3: Values for the effective threshold s_0 extracted from the SVZ sum rules.

contrary, we use data on the $K\pi$ form factor to fix the hadronic part and s_0 enters both sides of the sum rule equation. We determine the range of values of s_0 that best fit this equation and then use it in the LCSRs for the $B \rightarrow K\pi$ form factors. The extracted intervals of the effective threshold thus depend on the choice of Borel parameter. Hence, when taking a certain value of Borel parameter in the LCSR, we will use the corresponding fitted threshold.

Fitting the integral $\Pi(M^2, s_0)$ to its QCD sum rule counterpart $\Pi^{\text{OPE}}(M^2, s_0)$ we find the values for the effective threshold quoted in Table 3. These values depend on the Borel parameter M^2 and on the model used for the form factor $f_+(s)$. We set the Borel parameter to the three different values $M^2 = \{1.00, 1.25, 1.50\}$ GeV², and for each of these values we calculate the resulting s_0 from a χ^2 minimization of the difference $(\Pi - \Pi^{\text{OPE}})$, including the uncertainties in the OPE coefficients. This is done separately for each of the two models discussed in Section 5.2 for $f_+(s)$. These results are shown in the second column of Table 3. Finally, we combine both numbers for each value of the Borel parameter to produce an average that accounts for the “model dependence”, as shown in the third column. The estimated model dependence turns out to be small compared to the parametric uncertainty from the OPE coefficients.

Our estimates for the effective threshold are relatively low as compared to the duality interval $s_0^{K^*} = 1.7$ GeV² adopted in the original SVZ sum rule for the K^* meson [59], and used again in Ref. [57]. In the latter, the sum rule was employed to obtain the value of the decay constant f_{K^*} (quoted at the end of Section 5.2) and the choice of the threshold was done in a seemingly qualitative way⁸. Following our procedure, we notice that for $M^2 \sim 1$ GeV² the integral on r.h.s. of Eq. (88) practically does not depend on s_0 starting from $s_0 \sim 1.0$ GeV², which means that the contribution of the $K\pi$ state to the hadronic spectral density weighted with the Borel exponent dominates for $s \lesssim 1$ GeV². The OPE in Eq. (89),

⁸We can roughly reproduce this value assuming $s_0^{K^*} = (\sqrt{s_0^p} + m_s)^2$ where $s_0^p = 1.5$ GeV² is an established threshold in the ρ /dipion channel.

where the perturbative part dominates at $M^2 \sim 1 \text{ GeV}^2$ is, on the contrary, sensitive to increasing $s_0 > 1 \text{ GeV}^2$ and fits the r.h.s. of Eq. (88) only at $s_0 \sim 1.3 \text{ GeV}^2$. We conclude that the OPE spectral density at $s > s_0$ is to a large extent dual to the hadronic states with larger multiplicity ($K\pi\pi$, $K3\pi$, etc.) including their resonance contributions, and that the values of s_0 in Table 3 are truly reflecting the duality interval for the $K\pi$ P -wave state.

Our second observation is that these values are somewhat smaller than $s_0^{2\pi} \simeq 1.5 \text{ GeV}^2$ obtained in Ref. [19] for the dipion P -wave state. This might also seem unexpected but in reality it only reflects the complexity of hadronic spectral functions in both $K\pi$ and $\pi\pi$ channels, including some diversity – for instance, three-body $K\pi\pi$ states are allowed in the former case whereas the 3π ones are forbidden in the latter channel by isospin symmetry. These observations could open up a new perspective for revisiting the “classical” two-point SVZ sum rules with a more accurate hadronic description, such as the one adopted here.

5.4 Fitting the OPE to the z -expansion

We now use the OPE expressions $\mathcal{P}_i^{(T),\text{OPE}}$ in Appendix D to determine the OPE coefficients of the z -expansion in Eq. (67):

$$\mathcal{P}_i^{(T),\text{OPE}}(q^2, \sigma_0, M^2) = \frac{\kappa_i^{(T),\text{OPE}} + \eta_i^{(T),\text{OPE}} \zeta(q^2)}{1 - q^2/m_i^2}. \quad (91)$$

For this purpose, we first produce results for $\mathcal{P}_i^{(T),\text{OPE}}(q^2, \sigma_0, M^2)$ for all seven form factors, for $q^2 = \{0, 1, 2, 3, 4, 5\} \text{ GeV}^2$ and for $M^2 = \{1.00, 1.25, 1.50\} \text{ GeV}^2$ (with the corresponding values of s_0 in Table 3). This amounts to 18 determinations per form factor. In addition, we consider all three models for the B -meson LCDAs discussed Appendix B.2. These results for $\mathcal{P}_i^{(T),\text{OPE}}$ have central values and uncertainties that correspond to the mean and the standard deviation of a multivariate Gaussian scan over all input parameters. We have checked that these ensembles are approximately Gaussian and that the mean values are close to the most probable point, and also close to the result obtained from the central values of the input parameters.

From the results at $q^2 = 0$ we obtain directly the OPE parameters $\kappa_i^{(T),\text{OPE}}$,

$$\kappa_i^{(T),\text{OPE}}(\sigma_0, M^2) = \mathcal{P}_i^{(T),\text{OPE}}(0, \sigma_0, M^2). \quad (92)$$

For the “slope” OPE parameters $\eta_i^{(T),\text{OPE}}$ we use the formula

$$\eta_i^{(T),\text{OPE}}(\sigma_0, M^2) = \frac{(m_i^2 - q^2)\mathcal{P}_i^{(T),\text{OPE}}(q^2, \sigma_0, M^2)}{m_i^2 \zeta(q^2)} - \frac{\mathcal{P}_i^{(T),\text{OPE}}(0, \sigma_0, M^2)}{\zeta(q^2)}, \quad (93)$$

and taking into account that the left-hand side must be q^2 -independent, we perform a fit using the determinations at $q^2 = \{1, 2, 3, 4, 5\} \text{ GeV}^2$ as pseudo-data. Our final results for the OPE

Form F.	$M^2 = 1.00 \text{ GeV}^2$	$M^2 = 1.25 \text{ GeV}^2$	$M^2 = 1.50 \text{ GeV}^2$
F_{\perp}	$\kappa_{\perp}^{\text{OPE}} = +0.007(4)(0)$	$\kappa_{\perp}^{\text{OPE}} = +0.008(5)(0)$	$\kappa_{\perp}^{\text{OPE}} = +0.009(5)(0)$
	$\eta_{\perp}^{\text{OPE}} = -0.010(14)(14)$	$\eta_{\perp}^{\text{OPE}} = -0.012(17)(17)$	$\eta_{\perp}^{\text{OPE}} = -0.013(19)(21)$
F_{\parallel}	$\kappa_{\parallel}^{\text{OPE}} = +0.100(58)(7)$	$\kappa_{\parallel}^{\text{OPE}} = +0.120(69)(8)$	$\kappa_{\parallel}^{\text{OPE}} = +0.137(78)(8)$
	$\eta_{\parallel}^{\text{OPE}} = +0.25(9)(16)$	$\eta_{\parallel}^{\text{OPE}} = +0.30(11)(20)$	$\eta_{\parallel}^{\text{OPE}} = +0.36(13)(24)$
F_{-}	$\kappa_{-}^{\text{OPE}} = -0.004(3)(1)$	$\kappa_{-}^{\text{OPE}} = -0.004(4)(1)$	$\kappa_{-}^{\text{OPE}} = -0.005(5)(1)$
	$\eta_{-}^{\text{OPE}} = -0.020(17)(3)$	$\eta_{-}^{\text{OPE}} = -0.025(21)(4)$	$\eta_{-}^{\text{OPE}} = -0.029(24)(5)$
F_t	$\kappa_t^{\text{OPE}} = -0.043(9)(2)$	$\kappa_t^{\text{OPE}} = -0.052(11)(3)$	$\kappa_t^{\text{OPE}} = -0.060(12)(3)$
	$\eta_t^{\text{OPE}} = +0.210(30)(10)$	$\eta_t^{\text{OPE}} = +0.249(34)(14)$	$\eta_t^{\text{OPE}} = +0.282(37)(19)$
F_{\perp}^T	$\kappa_{\perp}^{T,\text{OPE}} = +0.036(21)(2)$	$\kappa_{\perp}^{T,\text{OPE}} = +0.043(25)(2)$	$\kappa_{\perp}^{T,\text{OPE}} = +0.050(29)(2)$
	$\eta_{\perp}^{T,\text{OPE}} = -0.056(73)(66)$	$\eta_{\perp}^{T,\text{OPE}} = -0.065(85)(84)$	$\eta_{\perp}^{T,\text{OPE}} = -0.07(9)(10)$
F_{\parallel}^T	$\kappa_{\parallel}^{T,\text{OPE}} = +0.49(29)(3)$	$\kappa_{\parallel}^{T,\text{OPE}} = +0.59(35)(3)$	$\kappa_{\parallel}^{T,\text{OPE}} = +0.67(39)(3)$
	$\eta_{\parallel}^{T,\text{OPE}} = +1.35(46)(85)$	$\eta_{\parallel}^{T,\text{OPE}} = +1.7(6)(11)$	$\eta_{\parallel}^{T,\text{OPE}} = +1.9(7)(12)$
F_{-}^T	$\kappa_{-}^{T,\text{OPE}} = -0.021(19)(5)$	$\kappa_{-}^{T,\text{OPE}} = -0.025(23)(6)$	$\kappa_{-}^{T,\text{OPE}} = -0.028(26)(7)$
	$\eta_{-}^{T,\text{OPE}} = -0.10(10)(1)$	$\eta_{-}^{T,\text{OPE}} = -0.12(13)(2)$	$\eta_{-}^{T,\text{OPE}} = -0.14(15)(2)$

Table 4: *Results for the OPE coefficients in the z -expansion in Model I for the B -meson LCDAs. The first error is parametric and the second one captures the model dependence from the LCDAs, as detailed in Appendix E.*

parameters $\kappa_i^{(T),\text{OPE}}$ and $\eta_i^{(T),\text{OPE}}$ are summarized in Table 4. The uncertainties of this set of 42 numbers are strongly correlated among themselves. The full 42×42 correlation matrix in electronic format (in the form of a Mathematica file) is available from the authors upon request (see Appendix E for details).

These results correspond to Model I for the B -meson LCDAs as described in Appendix B.2, which we regard as our default model. In order to estimate the model dependence of the OPE contributions, we look at the corresponding results in models IIA and IIB. These results are collected in Appendix E. We use these results to produce the second set of errors in Table 4, which capture the model dependence of the results. This estimate of model dependence does not imply that the three models discussed in Appendix B.2 and Ref. [24] must be regarded on the same footing. Models for LCDAs remain to be studied carefully and deserve further theoretical work (see e.g. Ref. [62]). In relation to this, it has been determined that some invariant amplitudes in the correlation function relevant to $B \rightarrow \gamma \ell \nu$ are independent of the

shape of some of the higher-twist LCDAs, within the types of models considered here [87]. This correlation function is equal to the one in Eq. (18) up to flavor, and thus the invariant amplitudes considered in Ref. [87] are related to some of the invariant amplitudes in Eq. (18) in the limit $m_s \rightarrow 0$. To which extent the shape-independence of the B -meson LCDAs applies to the invariant amplitudes relevant to $B \rightarrow K\pi$ form factors is a question that we leave for future consideration.

5.5 $B \rightarrow K^*$ form factors in the narrow-width limit

Having studied the OPE side of the sum rules in the previous section, we can move to the hadronic side. This is the part of the sum rules that has been generalized in this article to go beyond the Narrow-Width Limit (NWL). In Section 4.2, we have demonstrated explicitly that in the limit $\Gamma_{K^*} \rightarrow 0$ the integrand of the integral over the $K\pi$ invariant mass becomes a delta function, and thus the usual LCSRs for $B \rightarrow K^*$ form factors are recovered from our sum rules, analytically. Furthermore, we have also checked that the limit $\Gamma_{K^*} \rightarrow 0$ works also numerically, and that making Γ_{K^*} smaller and smaller the results for the form factors from the full LCSRs converge to the results from the $B \rightarrow K^*$ sum rules in Appendix A.

In this section we thus study the $B \rightarrow K^*$ form factors in the NWL and compare our results to those in the literature. For this purpose we take the formulae for the form factors in Appendix A and the numerical determination of the OPE functions in Table 4. In this way, we have:

$$V^{BK^*}(0) = \frac{m_B + m_{K^*}}{2f_{K^*}m_{K^*}} e^{m_{K^*}^2/M^2} \kappa_{\perp}^{\text{OPE}}(\sigma_0, M^2), \quad (94)$$

$$b_V^{BK^*} = \frac{m_B + m_{K^*}}{2f_{K^*}m_{K^*}} e^{m_{K^*}^2/M^2} \eta_{\perp}^{\text{OPE}}(\sigma_0, M^2), \quad (95)$$

and similarly for the other form factors.

We calculate the form factors $\mathcal{F}_i^{BK^*}(0)$ and the slope parameters $b_i^{BK^*}$ by performing a Gaussian scan over all input parameters, including the three different values for M^2 . Our results are collected in Table 5, together with the correlation coefficients.

In Table 6 we compare our results for the form factors at $q^2 = 0$ with the analogous results in Refs. [12, 15, 18, 25]. We see that our results are consistent with all the other determinations within uncertainties, but with central values that are somewhat lower. We ascribe this difference to four factors: the difference in the numerical input, the effect of twist-four two-particle contributions from $g_+(\omega)$ and $\bar{G}_{\pm}(\omega)$, the substantially lower value of the effective threshold parameter s_0 as described in Section 5.3, and the effect of three-particle contributions, which in our case reduce the form factors by around 10%, while they are negligible and excluded from the numerical analysis in Ref. [15]⁹. These effects are summarized in Table 7, where we show

⁹Using the same inputs as in Ref. [15], we agree with the results of that reference very precisely. The

$\mathcal{F}_\perp(0)$	b_\perp	$\mathcal{F}_\parallel(0)$	b_\parallel	$\mathcal{F}_-(0)$	b_-	$\mathcal{F}_t(0)$	b_t	$\mathcal{F}_\perp^T(0)$	b_\perp^T	$\mathcal{F}_\parallel^T(0)$	b_\parallel^T	$\mathcal{F}_-^T(0)$	b_-^T
0.26	-0.37	0.20	0.51	0.14	0.80	0.30	-1.44	0.22	-0.33	0.22	0.63	0.13	0.62
± 0.15	± 0.53	± 0.12	± 0.19	± 0.13	± 0.68	± 0.07	± 0.20	± 0.13	± 0.44	± 0.13	± 0.24	± 0.12	± 0.66
1.00	-0.97	1.00	0.86	1.00	-0.68	0.96	-0.67	1.00	-0.97	1.00	0.87	1.00	-0.72
-0.97	1.00	-0.97	-0.72	-0.98	0.78	-0.89	0.56	-0.97	1.00	-0.97	-0.74	-0.98	0.81
1.00	-0.97	1.00	0.86	1.00	-0.68	0.96	-0.67	1.00	-0.97	1.00	0.87	1.00	-0.72
0.86	-0.72	0.86	1.00	0.83	-0.25	0.91	-0.84	0.85	-0.70	0.85	1.00	0.83	-0.30
1.00	-0.98	1.00	0.83	1.00	-0.70	0.93	-0.64	1.00	-0.98	1.00	0.84	1.00	-0.74
-0.68	0.78	-0.68	-0.25	-0.70	1.00	-0.55	-0.06	-0.68	0.79	-0.68	-0.27	-0.70	1.00
0.96	-0.89	0.96	0.91	0.93	-0.55	1.00	-0.74	0.96	-0.88	0.95	0.92	0.94	-0.60
-0.67	0.56	-0.67	-0.84	-0.64	-0.06	-0.74	1.00	-0.67	0.55	-0.67	-0.83	-0.64	-0.01
1.00	-0.97	1.00	0.85	1.00	-0.68	0.96	-0.67	1.00	-0.97	1.00	0.87	1.00	-0.72
-0.97	1.00	-0.97	-0.70	-0.98	0.79	-0.88	0.55	-0.97	1.00	-0.97	-0.72	-0.98	0.82
1.00	-0.97	1.00	0.85	1.00	-0.68	0.95	-0.67	1.00	-0.97	1.00	0.87	1.00	-0.72
0.87	-0.74	0.87	1.00	0.84	-0.27	0.92	-0.83	0.87	-0.72	0.87	1.00	0.85	-0.32
1.00	-0.98	1.00	0.83	1.00	-0.70	0.94	-0.64	1.00	-0.98	1.00	0.85	1.00	-0.74
-0.72	0.81	-0.72	-0.30	-0.74	1.00	-0.60	-0.01	-0.72	0.82	-0.72	-0.32	-0.74	1.00

Table 5: Results for the form factors in the narrow-width limit. The first row contains the central values, the second row the uncertainties, and the rest the correlation coefficients.

Form Factor	This work	Ref. [12]	Ref. [25]	Ref. [15]	Ref. [18]
$\mathcal{F}_{K^*,\perp}(0) = V^{BK^*}(0)$	0.26(15)	0.39(11)	0.36(18)	0.32(11)	0.34(4)
$\mathcal{F}_{K^*,\parallel}(0) = A_1^{BK^*}(0)$	0.20(12)	0.30(8)	0.25(13)	0.26(8)	0.27(3)
$\mathcal{F}_{K^*,-}(0) = A_2^{BK^*}(0)$	0.14(13)	0.26(8)	0.23(15)	0.24(9)	0.23(5)
$\mathcal{F}_{K^*,t}(0) = A_0^{BK^*}(0)$	0.30(7)	–	0.29(8)	0.31(7)	0.36(5)
$\mathcal{F}_{K^*,\perp}^T(0) = T_1^{BK^*}(0)$	0.22(13)	0.33(10)	0.31(14)	0.29(10)	0.28(3)
$\mathcal{F}_{K^*,\parallel}^T(0) = T_2^{BK^*}(0)$	0.22(13)	0.33(10)	0.31(14)	0.29(10)	0.28(3)
$\mathcal{F}_{K^*,-}^T(0) = T_3^{BK^*}(0)$	0.13(12)	–	0.22(14)	0.20(8)	0.18(3)

Table 6: *Results for the form factors at $q^2 = 0$ in the narrow-width limit, compared to corresponding results in the literature. The approach in Ref. [18] is a completely different LCSR approach, in terms of K^* DAs.*

the central values for the form factors corresponding to: Ref. [12] (first row); our calculation but with the numerical inputs of Ref. [12]: $f_B = 180$ MeV, $f_{K^*} = 217$ MeV, $s_0 = 1.7$ GeV², $m_s = 130$ MeV, and excluding the twist-four two-particle contributions (second row); the same but including the twist-four contributions (third row); the calculation with $M^2 = 1$ and our inputs in Table 2, but with the effective threshold at $s_0 = 1.7$ GeV (fourth row); all our inputs but excluding the twist-four two-particle contributions (fifth row); and our final central values with the value of s_0 from Section 5.3, which coincide with the values quoted in Table 6 (sixth row). Our higher input value for f_B and lower value for f_{K^*} increase the values of the form factors, but this cancels approximately the decrease from the substantially lower value of s_0 . The effect of g_+ is ultimately responsible for the low values of our form factors (albeit consistent with other determinations within errors). The parametrical hierarchy of twists in the OPE deserves further careful study, which we postpone to a future work.

To close this subsection, we mention a very recent LCSR calculation of the “soft overlap” $B \rightarrow V$ form factors (in the narrow-width limit), done at NLO in SCET and including twist-6 contributions [16]. The results for $B \rightarrow K^*$ form factors are given in Tables 6 and 7 there.

5.6 Finite-width effects in $B \rightarrow K^*$ form factors

The LCSRs in the form of Eq. (66) imply that, in the one-resonance approximation, each $B \rightarrow K^*$ form factor normalized to its narrow-width limit is a constant that does not depend

reason that three-particle contributions are negligible in Ref. [15] is due to the use of the numerical values in Eq. (B.32) from Ref. [90] without the use of the EOM (see Appendix B.2).

$\mathcal{F}^{BK^*}(q^2 = 0)$	V^{BK^*}	$A_1^{BK^*}$	$A_2^{BK^*}$	$A_0^{BK^*}$	$T_{1,2}^{BK^*}$	$T_3^{BK^*}$
Ref. [12]	0.39	0.30	0.26	–	0.33	–
Inputs [12], no g_+	0.38	0.29	0.26	0.31	0.33	0.25
Inputs [12], with g_+	0.27	0.21	0.14	0.31	0.24	0.14
Our inputs, but $s_0 = 1.7 \text{ GeV}^2$	0.33	0.26	0.17	0.38	0.29	0.17
Our inputs, our s_0 , no g_+	0.36	0.28	0.25	0.30	0.31	0.23
Our inputs, our s_0 , with g_+	0.26	0.20	0.14	0.30	0.22	0.13

Table 7: *Deconstruction of the different effects explaining the difference between our results for the form factors at $q^2 = 0$ and those in Ref. [12]. The difference stems mainly from the inclusion of the twist-four two-particle contributions. See the text for more details.*

on the form factor type. To see this we consider the LCSRs (44) with a single K^* :

$$\mathcal{F}_{K^*,i}^{(T)}(q^2) d_{K^*,i}^{(T)} I_{K^*}(s_0, M^2) = \mathcal{P}_i^{(T)\text{OPE}}(q^2, \sigma_0, M^2). \quad (96)$$

The key observation is that the only quantity here that depends on both i and the width Γ_{K^*} is the form factor itself $\mathcal{F}_{K^*,i}^{(T)}(q^2)$. The other quantity that depends on Γ_{K^*} is the function $I_{K^*}(s_0, M^2)$, which is universal for all form factors and independent of q^2 . Therefore, defining the ratio \mathcal{W}_{K^*} of any of the form factors to its NWL, we find:

$$\mathcal{W}_{K^*} \equiv \frac{\mathcal{F}_{K^*,i}^{(T)}(q^2)}{\mathcal{F}_{K^*,i}^{(T)}(q^2)_{\text{NWL}}} = \frac{I_{K^*}(s_0, M^2)|_{\Gamma_{K^*} \rightarrow 0}}{I_{K^*}(s_0, M^2)} = \frac{2m_{K^*} f_{K^*} e^{-m_{K^*}^2/M^2}}{I_{K^*}(s_0, M^2)}, \quad (97)$$

where the NWL of the numerator has been performed as described in Section 4.2. Assuming K^* dominance, the quantities $\mathcal{F}_{K^*,i}^{(T)}(q^2)_{\text{NWL}}$ are precisely the ones determined in the previous subsection, and thus the form factors $\mathcal{F}_{K^*,i}^{(T)}(q^2)$ can be obtained by multiplying the results in Tables 5 and 6 by \mathcal{W}_{K^*} .

The ratio \mathcal{W}_{K^*} as a function of the K^* width Γ_{K^*} is shown in Figure 2. We can see that for $\Gamma_{K^*} \rightarrow 0$ we recover smoothly the NWL $\mathcal{W}_{K^*} \rightarrow 1$ (as discussed above for the form factors themselves). The dependence is very approximately linear:

$$\mathcal{W}_{K^*} \simeq 1 + 1.9 \frac{\Gamma_{K^*}}{m_{K^*}}, \quad (98)$$

with a coefficient (≈ 2) of order one multiplying the expected Γ_{K^*}/m_{K^*} correction. For the measured width $\Gamma_{K^*} \simeq 46 \text{ MeV}$ (see Table 2) we find that the finite-width correction in $B \rightarrow K^*$ form factors is of order of $\sim 10\%$, which is similar to the corresponding corrections to the $B \rightarrow \rho$ form factors investigated in Ref. [19]. More precisely, from Eq. (97) and the

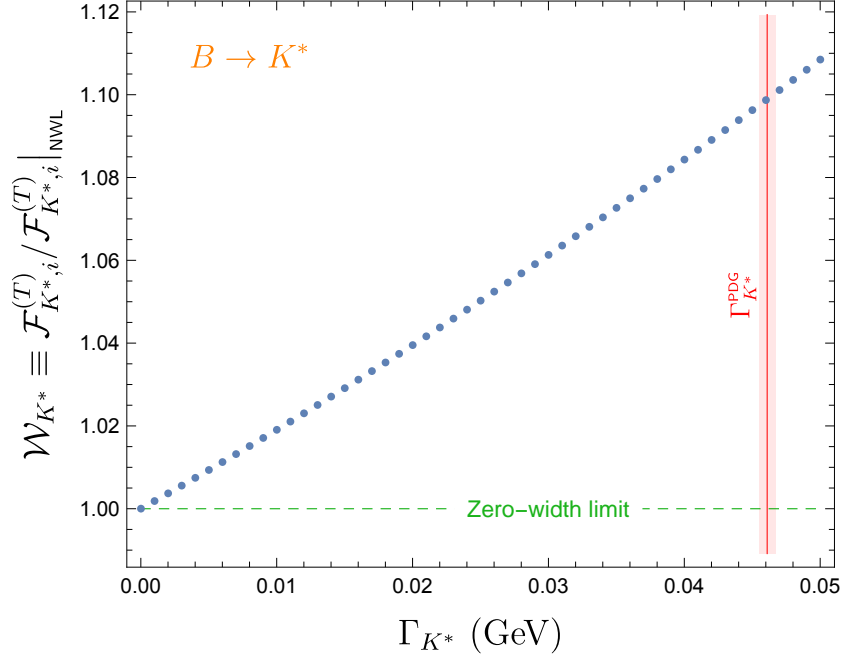


Figure 2: Ratio \mathcal{W}_{K^*} quantifying the finite-width correction to the $B \rightarrow K^*$ form factors, as a function of the K^* width Γ_{K^*} , for $M^2 = 1 \text{ GeV}^2$. The red vertical band corresponds to the physical width (PDG). This finite-width correction is universal and q^2 -independent.

numerical inputs in Table 2 we find:

$$\mathcal{W}_{K^*} = 1.09 \pm 0.01 . \quad (99)$$

We have used the Model 1 for $f_{K^*(892)} = 206 \text{ MeV}$, since in this model the τ data is consistent with the absence of a $K^*(1410)$ resonance (see Section 5.2). This number is an average of the results $\mathcal{W}_{K^*} = \{1.099(16), 1.091(9), 1.085(7)\}$ for $M^2 = \{1.00, 1.25, 1.50\} \text{ GeV}^2$, where the corresponding values for s_0 in Table 3 – for Model 1 – have been used. The parametric uncertainties in \mathcal{W}_{K^*} are negligible compared to those arising from the uncertainty in s_0 . The variation of s_0 and M^2 in \mathcal{W}_{K^*} will be correlated with the one in the calculation of the form factors, and therefore the separate determinations of \mathcal{W}_{K^*} for different values of M^2 may result in more accurate estimates of the finite-width effect. Nevertheless, the three values quoted for \mathcal{W}_{K^*} are consistent among themselves within errors, and the average in Eq. (99) is meaningful.

The robustness of the previous results is also supported by the expansion at $\mathcal{O}(\Gamma)$ discussed at the end of Section 4.2. From Eq. (61), we see that

$$\mathcal{W}_{K^*} = 1 - \frac{\Gamma_{K^*}}{m_{K^*}} \Delta_{K^*}(s_0, M^2) + \mathcal{O}(\Gamma_{K^*}^2) . \quad (100)$$

This linearised expression depends only on the mass and the width of the resonance as well as the sum rule parameters s_0 and M^2 , and it is thus less dependent on the details of the

hadronic model used. With the same inputs as above, we obtain

$$\mathcal{W}_{K^*} = 1.08 \pm 0.01 \quad [\text{linearised}] . \quad (101)$$

The range is obtained by varying the sum rule parameters in the same way as in Eq. (99). The slight difference with the central value of Eq. (99) can be attributed to higher orders in the expansion in powers of Γ_{K^*} , indicated by the slight curvature of the function $\mathcal{W}_{K^*}(\Gamma_{K^*})$ shown in Figure 2¹⁰.

The fact that the ratio \mathcal{W}_{K^*} is independent of the form factor helicity has two consequences, which will be discussed further in Section 6. First, corrections to the NWL in branching fractions of exclusive $B \rightarrow K^*$ observables will be proportional to $|\mathcal{W}_{K^*}|^2 \simeq 1.20$. This 20% increase in the theory predictions with respect to the narrow-width limit is very relevant phenomenologically in view of the systematically low experimental determinations of branching ratios in $b \rightarrow s\mu\mu$ modes reported by the LHCb collaboration (see for instance Refs. [1,2,64,65] and references therein). The correction to the NWL discussed here would tend to increase the discrepancy between the SM predictions and the LHCb measurements. Second, normalized observables such as P'_5 [66,67], which depend only on ratios of form factors, are insensitive to finite-width corrections. Technically, these considerations apply only to *factorizable* decay modes; it remains to be determined if non-local contributions to $b \rightarrow s\ell\ell$ also have this property.

5.7 Beyond the K^* window and the $K^*(1410)$ contribution

It is evident from Eq. (68) that the LCSRs can only constrain one particular combination of the $K^*(892)$ and $K^*(1410)$ contributions. As mentioned earlier, this is due to the fact that the sum rules only depend on an integral of the $B \rightarrow K\pi$ form factors over the $K\pi$ invariant mass, weighted by the $K\pi$ form factor $f_+(s)$. Since this form factor is peaked strongly around the $K^*(892)$ resonance, the LCSRs are mostly sensitive to the $B \rightarrow K\pi$ form factors in the region $s \simeq m_{K^*} \pm \Gamma_{K^*}$. This is the reason why the traditional LCSRs for $B \rightarrow K^*$ form factors work well. But this also means that the $K^*(1410)$ and other “non-resonant” contributions will be only weakly constrained by the LCSRs. In addition, the two models for $f_+(s)$ considered in Section 5.2 (consistent with the τ decay), will presumably provide a slightly different sensitivity to the $K^*(1410)$ contribution, as the form factor differs by a factor of two on the vicinity of this resonance.

More quantitatively, the contributions from $K^*(892)$ and $K^*(1410)$ to the sum rules (68) are proportional to the factors $I_{K^*(892)}$ and $I_{K^*(1410)}$. The numerical values for these factors are collected in Table 8, where one can see that $I_{K^*(1410)}/I_{K^*(892)} \simeq 0.03$. Thus, for the $K^*(1410)$

¹⁰Interestingly, a similar effect (in size and direction) was found in Ref. [63] in the case of the form factor for the $\gamma^*\rho \rightarrow \pi$ transition. Indeed, taking into account the measured width of the ρ -meson leads to an increase by 12% of the form factor compared to the LCSR prediction in the narrow-width limit.

		$M^2 = 1.00 \text{ GeV}^2$	$M^2 = 1.25 \text{ GeV}^2$	$M^2 = 1.50 \text{ GeV}^2$
Model 1	$I_{K^*(892)}$	0.1506(23)	0.1781(16)	0.1992(13)
	$I_{K^*(1410)}$	0.0050(07)	0.0062(07)	0.0072(06)
Model 2	$I_{K^*(892)}$	0.1491(22)	0.1766(20)	0.1975(16)
	$I_{K^*(1410)}$	0.0048(07)	0.0061(06)	0.0070(06)

Table 8: Values for the quantities I_R for $R = \{K^*(892), K^*(1410)\}$ for the different values of the Borel parameter M^2 and for the two models for the $K\pi$ form factor. The $K^*(1410)$ contribution is very suppressed in the sum rules, with $I_{K^*(1410)}/I_{K^*(892)} \simeq 0.03$ in all cases.

to have a significant weight in the sum rule for a given form factor, $\mathcal{F}_{K^*(1410)}$ must be at least an order or magnitude larger than $\mathcal{F}_{K^*(892)}$.

This issue was also pointed out in Ref. [19] where various alternative assumptions were adopted in order to estimate the ρ' and ρ'' contributions to $B \rightarrow \pi\pi$ form factors. As a first approach, the LCSRs with ρ -meson LCDAs were used to fix the ρ contribution, and thus the ρ' contribution could be estimated from our LCSRs for $B \rightarrow \pi\pi$ form factors. This assumed that the LCSRs with ρ -meson LCDAs are insensitive to the presence of the ρ' [18]. The corresponding results for $B \rightarrow \rho'$ form factors were relatively imprecise, given the insensitivity of the LCSRs to the region outside the ρ window. As a second approach, it was assumed that the relative contribution from each resonance is the same in the $B \rightarrow \pi\pi$ form factors as in the time-like pion form factor. This is a bolder assumption but provides relatively precise predictions. One may see this as a model which is consistent with the LCSRs.

As a more pragmatic and model-independent alternative, one may attempt to constrain the $B \rightarrow K\pi$ form factors in the $K^*(1410)$ region from data. Once this is done, our LCSRs can be used to determine the $B \rightarrow K^*$ form factors in a way which takes into account the contributions beyond the K^* window. Note that this data-driven determination of the form factors in the $K^*(1410)$ region needs not be very precise. In order to have a significant impact on the K^* region, these would need to be huge, but this is a possibility that has not been discarded.

In order to illustrate this point, we consider the form factors in the form of Eq. (69), and set $\mathcal{F}_{K^*(1410)} = \alpha \mathcal{F}_{K^*(892)}$ with α a floating parameter. For different values of α , we can use the sum rules (68) to fix the parameters $\mathcal{F}_{K^*,i}^{(T)}$ and $b_{K^*,i}^{(T)}$ as in Section 5.5, and plug these results into Eq. (69) to predict the $B \rightarrow K\pi$ form factors $F_i^{(T)(\ell=1)}(s, q^2)$. In Figure 3 we show the outcome of this exercise for the form factor $F_{\perp}^{(\ell=1)}(s, 0)$, choosing the values $\alpha = \{1, 10, 50\}$. One can see that for $\alpha = 1$, the presence of the $K^*(1410)$ is barely noticeable, but for $\alpha = 50$ it dominates the form factor. These two extremes are perfectly allowed by the LCSRs. But

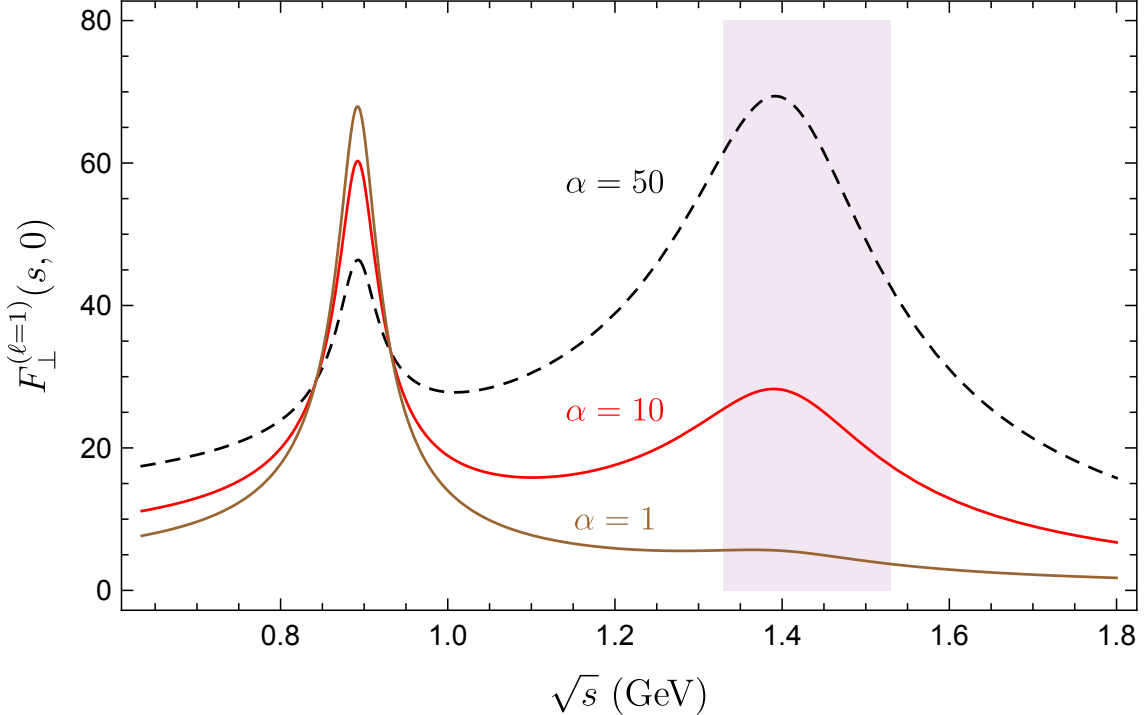


Figure 3: Form factor $F_{\perp}^{(\ell=1)}(s, 0)$ at $q^2 = 0$, as a function of the $K\pi$ invariant mass, for three different values of the parameter α , describing the relative size of $K^*(892)$ and $K^*(1410)$ contributions. All the curves are consistent with the Light-Cone Sum Rule. The vertical band indicates the region of the measurements in Ref. [68].

there is a competition between both contributions. Higher values of α suppress the $B \rightarrow K^*$ form factor in order to maintain the sum rule constraint ¹¹:

$$\alpha = 1 : \mathcal{F}_{K^*,\perp}(0) = 0.28 ; \quad \alpha = 10 : \mathcal{F}_{K^*,\perp}(0) = 0.22 ; \quad \alpha = 50 : \mathcal{F}_{K^*,\perp}(0) = 0.11 . \quad (102)$$

Therefore, a suppression of the $B \rightarrow K^*$ form factors favoured by $B \rightarrow K^* \mu \mu$ data could be the result of a very large $B \rightarrow K^*(1410)$ form factor, being all consistent with the LCSRs. However, this would at the same time produce a huge enhancement of the $B \rightarrow K \pi \mu \mu$ rate around $\sqrt{s} = 1.4$ GeV, as can be seen in Figure 3, which would impact significantly the measurements in this region performed by the LHCb collaboration [68]. Thus these measurements can be used to constrain the predictions for $B \rightarrow K^*$ form factors. We shall discuss this in more detail in Section 6.4.

As a side note, we point out that the exact interplay between both contributions depends on the relative phase ϕ_R in the form factor. Figure 3 and the above discussion correspond to the phase choice in Eq. (47). All in all, it would also be important to study these phases in more depth.

¹¹Note that the value 0.28 corresponding to $\alpha = 1$ is equal to the NWL result in Table 6 corrected by \mathcal{W}_{K^*} .

6 Applications to rare decays

We have derived the sum rules for the $B \rightarrow K\pi$ form factors and we have determined the constraints set on models based on a series of resonances. We want now to exploit these sum rules for $B \rightarrow K\pi\ell\ell$. We consider first a toy example to illustrate the connection between the general $K\pi$ case and the narrow-width K^* case at the level of the differential decay rates. Then we consider the $B \rightarrow K\pi\ell\ell$ decay: we derive the expression of the differential decay rate using the $B \rightarrow K\pi$ form factors, we discuss the connection with the narrow-width limit around the K^* peak, and we exploit experimental information obtained for a $K\pi$ invariant mass around the $K^*(1410)$ in order to further constrain our model for the $B \rightarrow K\pi$ form factors.

6.1 A toy example

We start with a toy example that captures the essence of the generalization beyond the narrow-width limit at the level of decay rates. We consider a new scalar particle Φ with mass-squared $m_\Phi^2 = q^2$ that couples to the pseudoscalar current $\bar{s}\gamma_5 b$:

$$\mathcal{L}_{sb\Phi} = -g \bar{s}\gamma_5 b \Phi + \text{h.c.} , \quad (103)$$

and study the decay $B \rightarrow \Phi K^- \pi^+$. The amplitude of the process to leading order in g is

$$i\mathcal{A} = -\frac{g \sqrt{q^2}}{m_b + m_s} F_t(k^2, q^2, q \cdot \bar{k}) , \quad (104)$$

and the differential decay rate is given by

$$\frac{d\Gamma}{dk^2 d\cos\theta_K} = \frac{1}{(2\pi)^3 32m_B^3} \frac{\sqrt{\lambda\lambda_{K\pi}}}{2k^2} |\mathcal{A}|^2 . \quad (105)$$

Expanding the form factor in partial waves, the squared amplitude is

$$|\mathcal{A}|^2 = \frac{g^2 q^2}{(m_b + m_s)^2} \sum_{\ell, m} \sqrt{(2\ell + 1)(2m + 1)} F_t^{(\ell)}(k^2, q^2) F_t^{(m)*}(k^2, q^2) P_\ell^{(0)}(\cos\theta_K) P_m^{(0)}(\cos\theta_K) . \quad (106)$$

Therefore, integrating over the angle θ_K and using the orthogonality of Legendre polynomials we find

$$\frac{d\Gamma}{dk^2} = \frac{1}{(2\pi)^3 32m_B^3} \frac{g^2 q^2 \sqrt{\lambda\lambda_{K\pi}}}{(m_b + m_s)^2 k^2} \sum_{\ell=0}^{\infty} |F_t^{(\ell)}(k^2, q^2)|^2 . \quad (107)$$

We now consider the K^* contribution to this decay rate, which means taking only the $\ell = 1$ term in the sum, and using the parametrization of Eq. (42) with only one resonance:

$$|F_t^{(\ell=1)}|^2 = \frac{32\pi^2 s\lambda}{3q^2 \lambda_{K\pi}^{1/2}} |\mathcal{F}_{K^*,t}(q^2)|^2 \Delta(s, m_{K^*}) ; \quad \Delta(s, m_{K^*}) \equiv \frac{1}{\pi} \frac{\sqrt{s} \Gamma_{K^*}(s)}{(m_{K^*}^2 - s)^2 + s \Gamma_{K^*}(s)} . \quad (108)$$

The function $\Delta(s, m_{K^*})$ has an integral equal to 1 and goes to $\delta(s - m_{K^*})$ in the narrow-width limit. We use the notation $s = k^2$. Thus, if we integrate the decay rate around a window that contains the K^* resonance, we find ¹²:

$$\Gamma(B \rightarrow \Phi K^* [\rightarrow K^- \pi^+]) = \frac{g^2 \lambda^{3/2}(m_{K^*}^*)}{24\pi m_B^3 (m_b + m_s)^2} |\mathcal{F}_{K^*,t}(q^2)|^2 . \quad (109)$$

We need to compare this result with its narrow-width approximation. In this case the amplitude would be:

$$i\mathcal{A}_{K^*} = -\frac{2g m_{K^*} \epsilon_\eta^{*\mu} \cdot q}{m_b + m_s} A_0^{BK^*}(q^2) , \quad (110)$$

where η is the polarization of the K^* (with $\epsilon_\eta^{*\mu}$ its polarization vector), and $A_0^{BK^*}$ is the timelike-helicity $B \rightarrow K^*$ form factor (see Eq. (A.1)). Squaring the amplitude and summing over polarizations:

$$\sum_\eta |\mathcal{A}_{K^*}|^2 = \frac{g^2 m_{K^*}^2 \lambda(m_{K^*})}{(m_b + m_s)^2 k^2} |A_0^{BK^*}(q^2)|^2 , \quad (111)$$

where we have used that $\sum_\eta 4q_\mu q_\nu \epsilon_\eta^\mu \epsilon_\eta^{*\nu} = \lambda(m_{K^*})/k^2$. The decay rate is then:

$$\Gamma(B \rightarrow \Phi K^*) = \frac{g^2 \lambda^{3/2}(m_{K^*}^*)}{16\pi m_B^3 (m_b + m_s)^2} |A_0^{BK^*}(q^2)|^2 . \quad (112)$$

Since the K^* decays with probability 2/3 to $K^- \pi^+$, Eqs. (109) and (112) coincide if we identify $\mathcal{F}_{K^*,t}(q^2) = A_0^{BK^*}(q^2)$. Thus, when we integrate the decay rate around a resonance in a region wide enough to contain it, the finite-width-corrected result is obtained multiplying the rate by the squared of the ratio \mathcal{W} discussed in Section 5.6. In the case of the K^* , where $\mathcal{W}_{K^*} = 1.09$, the impact is 20%:

$$\Gamma(B \rightarrow \Phi K^* [\rightarrow K^- \pi^+]) = 1.2 \times \Gamma(B \rightarrow \Phi K^* [\rightarrow K^- \pi^+])_{\text{NWL}} . \quad (113)$$

As a final note, since the ratio \mathcal{W}_K^* is independent of the form factor helicity (see Section 5.6), the correction $\mathcal{W}_{K^*}^2 = 1.19$ factorizes in the decay rate of any (factorizable) decay mode, even if the amplitude depends on all 7 form factors. Such is the case in $B \rightarrow K^* \nu \bar{\nu}$ or $B_s \rightarrow K^* \ell \nu$, and in the factorizable part of more complicated decay modes such as the non-leptonic decay $B \rightarrow MK^*$, and the rare decay $B \rightarrow K^* \ell \ell$ discussed in the following section.

6.2 Angular distribution of the non-resonant $B \rightarrow K \pi \ell \ell$ decay

After the study of this toy example, we can move to the more realistic case of the rare decay $B \rightarrow K \pi \ell \ell$. The amplitude $\mathcal{A} \equiv \mathcal{A}(\bar{B}^0 \rightarrow K^-(k_1) \pi^+(k_2) \ell^-(q_1) \ell^+(q_2))$ in the SM is given

¹²Here we assume that the prefactor multiplying $\Delta(s, m_{K^*})$ in Eq. (108) varies slowly in the resonance region. This is certainly true if the width is small. A more careful description of this effect is given in Appendix F.

by [25, 69, 70]:

$$i\mathcal{A} = g_F \frac{\alpha}{4\pi} \left[(C_9 L_{V\mu} + C_{10} L_{A\mu}) \mathcal{F}_L^\mu + \frac{L_{V\mu}}{q^2} \left\{ 2m_b C_7 \mathcal{F}_R^{T\mu} - i 16\pi^2 \mathcal{H}^\mu \right\} \right] \quad (114)$$

with $q = q_1 + q_2$, $g_F \equiv 4G_F/\sqrt{2} V_{ts}^* V_{tb}$, $L_{V(A)}^\mu \equiv \bar{u}_\ell(q_1) \gamma^\mu (\gamma_5) v_\ell(q_2)$, and the local and non-local hadronic matrix elements:

$$\mathcal{F}_L^\mu \equiv i \langle K^-(k_1) \pi^+(k_2) | \bar{s} \gamma^\mu P_L b | \bar{B}^0(p) \rangle = \frac{1}{2} (F_\perp k_\perp^\mu + F_\parallel k_\parallel^\mu + F_0 k_0^\mu + F_t k_t^\mu), \quad (115)$$

$$\mathcal{F}_R^{T\mu} \equiv \langle K^-(k_1) \pi^+(k_2) | \bar{s} \sigma^{\mu\nu} q_\nu P_R b | \bar{B}^0(p) \rangle = \frac{1}{2} (F_\perp^T k_\perp^\mu + F_\parallel^T k_\parallel^\mu + F_0^T k_0^\mu), \quad (116)$$

$$\mathcal{H}^\mu \equiv i \int dx e^{i q \cdot x} \langle K^-(k_1) \pi^+(k_2) | T \{ j_{\text{em}}^\mu(x) \mathcal{O}_{4q}(0) \} | \bar{B}^0(p) \rangle = \mathcal{H}_\perp k_\perp^\mu + \mathcal{H}_\parallel k_\parallel^\mu + \mathcal{H}_0 k_0^\mu, \quad (117)$$

with $p = q + k$. Besides the form factors $F_i^{(T)}$ discussed in this article, we have introduced here the functions $\mathcal{H}_i(k^2, q^2, q \cdot \bar{k})$ describing the non-local effects which appear when the lepton pair couples to the electromagnetic current, through a penguin contraction of four-quark $\mathcal{O}_{4q} \sim \bar{s} b \bar{q} q$ operators. In complete analogy with the form factors in Eqs. (11–12), the functions $\mathcal{H}_i(k^2, q^2, q \cdot \bar{k})$ can be expanded in partial waves, resulting in the corresponding functions $\mathcal{H}_i^{(\ell)}(k^2, q^2)$.

The Lorentz decomposition and the structure of the leptonic currents define the different *transversity amplitudes* $\mathcal{A}_i^{L,R}$ by:

$$i\mathcal{A} = \frac{\alpha g_F}{8\pi\mathcal{N}} \left\{ L_\mu (\mathcal{A}_\perp^L k_\perp^\mu + \mathcal{A}_\parallel^L k_\parallel^\mu + \mathcal{A}_0^L k_0^\mu + \mathcal{A}_t^L k_t^\mu) + R_\mu (\mathcal{A}_\perp^R k_\perp^\mu + \mathcal{A}_\parallel^R k_\parallel^\mu + \mathcal{A}_0^R k_0^\mu + \mathcal{A}_t^R k_t^\mu) \right\}, \quad (118)$$

where $L^\mu \equiv \bar{u}_\ell(q_1) \gamma^\mu P_L v_\ell(q_2)$ and $R^\mu \equiv \bar{u}_\ell(q_1) \gamma^\mu P_R v_\ell(q_2)$, with $P_{L,R} = (1 \mp \gamma_5)/2$, and \mathcal{N} is a normalization constant which is introduced for convenience and will be fixed later. Comparing with Eq. (114) one sees that

$$\mathcal{A}_i^{L,R} = \mathcal{N} \left[(C_9 \mp C_{10}) F_i + \frac{2m_b}{q^2} \left\{ C_7 F_i^T - i \frac{16\pi^2}{m_b} \mathcal{H}_i \right\} \right], \quad i = \{\perp, \parallel, 0, t\}, \quad (119)$$

keeping in mind that $\mathcal{A}_i^{L,R} \equiv \mathcal{A}_i^{L,R}(k^2, q^2, q \cdot \bar{k})$, etc. For $\mathcal{A}_t^{L,R}$ only the first term exists ($F_t^T = \mathcal{H}_t = 0$). In addition, when $m_1 = m_2$ one has $L_\mu k_t^\mu = -R_\mu k_t^\mu$ and the timelike-helicity amplitude depends only on the combination $\mathcal{A}_t \equiv \mathcal{A}_t^L - \mathcal{A}_t^R$, which is independent of C_9 . However this is not true if the two leptons have different mass. The transversity amplitudes $\mathcal{A}_i^{L,R}$ in Eq. (119) can be expanded in partial waves $\mathcal{A}_i^{L,R(\ell)}(k^2, q^2)$ in the same way as the form factors, i.e. Eqs. (11)-(12).

We follow the same approach as in Ref. [69], exploiting the fact that we use the same definitions for the various angles (the link with the experimental kinematics from the LHCb experiment [71] is given by Ref. [72]). We consider the decay as the chain $B \rightarrow V^*(\rightarrow \ell\ell) K \pi$,

and we introduce the polarisations of the virtual intermediate gauge boson V^* defined in the B -meson rest frame,

$$\epsilon_{\pm}^{\mu} = (0, 1, \mp i, 0)/\sqrt{2} \quad \epsilon_0^{\mu} = (-q_z, 0, 0, -q_0)/\sqrt{q^2} \quad \epsilon_t^{\mu} = (q_0, 0, 0, q_z)/\sqrt{q^2}, \quad (120)$$

where $q^{\mu} = (q_0, 0, 0, q_z)$. We can then use the completeness relation for this basis of polarisation vectors to write

$$i\mathcal{A} = \frac{\alpha g_F}{8\pi\mathcal{N}} \sum_i \sum_{\lambda} g_{\lambda\lambda} (L_{\lambda} \mathcal{A}_i^L + R_{\lambda} \mathcal{A}_i^R) (\epsilon_{\lambda}^* \cdot k_i) = \frac{\alpha g_F}{8\pi\mathcal{N}} \sum_{\lambda} g_{\lambda\lambda} (L_{\lambda} H_{\lambda}^L + R_{\lambda} H_{\lambda}^R), \quad (121)$$

with $i = \{\perp, \parallel, 0, t\}$, $\lambda = \{0, t, +, -\}$ and $g_{tt} = 1$, $g_{00} = g_{++} = g_{--} = -1$. We have also defined $L_{\lambda} = \epsilon_{\lambda} \cdot L$ and $R_{\lambda} = \epsilon_{\lambda} \cdot R$, with R^{μ}, L^{μ} given after Eq. (118). The quantities $H_{\lambda}^{L,R}$ are called *helicity amplitudes*.

We can define transversity amplitudes similar to the $\bar{B} \rightarrow \bar{K}^* \ell^+ \ell^-$ case, by considering the B -meson rest frame described in Appendix G, and performing the partial-wave expansion of the various amplitudes up to the P wave:

$$H_{+}^{L,R} = \sqrt{3} \frac{\hat{A}_{\parallel}^{L,R} + \hat{A}_{\perp}^{L,R}}{\sqrt{2}} (-\sin \theta_K) + \dots, \quad H_{-}^{L,R} = \sqrt{3} \frac{\hat{A}_{\parallel}^{L,R} - \hat{A}_{\perp}^{L,R}}{\sqrt{2}} (-\sin \theta_K) + \dots, \quad (122)$$

$$H_0^{L,R} = \sqrt{2}\sqrt{3}(\hat{S}_0^{L,R} + \hat{A}_0^{L,R} \cos \theta_K + \dots), \quad H_t = -\sqrt{2}\sqrt{3}(\hat{S}_t + \hat{A}_t \cos \theta_K + \dots), \quad (123)$$

with $H_t \equiv H_t^L - H_t^R$. Here \hat{S} and \hat{A} denote $\ell_{K\pi} = 0$ and $\ell_{K\pi} = 1$ amplitudes, respectively, and the ellipsis indicates D and higher partial waves. The normalisations have been chosen to make the connection between \mathcal{A}_i and \hat{A}_i amplitudes easier, taking into account the partial-wave decompositions and the powers of $\sin \theta_K$ stemming from $\epsilon(\lambda) \cdot k_{\parallel}$ and $\epsilon(\lambda) \cdot k_{\perp}$ in Eq. (121):

$$\begin{aligned} \hat{A}_{\perp}^{L,R} &= \frac{\sqrt{\lambda_{K\pi}}}{k^2} \mathcal{A}_{\perp}^{L,R(1)}, & \hat{A}_{\parallel}^{L,R} &= \frac{\sqrt{\lambda_{K\pi}}}{k^2} \mathcal{A}_{\parallel}^{L,R(1)}, \\ \hat{A}_0^{L,R} &= -\mathcal{A}_0^{L,R(1)}/\sqrt{2}, & \hat{A}_t &= -\mathcal{A}_t^{(1)}/\sqrt{2}. \end{aligned} \quad (124)$$

The differential decay rate is given by

$$\frac{d\Gamma}{dq^2 dk^2 d \cos \theta_{\ell} d \cos \theta_K d\phi} = \frac{1}{2^{15} \pi^6 m_B} \frac{\sqrt{\lambda \lambda_q \lambda_{K\pi}}}{m_B^2 q^2 k^2} \sum_{s_1, s_2} |\mathcal{A}|^2, \quad (125)$$

where $|\mathcal{A}|^2$ is a product of the hadronic amplitudes $\hat{A}_i^{L,R}$ (known in terms of the form factors F_i, F_i^T) and the leptonic amplitudes L_{λ} and R_{λ} (which can be easily evaluated in the B -meson rest frame) and $\lambda_q \equiv \lambda(q^2, m_{\ell}^2, m_{\ell}^2)$. We can then perform the summation over the spins of the outgoing leptons to obtain the final expression

$$\frac{d\Gamma}{dq^2 dk^2 d \cos \theta_{\ell} d \cos \theta_K d\phi} = \frac{9}{32\pi} \bar{I}(q^2, k^2, \theta_{\ell}, \theta_K, \phi). \quad (126)$$

If we choose the normalisation

$$\mathcal{N} = \alpha G_F V_{tb} V_{ts}^* \sqrt{\frac{\sqrt{\lambda \lambda_{K\pi} \lambda_q}}{3 \cdot 2^{13} \pi^7 m_B^3 k^2}} \quad (127)$$

the expression of Eq. (126) is indeed very simple. \bar{I} is formally the same expression obtained in Eqs (3.10) and (3.21) of Ref. [69] with the angular coefficients $\bar{I}_{1s,1c,2s,2c,3,4,5,6s,6c,7,8,9}$ given by Eqs. (3.34)-(3.45) of the same reference. The main difference comes from the transversity amplitudes A_i , which are not be given by Eqs. (3.28)-(3.31) of Ref. [69] but should be replaced by the transversity amplitudes \hat{A}_i given in Eq. (124).

6.3 Finite-width effects in $B \rightarrow K^* \ell \ell$

Following the same arguments as in Section 6.1, we expect the results of Section 6.2 to be compatible with Ref. [69] if we assume that the $K^- \pi^+$ pair comes only from the decay of a narrow K^* . In order to prove this agreement, we can take the expressions of Section 6.2 and determine the expressions of the amplitudes \hat{A}_i assuming that they are dominated by a narrow K^* contribution. We can connect \hat{A}_i to \mathcal{A}_i using Eq. (124), express them in terms of $F_i^{(1)}$ and $F_i^{T(1)}$ using Eq. (119), and describe the latter using the model in Eq. (42). One can then use the narrow-width limit expression of $\mathcal{F}_{R,i}^{(T)}$ in terms of the $B \rightarrow K^*$ form factors described in Appendix A.

The resulting expressions can be related to the $B \rightarrow K^*$ amplitudes A_i given in Eqs. (3.28)-(3.31) of Ref. [69]:

$$\hat{A}_i^{L,R} = -\frac{1}{4\pi\sqrt{3}} \frac{\lambda_{K\pi}^{3/4}}{m_R^2} \frac{g_{RK\pi} e^{i\phi_R(s)}}{m_R^2 - s - i\sqrt{s}\Gamma_{K^*}(s)} \left[A_i^{L,R} + \mathcal{O}(\Gamma_{K^*}) \right] \quad (128)$$

where we have already considered the narrow-width limit for the form factors, but we have still to take this limit for the propagator.

Interferences between these amplitudes will thus become

$$\hat{A}_i^{L,R} (\hat{A}_j^{L,R})^* = \frac{1}{48\pi^2} \frac{\lambda_{K\pi}^{3/2}}{m_R^4} \frac{g_{RK\pi}^2}{(m_R - s)^2 + s\Gamma_R^2} A_i^{L,R} (A_j^{L,R})^* + \mathcal{O}(\Gamma_{K^*}) . \quad (129)$$

In the narrow-width limit, the squared propagator becomes

$$\frac{1}{(k^2 - m_{K^*}^2)^2 + (m_{K^*}\Gamma_{K^*})^2} \xrightarrow{\Gamma_{K^*} \rightarrow 0} \frac{\pi}{m_{K^*}\Gamma_{K^*}} \delta(k^2 - m_{K^*}^2) \quad (130)$$

whereas the width can be reexpressed using Eqs. (36) and (37)

$$\Gamma_{K^*} = \frac{g_{K^*K\pi}^2 \lambda_{K\pi}^{3/2}}{48\pi m_{K^*}^5} \mathcal{B}(K^* \rightarrow K^- \pi^+) \quad (131)$$

so that we have

$$\widehat{A}_i^{L,R}(\widehat{A}_j^{L,R})^* \xrightarrow{\Gamma_{K^* \rightarrow 0}} A_i^{L,R}(A_j^{L,R})^* \delta(k^2 - m_{K^*}^2) \mathcal{B}(K^* \rightarrow K^- \pi^+) , \quad (132)$$

proving that the narrow-width limit of the differential decay rate in Eq. (126) agrees with the results of Ref. [69].

As discussed in Section 4.2, the $\mathcal{O}(\Gamma)$ correction to the narrow-width limit can be determined quite easily. If we take finite-width effects into account, the sum-rule determination of the form factors entering the amplitudes \widehat{A}_i are enhanced by a factor \mathcal{W}_{K^*} , leading to an enhancement of all angular coefficients I_i by a factor $\simeq 1.2$ compared to the value obtained using the $B \rightarrow K^*$ form factors in the narrow-width limit.

6.4 High $K\pi$ -mass moments of the $B \rightarrow K\pi\ell\ell$ angular distribution

We can combine the analysis of the $B \rightarrow K\pi\ell\ell$ angular distribution in terms of $B \rightarrow K\pi$ form factors with the sum rules derived in Section 3 to constrain the $K^*(1410)$ contribution to the models in Section 4, thanks to recent experimental measurements. Indeed, in Ref. [68] the LHCb experiment has analysed the moments Γ_i ($i = 1 \dots 41$) of the angular distribution of $B \rightarrow K\pi\mu\mu$ in the region of $K\pi$ and dilepton invariant masses $\sqrt{k^2} \in [1.33, 1.53]$ GeV and $q^2 \in [1.1, 6]$ GeV², respectively. This region of $K\pi$ masses contains contributions from K^* resonances in the S , P and D waves, and the moments analysed in Ref. [68] contain contributions from all partial waves, following the analysis in Ref. [73]. The corresponding expansion can be written as

$$\frac{d\Gamma}{dq^2 dk^2 d\Omega} = \frac{1}{4\pi} \sum_{i=1}^{41} f_i(\Omega) \tilde{\Gamma}_i(q^2, k^2) \quad (133)$$

where $d\Omega = d\cos\theta_\ell d\cos\theta_K d\phi$. Since the decomposition takes into account the possibility of S , P and D -wave contributions, it features many different angular structures $f_i(\Omega)$.

We can compare these results with our predictions using our $B \rightarrow K\pi$ form factors for the combinations of moments that depend only on the P -wave contributions. The normalisations chosen are such that

$$\frac{d\Gamma}{dq^2 dk^2} = \tilde{\Gamma}_1 = |\widehat{A}_{\parallel}^L|^2 + |\widehat{A}_{\parallel}^R|^2 + |\widehat{A}_{\perp}^L|^2 + |\widehat{A}_{\perp}^R|^2 + |\widehat{A}_0^L|^2 + |\widehat{A}_0^R|^2 + \dots \quad (134)$$

where the ellipsis denote other partial-waves. The other moments can be obtained from Table 5 of Ref. [68] in a similar way. The experimental value integrated over the ranges in k^2 and q^2 can be obtained from Table 3 of the same reference using $\tilde{\Gamma}_i = \bar{\Gamma}_i \tilde{\Gamma}_1$.

One should be careful that Ref. [68] uses the same definition of the kinematics as in Ref. [73], whereas we follow a prescription for the angles in agreement with Ref. [69]: we have thus to

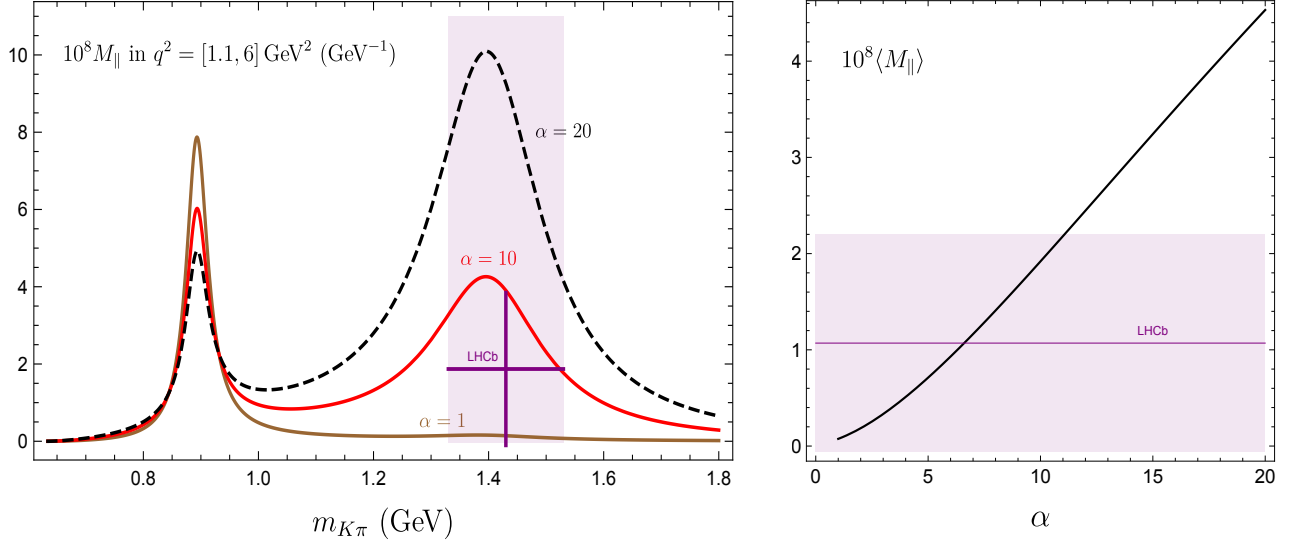


Figure 4: *Left: The moment $\langle M_{\parallel} \rangle$ differentially in $m_{K\pi}$ for three values of $\alpha = \{1, 10, 20\}$, compared to the LHCb measurement in the bin $m_{K\pi}^2 \in [1.33^2, 1.53^2]$ GeV 2 . For easy comparison, the LHCb binned measurement has been divided by the bin size. Right: The integrated moment $\langle M_{\parallel} \rangle$ as a function of α , compared to the LHCb measurement (horizontal band).*

perform the redefinition¹³

$$\theta_{\ell} \rightarrow \pi - \theta_{\ell}, \quad (135)$$

leading to a change of sign for Γ_i for i from 11 to 18 and 29 to 33 between our definition and the one used in Ref. [68].

We could try to compute the various moments Γ_i using our model for the $B \rightarrow K\pi$ form factors. Although possible, this is probably not the best use that can be made of the LHCb measurements. Indeed, by construction, our sum rules involve the $K\pi$ form factor, which yields a better sensitivity to the low-energy resonances (and most prominently to the $K^*(892)$ resonance). As discussed in Section 5.7 the sensitivity to the parameters of the excited K^* resonances is limited, which would lead to predictions for the moments Γ_i with large uncertainties. On the contrary, one can think of using the LHCb measurements to constrain the parameters describing the contributions of the higher resonances.

In order to perform this analysis, we have to isolate combinations of the moments that are only dependent on the P -wave contributions. Using Appendix A of Ref. [68], we find the

¹³As indicated in Ref. [72], the definitions in the LHCb analyses (see Ref. [74]) and the theoretical analyses (e.g. Ref. [69]) for the decay of $B \rightarrow K^*(\rightarrow K\pi)\mu\mu$ can be related by the changes $\theta_{\ell} \rightarrow \pi - \theta_{\ell}$ and $\phi \rightarrow -\phi$. However, the LHCb analysis at higher invariant $K\pi$ mass Ref. [68] uses a different convention for ϕ from the LHCb analysis of the $B \rightarrow K^*(\rightarrow K\pi)\mu\mu$ decay Ref. [74], which explains that we only have to change the definition of θ_{ℓ} here.

following combinations free from S and D -wave contributions

$$|\widehat{A}_{\parallel}^L|^2 + |\widehat{A}_{\parallel}^R|^2 = \frac{1}{36}(5\tilde{\Gamma}_1 - 7\sqrt{5}\tilde{\Gamma}_3 + 5\sqrt{5}\tilde{\Gamma}_6 - 35\tilde{\Gamma}_8 - 5\sqrt{15}\tilde{\Gamma}_{19} + 35\sqrt{3}\tilde{\Gamma}_{21}) , \quad (136)$$

$$|\widehat{A}_{\perp}^L|^2 + |\widehat{A}_{\perp}^R|^2 = \frac{1}{36}(5\tilde{\Gamma}_1 - 7\sqrt{5}\tilde{\Gamma}_3 + 5\sqrt{5}\tilde{\Gamma}_6 - 35\tilde{\Gamma}_8 + 5\sqrt{15}\tilde{\Gamma}_{19} - 35\sqrt{3}\tilde{\Gamma}_{21}) , \quad (137)$$

$$\text{Im}(\widehat{A}_{\perp}^L \widehat{A}_{\parallel}^{L*} + \widehat{A}_{\perp}^R \widehat{A}_{\parallel}^{R*}) = \frac{5}{36}(\sqrt{15}\tilde{\Gamma}_{24} - 7\sqrt{3}\tilde{\Gamma}_{26}) , \quad (138)$$

$$\text{Re}(\widehat{A}_{\perp}^L \widehat{A}_{\parallel}^{L*} - \widehat{A}_{\perp}^R \widehat{A}_{\parallel}^{R*}) = \frac{1}{36}(-5\sqrt{3}\tilde{\Gamma}_{29} + 7\sqrt{15}\tilde{\Gamma}_{31}) . \quad (139)$$

There is some ambiguity in the previous expressions due to the following degeneracies among the moments¹⁴:

$$\begin{aligned} 0 &= \tilde{\Gamma}_1 + \sqrt{5}\tilde{\Gamma}_3 + 3\tilde{\Gamma}_5 + \sqrt{5}\tilde{\Gamma}_6 + 5\tilde{\Gamma}_8 + 3\sqrt{5}\tilde{\Gamma}_{10} \\ &= \tilde{\Gamma}_{19} + \sqrt{5}\tilde{\Gamma}_{21} + 3\tilde{\Gamma}_{23} = \tilde{\Gamma}_{24} + \sqrt{5}\tilde{\Gamma}_{26} + 3\tilde{\Gamma}_{28} = \tilde{\Gamma}_{29} + \sqrt{5}\tilde{\Gamma}_{31} + 3\tilde{\Gamma}_{33} . \end{aligned} \quad (141)$$

Using the experimental values and correlations of the moments, we obtain from Eqs. (136–139):

$$\tau_B \langle |\widehat{A}_{\parallel}^L|^2 + |\widehat{A}_{\parallel}^R|^2 \rangle \equiv \langle M_{\parallel} \rangle = (1.07 \pm 1.13) \times 10^{-8} , \quad (142)$$

$$\tau_B \langle |\widehat{A}_{\perp}^L|^2 + |\widehat{A}_{\perp}^R|^2 \rangle \equiv \langle M_{\perp} \rangle = (0.94 \pm 1.06) \times 10^{-8} , \quad (143)$$

$$\tau_B \langle \text{Im}(\widehat{A}_{\perp}^L \widehat{A}_{\parallel}^{L*} + \widehat{A}_{\perp}^R \widehat{A}_{\parallel}^{R*}) \rangle \equiv \langle M_{\text{im}} \rangle = (-0.75 \pm 0.79) \times 10^{-8} , \quad (144)$$

$$\tau_B \langle \text{Re}(\widehat{A}_{\perp}^L \widehat{A}_{\parallel}^{L*} - \widehat{A}_{\perp}^R \widehat{A}_{\parallel}^{R*}) \rangle \equiv \langle M_{\text{re}} \rangle = (0.27 \pm 0.50) \times 10^{-8} , \quad (145)$$

where $\langle X \rangle$ denotes the integration with respect to q^2 and k^2 over the experimental ranges, and $\tau_B \simeq 2.3 \cdot 10^{12} \text{ GeV}^{-1}$ is the lifetime of the B meson.

As an illustration we show in Figure 4 the comparison between our predictions for the moment M_{\parallel} and the LHCb measurement in Eq. (142). From these measurements we obtain the following bounds on the parameter α :

$$\text{From } \langle M_{\parallel} \rangle : \quad \alpha \lesssim 11 , \quad (146)$$

$$\text{From } \langle M_{\perp} \rangle : \quad \alpha \lesssim 17 , \quad (147)$$

$$\text{From } \langle M_{\text{re}} \rangle : \quad \alpha \lesssim 18 , \quad (148)$$

¹⁴One has also the following degeneracies, of no use here:

$$0 = \tilde{\Gamma}_2 + \sqrt{\frac{7}{3}}\tilde{\Gamma}_4 + \sqrt{5}\tilde{\Gamma}_7 + \sqrt{\frac{35}{3}}\tilde{\Gamma}_9 = \tilde{\Gamma}_{20} + \sqrt{\frac{7}{3}}\tilde{\Gamma}_{22} = \tilde{\Gamma}_{25} + \sqrt{\frac{7}{3}}\tilde{\Gamma}_{27} = \tilde{\Gamma}_{30} + \sqrt{\frac{7}{3}}\tilde{\Gamma}_{32} \quad (140)$$

The current LHCb data [68] obeys all the degeneracy relations at 1.4σ or less (taking into account the experimental correlations).

by imposing that the corresponding observable is lower than the central value plus the uncertainty quoted in Eqs. (142)-(145). From the measurement of $\langle M_{\text{im}} \rangle$ we do not obtain any meaningful bound since within our phase ansatz the product $\langle (\widehat{A}_{\perp}^L \widehat{A}_{\parallel}^{L*} + \widehat{A}_{\perp}^R \widehat{A}_{\parallel}^{R*}) \rangle$ is real. For the non-local contributions \mathcal{H}_{\perp} and \mathcal{H}_{\parallel} in Eq. (119) we have used the leading-order OPE approximation¹⁵, where they are proportional to the form factors F_{\perp} and F_{\parallel} , by absorbing them into the “effective” Wilson coefficients C_9^{eff} and C_7^{eff} [77]. For the values of these Wilson Coefficients we have used their SM values (see e.g. Table 1 of Ref. [78]), as the bounds given here on α should be understood as ballpark estimates. But in more refined analyses one should correlate the determination of the high-mass moments with the analysis of $B \rightarrow K^* \ell \ell$.

We can also use the branching ratio in Eq. (134) directly to obtain an upper bound on the P -wave contribution, since the contributions from the other partial waves are necessarily positive. LHCb has measured this branching ratio within the considered k^2 bin and in several bins of q^2 , and resulting in the following upper bounds on the parameter α :

$$10^8 \cdot \langle \mathcal{B} \rangle_{[0.10, 0.98]} = 1.41 \pm 0.27 \rightarrow \alpha \lesssim 5, \quad (149)$$

$$10^8 \cdot \langle \mathcal{B} \rangle_{[1.10, 2.50]} = 1.60 \pm 0.29 \rightarrow \alpha \lesssim 6, \quad (150)$$

$$10^8 \cdot \langle \mathcal{B} \rangle_{[2.50, 4.00]} = 1.37 \pm 0.26 \rightarrow \alpha \lesssim 5, \quad (151)$$

$$10^8 \cdot \langle \mathcal{B} \rangle_{[4.00, 6.00]} = 1.12 \pm 0.26 \rightarrow \alpha \lesssim 4, \quad (152)$$

$$10^8 \cdot \langle \mathcal{B} \rangle_{[6.00, 8.00]} = 0.98 \pm 0.23 \rightarrow \alpha \lesssim 3. \quad (153)$$

which are obtained as described above, and turn out to be somewhat stronger than the bounds from the angular moments. Again, the SM has been assumed here.

The ballpark bounds obtained here, while still rather loose, already constrain the very large values for the $B \rightarrow K^*(1410)$ form factors that would affect significantly the LCSR predictions for the $B \rightarrow K^*$ form factors. In particular, for $\alpha \lesssim 3$ the reduction of the $B \rightarrow K^*$ form factors is at most of order $\sim 10\%$. This simple analysis presented here should be refined in future studies, which together with more precise experimental measurements of the moments will provide more solid and stringent constraints on both the $B \rightarrow K^*(1410)$ and the $B \rightarrow K^*$ form factors. Moreover, further generalization of the sum rules to the S -wave $K\pi$ system [35] will make it possible to include other combination of moments beyond those considered here, and depending on the S -wave amplitudes.

7 Conclusions and Perspectives

Accurate theoretical predictions for exclusive B -meson decay observables are of utmost importance for studies of the the Standard Model and New Physics, but require a careful assessment

¹⁵The OPE coefficients at dimension three are known to NLO [75, 76].

of the theoretical inputs used. LCSRs are particularly prominent tools to compute the form factors involved. In this article, we focused on the determination of $B \rightarrow K^*$ form factors from LCSRs with B -meson LCDAs. We extended the framework to consider $B \rightarrow K\pi$ form factors for the $K\pi$ P wave, which include effects such as the non-resonant $K\pi$ production and the width of the K^* meson. We analysed all vector, axial and tensor form factors needed for the phenomenological analysis of $B \rightarrow K\pi\ell\ell$ in the P wave in the Standard Model.

We first derived light-cone sum rules with B -meson LCDAs for these form factors, generalising the results of Ref. [23] for the case of two pseudoscalar mesons of different masses in the final state. These sum rules provide relationships between the convolution of the $K\pi$ vector form factor and a $B \rightarrow K\pi$ form factor on one side, and the OPE of a well-chosen correlation function expressed in terms of B -meson LCDAs on the other side. On the OPE side of the sum rules, we computed higher-twist two- and three-particle contributions (see also Ref. [15]), and we proceeded to a new, well motivated, determination of the threshold parameter s_0 , somewhat lower than earlier determinations. On the hadronic side, we introduced a resonance model for the $B \rightarrow K\pi$ including the $K^*(980)$ and the $K^*(1410)$, so that our sum rules can be used to constrain the parameters describing the two contributions. This resonance model is related to the model used by the Belle collaboration to determine the $K\pi$ vector form factor from the $\tau \rightarrow K\pi\nu$ differential decay rate, and which describes the spectrum very well.

We then exploited our set-up phenomenologically with the following results:

- We considered the narrow-width limit of our LCSRs to check that we recover the known $B \rightarrow K^*$ sum rules, and to assess the correction due to the finite width of the K^* meson. We find that this correction is universal for all form factors and amounts to a multiplicative factor $\mathcal{W}_K^* \simeq 1.1$, corresponding to a 20% enhancement of the decay rate. This result does not depend strongly on the details of our model and it should be taken into account when computing observables with $B \rightarrow K^*$ form factors obtained from LCSRs derived in the narrow-width limit.
- Comparing with earlier determinations, we find that our results for the form factors in the narrow width-limit are consistent but with lower central values. Several competing effects compensate each other (choice of the B -meson decay constant, the $K^*(980)$ coupling constant, the threshold parameters s_0) so that the difference can be mainly attributed to the contribution from the twist-four two-particle contribution $g_+(\omega)$.
- We then considered the impact of an additional $K^*(1410)$ contribution to our model. This contribution is small in the case of the $K\pi$ vector form factor, but in principle it could be large for the $B \rightarrow K\pi$ case. Our sum rules provide a combined constraint on the $K^*(980)$ and $K^*(1410)$ coupling constants describing the height of the two resonances in the $B \rightarrow K\pi$ form factors (with a much smaller weight for $K^*(1410)$). An increased

$K^*(1410)$ contribution would correspond to a smaller $K^*(980)$ contribution, and thus a lower value for $B \rightarrow K^*$ form factors.

- We turned to the $B \rightarrow K\pi\mu\mu$ differential decay rate in the $K^*(1410)$ region, which has been measured recently by the LHCb collaboration. The branching ratio and the angular decay distribution in this $K\pi$ window provide bounds on the contribution of the $K^*(1410)$. If a huge contribution is ruled out, the current data leave room for a $K^*(1410)$ contribution of moderate size, which could lead to a decrease of the $K^*(890)$ contribution (and thus the values of the $B \rightarrow K^*$ form factors) of around 10%.

Considering the more general $B \rightarrow K\pi$ form factors and constraining them using LCSRs with B -meson LCDAs, we have identified three effects of rather different nature that affect the determination of the $B \rightarrow K^*$ form factors: a universal effect related to the finite-width of the K^* increasing by 1.1 the value compared to the narrow-width limit, an effect related to the inclusion of the two-particle twist-four B -meson LCDAs leading to smaller values in our case compared to earlier calculations, and an effect of the $K^*(1410)$ contribution that could decrease the $K^*(980)$ peak up to 10% according to the data currently available. All three effects have a direct impact on the prediction of the $B \rightarrow K^*\mu\mu$ branching ratio and thus on the importance of the current discrepancy between SM expectations and LHCb measurements of $b \rightarrow s\mu\mu$ branching ratios. Let us add that $B \rightarrow K^*\mu\mu$ angular observables (such as P_5') are less affected by this discussion as they are insensitive to the overall normalisation of the form factors.

One may wonder whether previous determinations or other approaches are sensitive to these issues. Previous light-cone sum rule determinations using the B -meson LCDAs have worked under the assumption of the narrow-width limit, so that any correction related to a finite width is missed. The $K^*(1410)$ contribution is included through quark-hadron duality in the choice of the threshold parameter, but this contribution is obviously hard to disentangle from the continuum contribution and it suffers from significant uncertainties (suppressed after Borel transformation). A huge contribution from the $K^*(1410)$ would require a significant failure of the quark-hadron duality, but the moderate contribution discussed here could be included in uncertainties associated with the continuum contribution.

Other LCSRs exploit different correlation functions, so that the OPE contribution is expressed in terms of light-meson LCDAs (either K^* or $K\pi$). They have the advantage of providing an expression of the form factors directly in terms of the OPE part, and not through a convolution with the $K\pi$ form factor as in our case (which required us to design a resonance model for the $B \rightarrow K\pi$ form factors). However, this simplicity prevents these sum rules from providing corrections to the narrow-width limit (the LCSRs with a vector resonance are not smooth limits of the LCSRs of the dimeson DAs). The size of the contribution of the $K^*(1410)$ is in principle partially encoded in the dimeson LCDAs, which are however poorly known, whereas the K^* LCDAs are essentially unable to probe this question.

Finally, lattice QCD simulations investigate a different kinematic range for the transfer momentum. The first results on $B \rightarrow K^*$ form factors [17] include configurations where the K^* meson may decay into $K\pi$, but there was not enough data to investigate the impact of finite-width effects in this kinematic regime. This could in principle be studied more extensively using a lattice set-up dedicated to the analysis of unstable resonances [79]. Concerning the $K^*(1410)$ contribution to the $B \rightarrow K\pi$ form factors, a huge effect would require an usually large q^2 -dependence of the form factors to bridge the LCSR and the lattice results and it could have led to difficulties in extracting the $K^*(980)$ signal from lattice data under a very large background of excited states, but the moderate contribution discussed here does not seem to contradict the current results from lattice QCD on these form factors.

Our study of $B \rightarrow K\pi$ form factors through an extension of well-known sum rules has highlighted several effects that may impact the current determination of the form factors used to analyse $B \rightarrow K^*\ell\ell$ and other decays of the form $B \rightarrow K^*X$. Several improvements would help assessing these effects more precisely. The models for the B -meson LCDAs should be investigated and constrained more tightly to assess the role played by higher-twist contributions. The LCSRs could be exploited with additional models for the $K\pi$ and $B \rightarrow K\pi$ form factors to consolidate our results. Finally, the differential decay rate for $B \rightarrow K\pi\mu\mu$ at high $K\pi$ invariant mass could be measured more precisely to provide tighter constraints on the $K^*(1410)$ contributions. This would also require a better knowledge of the other partial waves that are contributing in this invariant mass window. If the D wave seems small [68], the S wave interferes significantly with the P wave analysed here. The relevant $B \rightarrow K\pi$ form factors could be investigated with similar LCSRs to the ones considered here [35]. This should lead to a consistent picture of the contributions from higher resonances to the $B \rightarrow K\pi\ell\ell$ decay, and to a deeper understanding of the anomalies currently observed in $b \rightarrow s\ell\ell$ transitions.

Acknowledgments

We thank Marcin Chrzaszcz, Nico Gubernari, Pablo Roig, Danny van Dyk, Keri Vos and Yuming Wang for useful discussions. This work is supported by the DFG Research Unit FOR 1873 “Quark Flavour Physics and Effective Theories”, contract No KH 205/2-2. This project has received funding from the European Unions Horizon 2020 research and innovation programme under the Marie Skłodowska-Curie grant agreements No 690575 and No 674896. J.V. acknowledges funding from the European Union’s Horizon 2020 research and innovation programme under the Marie Skłodowska-Curie grant agreement No 700525 ‘NIOBE’, and support from SEJI/2018/033 (Generalitat Valenciana).

A Light-Cone Sum Rules for $B \rightarrow V$ Form Factors

Here we rederive the LCSR for the $B \rightarrow V$ form factors, assuming that the vector V is stable in QCD and leads to a pole in the correlation functions. The original derivation of these LCSRs was given in Ref. [12], but the sum rules for $T_{2,3}$ were not explicitly given there.

The $B \rightarrow V$ form factors are defined here as¹⁶:

$$i \langle V(k, \varepsilon) | \bar{s} \gamma^\mu (1 - \gamma_5) b | \bar{B}(p) \rangle = i \epsilon^{\mu\nu\alpha\beta} \varepsilon_\nu^* q_\alpha k_\beta \frac{2V^{BV}(q^2)}{m_B + m_V} + 2m_V \frac{\varepsilon^* \cdot q}{q^2} q^\mu A_0^{BV}(q^2) \quad (\text{A.1})$$

$$+ (m_B + m_V) A_1^{BV}(q^2) \left[\varepsilon^{*\mu} - \frac{\varepsilon^* \cdot q}{q^2} q^\mu \right] - \frac{\varepsilon^* \cdot q}{m_B + m_V} A_2^{BV}(q^2) \left[(p+k)^\mu - \frac{m_B^2 - m_V^2}{q^2} q^\mu \right],$$

$$i \langle V(k, \varepsilon) | \bar{s} \sigma^{\mu\nu} q_\nu (1 + \gamma_5) b | \bar{B}(p) \rangle = -2\epsilon^{\mu\nu\alpha\beta} \varepsilon_\nu^* q_\alpha k_\beta T_1^{BV}(q^2) \quad (\text{A.2})$$

$$+ i T_2^{BV}(q^2) \left[(m_B^2 - m_V^2) \varepsilon^{*\mu} - (\varepsilon^* \cdot q) (p+k)^\mu \right] + i (\varepsilon^* \cdot q) T_3^{BV}(q^2) \left[q^\mu - \frac{q^2 (p+k)^\mu}{m_B^2 - m_V^2} \right].$$

We start from the correlation functions in Eqs (18), (25) and (28), but in calculating the imaginary part of the invariant amplitudes through the unitarity relation we include the single-particle states $\sum_\lambda |V_\lambda\rangle \langle V_\lambda|$ (with λ the polarization of the vector particle) instead of the two-particle states $|K\pi\rangle \langle K\pi|$. Using the same invariant functions and conventions for the OPE functions as for the $B \rightarrow K\pi$ form factors, we find:

$$V^{BV}(q^2) = \mathcal{F}_{V,\perp}(q^2) = \frac{m_B + m_V}{2f_V m_V} e^{m_V^2/M^2} \cdot \mathcal{P}_\perp^{\text{OPE}}(q^2, \sigma_0, M^2), \quad (\text{A.3})$$

$$A_1^{BV}(q^2) = \mathcal{F}_{V,\parallel}(q^2) = \frac{1}{f_V m_V (m_B + m_V)} e^{m_V^2/M^2} \cdot \mathcal{P}_\parallel^{\text{OPE}}(q^2, \sigma_0, M^2), \quad (\text{A.4})$$

$$A_2^{BV}(q^2) = \mathcal{F}_{V,-}(q^2) = -\frac{m_B + m_V}{2f_V m_V} e^{m_V^2/M^2} \cdot \mathcal{P}_-^{\text{OPE}}(q^2, \sigma_0, M^2), \quad (\text{A.5})$$

$$A_0^{BV}(q^2) = \mathcal{F}_{V,t}(q^2) = -\frac{1}{2f_V m_V^2} e^{m_V^2/M^2} \cdot \mathcal{P}_t^{\text{OPE}}(q^2, \sigma_0, M^2), \quad (\text{A.6})$$

$$T_1^{BV}(q^2) = \mathcal{F}_{V,\perp}^T(q^2) = \frac{1}{2f_V m_V} e^{m_V^2/M^2} \cdot \mathcal{P}_\perp^{T,\text{OPE}}(q^2, \sigma_0, M^2), \quad (\text{A.7})$$

$$T_2^{BV}(q^2) = \mathcal{F}_{V,\parallel}^T(q^2) = \frac{1}{f_V m_V (m_B^2 - m_V^2)} e^{m_V^2/M^2} \cdot \mathcal{P}_\parallel^{T,\text{OPE}}(q^2, \sigma_0, M^2), \quad (\text{A.8})$$

$$T_3^{BV}(q^2) = \mathcal{F}_{V,-}^T(q^2) = -\frac{1}{2f_V m_V} e^{m_V^2/M^2} \cdot \mathcal{P}_-^{T,\text{OPE}}(q^2, \sigma_0, M^2), \quad (\text{A.9})$$

where the functions $\mathcal{P}_i^{T,\text{OPE}}$ are the same as the ones for the $B \rightarrow K\pi$ sum rules, and are given in Appendix D.

¹⁶ This definition agrees with Refs. [12, 19] but differs by a factor of i with respect to Ref. [80]: $F_{[80]} = iF_{[19]}$. The reason for this factor of i is that we want to define the phase of the $B \rightarrow K\pi$ form factors such that it is real below threshold, it reaches $\pi/2$ on the vector resonance and π once the resonance is left behind.

B B -meson distribution amplitudes up to twist 4

B.1 Definition of B -meson distribution amplitudes

We consider the two- and three-particle B -meson light-cone distribution amplitudes (LCDAs) up to twist four as recently discussed in Ref. [24]¹⁷.

B.1.1 Two-particle LCDAs

The two-particle LCDAs up to twist-four are given by [24]:

$$\begin{aligned} \mathcal{D}_\Gamma^{(2)}(x) \equiv \langle 0 | \bar{q}(x) \Gamma h_v(0) | \bar{B}(v) \rangle &= -\frac{if_B m_B}{2} \text{Tr} \left[\gamma_5 \Gamma P_+ \right] \int_0^\infty d\omega e^{-i\omega v \cdot x} \left\{ \phi_+(\omega) + x^2 g_+(\omega) \right\} \\ &+ \frac{if_B m_B}{4} \text{Tr} \left[\gamma_5 \Gamma P_+ \not{x} \right] \frac{1}{v \cdot x} \int_0^\infty d\omega e^{-i\omega v \cdot x} \left\{ [\phi_+ - \phi_-](\omega) + x^2 [g_+ - g_-](\omega) \right\} + \mathcal{O}(x^4) \end{aligned} \quad (\text{B.1})$$

for an arbitrary Dirac matrix Γ . Here $P_+ \equiv (1 + \not{v})/2$ and we have omitted the collinear Wilson line $W(0, x)$ that makes the matrix element gauge invariant. The functions $\phi_+(\omega)$, $\phi_-(\omega)$, $g_+(\omega)$ and $g_-(\omega)$ are respectively twist-two, three, four and five LCDAs. We will therefore neglect $g_-(\omega)$. We use the same normalization conventions for the LCDAs as in Ref. [12] (see also [80]), with the B -meson decay constant f_B defined in full QCD and with the relativistic normalization of the state $|B(v)\rangle$. These conventions differ from the ones used in Ref. [24], where the LCDAs are normalized to the scale-dependent decay constant F_B defined in the Heavy Quark Effective Theory (HQET) and the HQET normalization for the $|B(v)\rangle$ state is adopted. This explains an extra factor m_B in Eq. (B.1) as compared to the definition in [24]. Since we will not include gluon radiative corrections in the correlation function, the difference between F_B and f_B – which starts at $\mathcal{O}(\alpha_s)$ – remains within the considered accuracy.

We write Eq. (B.1) as:

$$\mathcal{D}_\Gamma^{(2)}(x) = -\frac{i}{2} f_B m_B \text{Tr} \left[\gamma_5 \Gamma P_+ \right] \mathcal{A}(x) + \frac{i}{4} f_B m_B \text{Tr} \left[\gamma_5 \Gamma P_+ \not{x} \right] \mathcal{B}(x) \quad (\text{B.2})$$

where:

$$\mathcal{A}(x) = \int_0^\infty d\omega e^{-i\omega v \cdot x} \left\{ \phi_+(\omega) + x^2 g_+(\omega) \right\}, \quad (\text{B.3})$$

$$\mathcal{B}(x) = \int_0^\infty d\omega e^{-i\omega v \cdot x} \left\{ i\bar{\Phi}_\pm(\omega) + x^2 i\bar{G}_\pm(\omega) \right\}, \quad (\text{B.4})$$

$$\bar{\Phi}_\pm(\omega) = \int_0^\omega d\tau (\phi_+(\tau) - \phi_-(\tau)), \quad \bar{G}_\pm(\omega) = \int_0^\omega d\tau g_+(\tau). \quad (\text{B.5})$$

¹⁷ For earlier articles discussing B -meson LCDAs, see [12, 80–89].

The functions $\bar{\Phi}_\pm(\omega)$, $\bar{G}_\pm(\omega)$ satisfy the normalization condition $\bar{\Phi}_\pm(\infty) = \bar{G}_\pm(\infty) = 0$, in order for $\mathcal{D}_\Gamma^{(2)}(x)$ to be well-defined as $v \cdot x \rightarrow 0$. The appearance of these functions in $\mathcal{B}(x)$ follows from integration by parts:

$$0 = \int_0^\infty d\omega \frac{d}{d\omega} (e^{-i\omega v \cdot x} F_\pm(\omega)) = \int_0^\infty d\omega e^{-i\omega v \cdot x} \left[(-iv \cdot x) F_\pm(\omega) + f_\pm(\omega) \right] \quad (\text{B.6})$$

where $\{f_\pm, F_\pm\}$ denote $\{\phi_+ - \phi_-, \bar{\Phi}_\pm\}$ or $\{g_+, \bar{G}_\pm\}$ and the first equality follows from the aforementioned normalization conditions $F_\pm(\infty) = 0$. This implies that under the integral one may perform the substitution

$$\frac{f_\pm(\omega)}{v \cdot x} \rightarrow iF_\pm(\omega) , \quad (\text{B.7})$$

which is what we have done in Eq. (B.4).

B.1.2 Three-particle LCDAs

The three-particle quark-gluon LCDAs up to twist four are given by [24]:

$$\begin{aligned} \mathcal{D}_\Gamma^{(3)}(x, u) &\equiv \langle 0 | \bar{q}(x) G_{\mu\nu}(ux) \Gamma^{\mu\nu} h_v(0) | \bar{B}(v) \rangle = \frac{f_B m_B}{2} \int_0^\infty d\omega_1 d\omega_2 e^{-i(\omega_1 + u\omega_2)v \cdot x} \\ &\text{Tr} \left\{ \gamma_5 \Gamma^{\mu\nu} P_+ \left[(v_\mu \gamma_\nu - v_\nu \gamma_\mu) \phi_3 + \frac{i}{2} \sigma_{\mu\nu} [\phi_3 - \phi_4] + \frac{x_\mu v_\nu - x_\nu v_\mu}{2v \cdot x} [\phi_3 + \phi_4 - 2\psi_4] \right. \right. \\ &\quad - \frac{x_\mu \gamma_\nu - x_\nu \gamma_\mu}{2v \cdot x} [\phi_3 + \tilde{\psi}_4] + \frac{i\epsilon_{\mu\nu\alpha\beta} x^\alpha v^\beta}{2v \cdot x} \gamma_5 [\phi_3 - \phi_4 + 2\tilde{\psi}_4] - \frac{i\epsilon_{\mu\nu\alpha\beta} x^\alpha}{2v \cdot x} \gamma^\beta \gamma_5 [\phi_3 - \phi_4 + \tilde{\psi}_4] \\ &\quad \left. \left. - \frac{(x_\mu v_\nu - x_\nu v_\mu) \not{x}}{2(v \cdot x)^2} [\phi_4 - \psi_4 - \tilde{\psi}_4] - \frac{(x_\mu \gamma_\nu - x_\nu \gamma_\mu) \not{x}}{4(v \cdot x)^2} [\phi_3 - \phi_4 + 2\tilde{\psi}_4] \right] \right\} (\omega_1, \omega_2) , \quad (\text{B.8}) \end{aligned}$$

where the functional dependence $\phi_3 = \phi_3(\omega_1, \omega_2)$, etc., is indicated outside the curly bracket. Again, $\Gamma^{\mu\nu}$ denotes an arbitrary Dirac matrix and Wilson lines have been suppressed. This form of the matrix element has been obtained from the one in [24] by defining $x_\mu = z_1 n_\mu$ and $u = z_2/z_1$. In analogy to Eq. (B.5) we define [12]

$$\bar{\Phi}(\omega_1, \omega_2) = \int_0^{\omega_1} d\tau \Phi(\tau, \omega_2) , \quad \bar{\bar{\Phi}}(\omega_1, \omega_2) = \int_0^{\omega_1} d\tau \bar{\Phi}(\tau, \omega_2) , \quad (\text{B.9})$$

for $\Phi = \{\phi_3, \phi_4, \psi_4, \tilde{\psi}_4\}$. This allows us to make the substitutions such as Eq. (B.7) in Eq. (B.8) and get rid of the $v \cdot x$ denominators. In the last two terms one needs to do this twice (thus appearing ‘double-barred’ LCDAs), but the final results for the correlation functions will only contain ‘single-barred’ LCDAs. In addition we define the variable

$$\sigma(u) \equiv (\omega_1 + u\omega_2)/m_B \quad (\text{B.10})$$

such that

$$\mathcal{D}_\Gamma^{(3)}(x, u) = \frac{f_B m_B}{2} \int_0^\infty d\omega_1 d\omega_2 e^{-i\sigma m_B v \cdot x} \text{Tr} \left[\gamma_5 \Gamma^{\mu\nu} P_+ \Psi_{\mu\nu}(x, \omega_1, \omega_2) \right], \quad (\text{B.11})$$

with

$$\begin{aligned} \Psi_{\mu\nu}(x, \omega_1, \omega_2) = & \left[(v_\mu \gamma_\nu - v_\nu \gamma_\mu) \phi_3 + \frac{i}{2} \sigma_{\mu\nu} [\phi_3 - \phi_4] + \frac{i}{2} (x_\mu v_\nu - x_\nu v_\mu) [\bar{\phi}_3 + \bar{\phi}_4 - 2\bar{\psi}_4] \right. \\ & - \frac{i}{2} (x_\mu \gamma_\nu - x_\nu \gamma_\mu) [\bar{\phi}_3 + \bar{\psi}_4] - \frac{1}{2} \epsilon_{\mu\nu\alpha\beta} x^\alpha v^\beta \gamma_5 [\bar{\phi}_3 - \bar{\phi}_4 + 2\bar{\psi}_4] + \frac{1}{2} \epsilon_{\mu\nu\alpha\beta} x^\alpha \gamma^\beta \gamma_5 [\bar{\phi}_3 - \bar{\phi}_4 + \bar{\psi}_4] \\ & \left. + \frac{1}{2} (x_\mu v_\nu - x_\nu v_\mu) \not{x} [\bar{\phi}_4 - \bar{\psi}_4 - \bar{\bar{\psi}}_4] + \frac{1}{4} (x_\mu \gamma_\nu - x_\nu \gamma_\mu) \not{x} [\bar{\phi}_3 - \bar{\phi}_4 + 2\bar{\bar{\psi}}_4] \right] (\omega_1, \omega_2). \quad (\text{B.12}) \end{aligned}$$

B.2 Models and numerics for LCDAs

We will use the three models for the two- and three-particle B -meson LCDAs considered in Ref. [24], called **Model I**, **Model IIA** and **Model IIB** in that reference, and we keep these names. All models are characterized by two input parameters: λ_B and R . Our numerical values for these two parameters are collected in Table 2, and will be justified at the end of this section.

Model I : The first model is based on the exponential model of Refs. [12, 81]:

$$\phi_+^{\mathbf{I}}(\omega) = \frac{\omega}{\lambda_B^2} e^{-\omega/\lambda_B} \quad (\text{B.13})$$

$$\phi_-^{\mathbf{I}}(\omega) = \frac{1}{\lambda_B} e^{-\omega/\lambda_B} + \frac{1}{2\lambda_B} \left[1 - \frac{2\omega}{\lambda_B} + \frac{\omega^2}{2\lambda_B^2} \right] \frac{1-R}{1+2R} e^{-\omega/\lambda_B} \quad (\text{B.14})$$

$$g_+^{\mathbf{I}}(\omega) = \frac{3\omega^2}{16\lambda_B} \frac{3+4R}{1+2R} e^{-\omega/\lambda_B} \quad (\text{B.15})$$

$$\phi_3^{\mathbf{I}}(\omega_1, \omega_2) = -\frac{3\omega_1\omega_2^2}{4\lambda_B^3} \frac{1-R}{1+2R} e^{-\bar{\omega}/\lambda_B} \quad (\text{B.16})$$

$$\phi_4^{\mathbf{I}}(\omega_1, \omega_2) = \frac{3\omega_2^2}{4\lambda_B^2} \frac{1+R}{1+2R} e^{-\bar{\omega}/\lambda_B} \quad (\text{B.17})$$

$$\psi_4^{\mathbf{I}}(\omega_1, \omega_2) = R \tilde{\psi}_4^{\mathbf{I}}(\omega_1, \omega_2) = \frac{3\omega_1\omega_2}{2\lambda_B^2} \frac{R}{1+2R} e^{-\bar{\omega}/\lambda_B}, \quad (\text{B.18})$$

where $\bar{\omega} \equiv \omega_1 + \omega_2$.

Model IIA : The second model is based on the ‘local duality’ assumption [24] with linear

behaviour $\sim (3\lambda_B - \omega)$ for all LCDAs (and constant for ϕ_3):

$$\phi_+^{\text{IIA}}(\omega) = \frac{2\omega}{9\lambda_B^3} (3\lambda_B - \omega) \theta(3\lambda_B - \omega) \quad (\text{B.19})$$

$$\phi_-^{\text{IIA}}(\omega) = \left[\frac{(3\lambda_B - \omega)^2}{9\lambda_B^3} + \frac{2\omega^2 - 6\omega\lambda_B + 3\lambda_B^2}{24\lambda_B^3} \frac{1 - R}{1 + 2R} \right] \theta(3\lambda_B - \omega) \quad (\text{B.20})$$

$$g_+^{\text{IIA}}(\omega) = \frac{\omega^2(3\lambda_B - \omega)^2}{192\lambda_B^3} \frac{7 + 12R}{1 + 2R} \theta(3\lambda_B - \omega) \quad (\text{B.21})$$

$$\phi_3^{\text{IIA}}(\omega_1, \omega_2) = -\frac{\omega_1\omega_2^2}{24\lambda_B^3} \frac{1 - R}{1 + 2R} \theta(3\lambda_B - \bar{\omega}) \quad (\text{B.22})$$

$$\phi_4^{\text{IIA}}(\omega_1, \omega_2) = \frac{\omega_2^2(3\lambda_B - \bar{\omega})}{24\lambda_B^3} \frac{1 + R}{1 + 2R} \theta(3\lambda_B - \bar{\omega}) \quad (\text{B.23})$$

$$\psi_4^{\text{IIA}}(\omega_1, \omega_2) = R \tilde{\psi}_4^{\text{IIA}}(\omega_1, \omega_2) = \frac{\omega_1\omega_2(3\lambda_B - \bar{\omega})}{12\lambda_B^3} \frac{R}{1 + 2R} \theta(3\lambda_B - \bar{\omega}) . \quad (\text{B.24})$$

Model IIB : The third model is the same type as IIA, but with cubic behaviour $\sim (5\lambda_B - \omega)^3$ for all LCDAs (and quadratic for ϕ_3):

$$\phi_+^{\text{IIB}}(\omega) = \frac{4\omega}{625\lambda_B^5} (5\lambda_B - \omega)^3 \theta(5\lambda_B - \omega) \quad (\text{B.25})$$

$$\phi_-^{\text{IIB}}(\omega) = \frac{(5\lambda_B - \omega)^4}{125\lambda_B^5} \left[\frac{1}{5} + \frac{3\omega^2 - 10\omega\lambda_B + 5\lambda_B^2}{4(5\lambda_B - \omega)^2} \frac{1 - R}{1 + 2R} \right] \theta(5\lambda_B - \omega) \quad (\text{B.26})$$

$$g_+^{\text{IIB}}(\omega) = \frac{\omega^2(5\lambda_B - \omega)^4}{20000\lambda_B^5} \frac{13 + 20R}{1 + 2R} \theta(5\lambda_B - \omega) \quad (\text{B.27})$$

$$\phi_3^{\text{IIB}}(\omega_1, \omega_2) = -\frac{9\omega_1\omega_2^2}{1250\lambda_B^5} \frac{(5\lambda_B - \bar{\omega})^2}{1 + 2R} \theta(5\lambda_B - \bar{\omega}) \quad (\text{B.28})$$

$$\phi_4^{\text{IIB}}(\omega_1, \omega_2) = \frac{3\omega_2^2(5\lambda_B - \bar{\omega})^3}{1250\lambda_B^5} \frac{1 + R}{1 + 2R} \theta(5\lambda_B - \bar{\omega}) \quad (\text{B.29})$$

$$\psi_4^{\text{IIB}}(\omega_1, \omega_2) = R \tilde{\psi}_4^{\text{IIB}}(\omega_1, \omega_2) = \frac{3\omega_1\omega_2(5\lambda_B - \bar{\omega})^3}{625\lambda_B^5} \frac{R}{1 + 2R} \theta(5\lambda_B - \bar{\omega}) . \quad (\text{B.30})$$

All these expressions for the LCDAs up to twist-four in the three models have been obtained from the expressions in Ref. [24] by enforcing the Equation-Of-Motion (EOM) constraints derived in that article. The expressions given here for $g_+(\omega)$ correspond to the simplified expressions in Ref. [24]. We have checked that they reproduce numerically the full expressions in [24] for a very wide range of parameters with a very high precision.

We now discuss briefly the numerical values chosen here for the two input parameters λ_B and R on which the models depend. These values are also collected for reference in Table 2.

For λ_B we follow [19] and take:

$$\lambda_B = \lambda_B(1 \text{ GeV}) = 460 \pm 110 \text{ MeV}, \quad (\text{B.31})$$

which is the value derived from the QCD sum rules in Ref. [45]. This value is consistent with the experimental bound obtained in Ref. [46] and with the determination from the $B \rightarrow \pi$ form factor LCSRs [13].

The parameter R is defined as the ratio $R = \lambda_E^2/\lambda_H^2$, where $\lambda_{E,H}^2$ parametrize the local correlation function $\mathcal{D}_\Gamma^{(3)}(0,0)$ (see Eq. (B.8)), for example $\lambda_E^2 = 3 \int d\omega_1 d\omega_2 \psi_4(\omega_1, \omega_2)$ and $\lambda_H^2 = 3 \int d\omega_1 d\omega_2 \tilde{\psi}_4(\omega_1, \omega_2)$. Ref. [24] considers the following two determinations of the local matrix element from QCD sum rules:

$$\lambda_E^2 = 110 \pm 60 \text{ MeV}^2, \quad \lambda_H^2 = 180 \pm 70 \text{ MeV}^2, \quad [81] \quad (\text{B.32})$$

$$\lambda_E^2 = 30 \pm 20 \text{ MeV}^2, \quad \lambda_H^2 = 60 \pm 30 \text{ MeV}^2. \quad [90]$$

These results are only marginally compatible with each other, and in addition when combined with the EOM they lead to values of λ_B significantly lower than Eq. (B.31). However, as pointed out in Ref. [24], the ratio R is expected to be more reliable: indeed both determinations are consistent with each other with $R \sim 0.5$. Here we average both determinations:

$$R = 0.4_{-0.3}^{+0.5}. \quad (\text{B.33})$$

This number is obtained in the following way. We assume the errors in Eq. (B.32) are Gaussian and uncorrelated. We generate a large and equal number of normally distributed pairs $\{\lambda_E^2, \lambda_H^2\}$ for each of the two determinations, and calculate the ratio R for each pair. This leads to a set of values of R that are not normally distributed but have a tail to the positive side. From this distribution we take the central value as the most probable one (the maximum of the distribution), and for the “ 1σ ” region we take the most probable region containing the 68% of the probability. This error bar has to be regarded as a conservative estimate, given the fact that the errors in Eq. (B.32) are certainly correlated. A reevaluation of the QCD sum rules leading to Eq. (B.32) should be performed, with a simultaneous determination of the ratio R taking into account such correlations.

In Figure 5 we show plots for the different LCDAs in the different models.

C Calculation of Correlation Functions

We need to calculate the correlation functions:

$$\mathcal{P}_{ab}(k, q) = i \int d^4x e^{ik \cdot x} \langle 0 | T \{ \bar{d}(x) \Gamma_a s(x), \bar{s}(0) \Gamma_b b(0) \} | \bar{B}^0(q+k) \rangle \quad (\text{C.1})$$

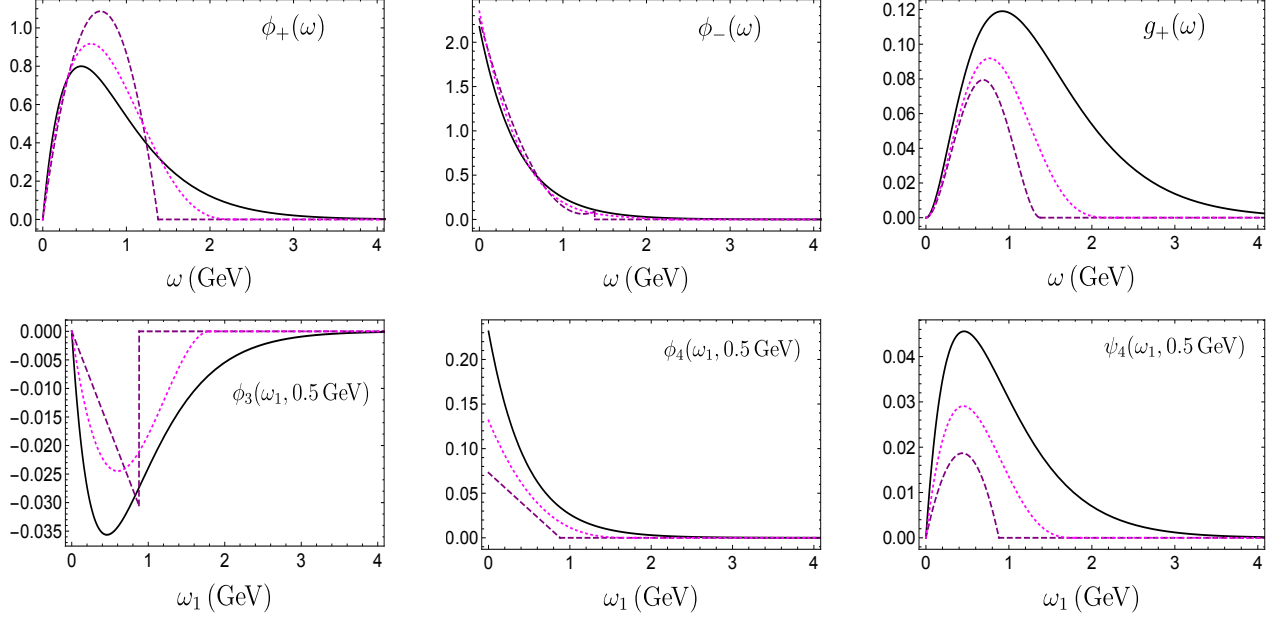


Figure 5: *Two- and three-particle LCDAs within the three different models considered: Model I (solid), Model IIA (dashed) and Model IIIA (dotted). These plots are obtained fixing λ_B and R to their central values, and $\omega_2 = 0.5$ GeV.*

with generic Dirac structures $\Gamma_{a,b}$. Contracting the s fields, we write:

$$\mathcal{P}_{ab}(k, q) = i \int d^4x e^{ik \cdot x} \langle 0 | \bar{d}(x) \Gamma_a \hat{S}(x) \Gamma_b b(0) | \bar{B}^0(q+k) \rangle \quad (\text{C.2})$$

where $\hat{S}(x) = \hat{S}^{(2)}(x) + \hat{S}^{(3)}(x) + \dots$ is the light-cone expansion of the quark propagator, with [91]

$$\hat{S}^{(2)}(x) = \int \frac{d^4p}{(2\pi)^4} e^{-ip \cdot x} \frac{i(\not{p} + m_s)}{p^2 - m_s^2}, \quad (\text{C.3})$$

$$\hat{S}^{(3)}(x) = -i \int_0^1 du G_{\alpha\beta}(ux) \int \frac{d^4p}{(2\pi)^4} e^{-ip \cdot x} \frac{[\bar{u}(\not{p} + m_s)\sigma^{\alpha\beta} + u\sigma^{\alpha\beta}(\not{p} + m_s)]}{2(p^2 - m_s^2)^2}. \quad (\text{C.4})$$

The contributions from $\hat{S}^{(2)}(x)$ and $\hat{S}^{(3)}(x)$ to the correlation functions are called two- and three-particle contributions, respectively:

$$\mathcal{P}_{ab}(k, q) = \mathcal{P}_{ab}^{(2)}(k, q) + \mathcal{P}_{ab}^{(3)}(k, q) + \dots \quad (\text{C.5})$$

$$\mathcal{P}_{ab}^{(j)}(k, q) = i \int d^4x e^{ik \cdot x} \langle 0 | \bar{d}(x) \Gamma_a \hat{S}^{(j)}(x) \Gamma_b b(0) | \bar{B}^0(q+k) \rangle. \quad (\text{C.6})$$

In the following two subsections we outline the calculation of these two- and three-particle contributions.

C.1 Two-particle contributions

Collecting the results in the previous subsections we have, for the two-particle contribution:

$$\begin{aligned} \mathcal{P}_{ab}^{(2)}(k, q) &= i \int d^4x e^{ik \cdot x} \mathcal{D}_{[\Gamma_a \hat{S}^{(2)}(x) \Gamma_b]}^{(2)}(x) \\ &= \frac{f_B m_B}{2} \int d^4x e^{ik \cdot x} \left\{ \text{Tr} \left[\gamma_5 \Gamma_a \hat{S}^{(2)}(x) \Gamma_b P_+ \right] \mathcal{A}(x) - \frac{1}{2} \text{Tr} \left[\gamma_5 \Gamma_a \hat{S}^{(2)}(x) \Gamma_b P_+ \not{x} \right] \mathcal{B}(x) \right\}. \end{aligned} \quad (\text{C.7})$$

The d^4x integrals can be performed by applying the general formula

$$\int d^4x \frac{d^4p}{(2\pi)^4} e^{i(k_\omega - p) \cdot x} f(x) S(p) = f(-i\partial_p) S(p) \Big|_{p=k_\omega}, \quad (\text{C.8})$$

leading to

$$\int d^4x e^{ik_\omega \cdot x} \hat{S}^{(2)}(x) = \frac{i(\not{k}_\omega + m_s)}{k_\omega^2 - m_s^2}, \quad (\text{C.9})$$

$$\int d^4x e^{ik_\omega \cdot x} x^2 \hat{S}^{(2)}(x) = \frac{4i\not{k}_\omega}{(k_\omega^2 - m_s^2)^2} - \frac{8im_s^2(\not{k}_\omega + m_s)}{(k_\omega^2 - m_s^2)^3}, \quad (\text{C.10})$$

$$\int d^4x e^{ik_\omega \cdot x} x^\mu \hat{S}^{(2)}(x) = \frac{\gamma^\mu}{k_\omega^2 - m_s^2} - \frac{2k_\omega^\mu(\not{k}_\omega + m_s)}{(k_\omega^2 - m_s^2)^2}, \quad (\text{C.11})$$

$$\int d^4x e^{ik_\omega \cdot x} x^\mu x^2 \hat{S}^{(2)}(x) = \frac{4\gamma^\mu}{(k_\omega^2 - m_s^2)^2} - \frac{8m_s^2\gamma^\mu + 16k_\omega^\mu \not{k}_\omega}{(k_\omega^2 - m_s^2)^3} + \frac{48m_s^2 k_\omega^\mu (\not{k}_\omega + m_s)}{(k_\omega^2 - m_s^2)^4}. \quad (\text{C.12})$$

In our case,

$$k_\omega = k - \omega v = \bar{\sigma} k - \sigma q, \quad (\text{C.13})$$

where $\sigma \equiv \omega/m_B$ and $\bar{\sigma} = 1 - \sigma$.

Inserting these expressions in Eq. (C.7) we reduce the latter to integrals over the variable ω – see Eqs. (B.3)-(B.4) – which is then traded for the variable σ , with a support in the range $[0, 1]$. Performing the Lorentz algebra and the Dirac traces, we can now identify the invariant amplitudes such as in Eq. (18). Each invariant amplitude can now be written as:

$$\mathcal{P}_{ab,(i)}^{(2)}(k^2, q^2) = f_B m_B \sum_n \int_0^1 d\sigma \frac{\bar{\sigma}^{n+1} \hat{I}_n^{(i)}(\sigma)}{(k_\omega^2 - m_s^2)^{n+1}}. \quad (\text{C.14})$$

where the functions $\hat{I}_n^{(i)}(\sigma)$ are linear combinations of the distribution amplitudes with σ -dependent coefficients. In order to implement duality, we cast the OPE expression of each invariant amplitude as a dispersion relation, with a subsequent subtraction above threshold and the Borel transformation:

$$\mathcal{P}(k^2, q^2) = \frac{1}{\pi} \int_{m_s^2}^{\infty} ds \frac{\text{Im} \mathcal{P}(s, q^2)}{s - k^2} \quad \longrightarrow \quad \mathcal{P}(q^2, s_0, M^2) = \frac{1}{\pi} \int_{m_s^2}^{s_0} ds \text{Im} \mathcal{P}(s, q^2) e^{-s/M^2}. \quad (\text{C.15})$$

To write the terms in Eq. (C.14) in the form of a dispersion relation, it is useful to define the variable $s(\sigma)$:

$$s(\sigma) \equiv \sigma m_B^2 - \frac{\sigma q^2 - m_s^2}{\bar{\sigma}}, \quad (\text{C.16})$$

such that $k_\omega^2 - m_s^2 = -\bar{\sigma} [s(\sigma) - k^2]$, before changing the integration variable from σ to s . This works directly for the terms with $n = 0$ in (C.14). For the terms with $n \geq 1$ we perform the integration by parts sequentially, in order to express them in terms of terms with $n = 0$ plus “boundary terms”. Once all the terms have been written in dispersive form, we apply duality by cutting out the s integrals above $s > s_0$, after which we work backwards to the original non-dispersive form of the $d\sigma$ integrals with a cut-off at $\sigma_0 \equiv \sigma(s_0)$. Then we perform the Borel transformation in the variable k^2 :

$$\mathcal{B}_{M^2} \left[\frac{1}{(s - k^2)^N} \right] = \frac{1}{(N - 1)!} \frac{e^{-s/M^2}}{M^{2(N-1)}} \quad (\text{C.17})$$

for generic (s, N) – and vanishing for $N \leq 0$.

At the end of the day, we find that the whole procedure can be implemented by performing the following substitution in the terms of the r.h.s of Eq. (C.14):

$$\int_0^1 d\sigma \frac{\bar{\sigma}^{n+1} \hat{I}_n^{(i)}(\sigma)}{(k_\omega^2 - m_s^2)^{n+1}} \longrightarrow \left\{ \int_0^{\sigma_0} d\sigma \frac{I_n^{(i)}(\sigma) e^{-s(\sigma)/M^2}}{(M^2)^n} + e^{-s_0/M^2} \sum_{\ell=0}^{n-1} \frac{\eta(\sigma_0) \mathcal{D}_\eta^\ell [I_n^{(i)}](\sigma_0)}{(M^2)^{n-\ell-1}} \right\} \quad (\text{C.18})$$

where the second term in the r.h.s. (the boundary term) arises only for $n \geq 1$. We have defined $s_0 \equiv s(\sigma_0)$ and $\hat{I}_n^{(i)}(\sigma) = (-1)^{n+1} n! I_n^{(i)}(\sigma)$. The operator \mathcal{D}_η is defined by:

$$\mathcal{D}_\eta[F](\sigma_0) = \frac{d}{d\sigma} [\eta(\sigma) F(\sigma)]_{\sigma=\sigma_0}, \quad (\text{C.19})$$

which is applied ℓ times in each term of the above formula, so that:

$$\mathcal{D}_\eta^0[F](\sigma) = F(\sigma); \quad \mathcal{D}_\eta^2[F](\sigma) = \frac{d}{d\sigma} \left[\eta(\sigma) \frac{d}{d\sigma} [\eta(\sigma) F(\sigma)] \right]; \quad \text{etc.} \quad (\text{C.20})$$

The function $\eta(\sigma)$ is the Jacobian of the change of integration variable $\sigma(s)$:

$$\eta(\sigma) \equiv \frac{d\sigma}{ds} = \frac{\bar{\sigma}^2}{\bar{\sigma}^2 m_B^2 - (q^2 - m_s^2)}. \quad (\text{C.21})$$

Collecting everything leads to the structure in Eq. (D.1) for each invariant amplitude. All the results for the choices of currents $\Gamma_{a,b}$ relevant for P -wave form factors are collected in Appendix D.

C.2 Three-particle contributions

Collecting the different pieces, we have:

$$\mathcal{P}_{ab}^{(3)}(k, q) = \frac{f_B m_B}{2} \int_0^1 du \int_0^\infty d\omega_1 d\omega_2 \mathcal{F}_{ab}(u, \omega_1 \omega_2) \quad (\text{C.22})$$

with

$$\mathcal{F}_{ab}(u, \omega_1 \omega_2) \equiv \int d^4x e^{ik_\omega \cdot x} \text{Tr} \left[\gamma_5 \Gamma_a \tilde{S}_{(3)}^{\mu\nu}(x, u) \Gamma_b P_+ \Psi_{\mu\nu}(x, \omega_1, \omega_2) \right], \quad (\text{C.23})$$

where $k_\omega = k - \sigma m_B v = \bar{\sigma} k - \sigma q$,¹⁸ and

$$\tilde{S}_{(3)}^{\mu\nu}(x, u) \equiv \int \frac{d^4p}{(2\pi)^4} e^{-ip \cdot x} \frac{[\bar{u}(\not{p} + m_s) \sigma^{\mu\nu} + u \sigma^{\mu\nu} (\not{p} + m_s)]}{2(p^2 - m_s^2)^2}. \quad (\text{C.24})$$

We perform the change of variable $u \rightarrow \sigma(u) \equiv (\omega_1 + u\omega_2)/m_B$, so that:

$$\int_0^1 du \int_0^\infty d\omega_1 d\omega_2 \mathcal{F}_{ab}(u, \omega_1, \omega_2) = \int_0^1 m_B d\sigma \int_0^{m_B \sigma} d\omega_1 \int_{m_B \sigma - \omega_1}^\infty \frac{d\omega_2}{\omega_2} \mathcal{F}_{ab}(u(\sigma), \omega_1, \omega_2) \quad (\text{C.25})$$

with $u(\sigma) = (\sigma m_B - \omega_1)/\omega_2$. With this, we write:

$$\mathcal{P}_{ab}^{(3)}(k, q) = \frac{f_B m_B^2}{2} \int_0^1 d\sigma \int_0^{m_B \sigma} d\omega_1 \int_{m_B \sigma - \omega_1}^\infty \frac{d\omega_2}{\omega_2} \mathcal{F}_{ab}(u(\sigma), \omega_1, \omega_2). \quad (\text{C.26})$$

The integrals over d^4x in Eq. (C.23) are performed by using the following results:

$$\int d^4x \frac{d^4p}{(2\pi)^4} e^{i(k_\omega - p) \cdot x} \frac{x^\mu (\not{p} + m_s)}{(p^2 - m_s^2)^2} = \frac{-i\gamma^\mu}{(k_\omega^2 - m_s^2)^2} + \frac{4ik_\omega^\mu (\not{k}_\omega + m_s)}{(k_\omega^2 - m_s^2)^3}, \quad (\text{C.27})$$

$$\int d^4x \frac{d^4p}{(2\pi)^4} e^{i(k_\omega - p) \cdot x} \frac{x^\mu x^\nu (\not{p} + m_s)}{(p^2 - m_s^2)^2} = \frac{4[k_\omega^\mu \gamma^\nu + k_\omega^\nu \gamma^\mu + g^{\mu\nu} (\not{k}_\omega + m_s)]}{(k_\omega^2 - m_s^2)^3} - \frac{24k_\omega^\mu k_\omega^\nu (\not{k}_\omega + m_s)}{(k_\omega^2 - m_s^2)^4}, \quad (\text{C.28})$$

which follow from Eq. (C.8). After the integration over d^4x and the traces in Eq. (C.23) have been performed, one identifies the various invariant amplitudes. These depend on k_ω as in the two-particle case discussed above, and the Borel transformation over k^2 is done analogously. In particular, in analogy with Eq. (C.14), we have

$$\frac{m_B}{2} \int_0^{m_B \sigma} d\omega_1 \int_{m_B \sigma - \omega_1}^\infty \frac{d\omega_2}{\omega_2} \mathcal{F}_{ab}(u(\sigma), \omega_1, \omega_2) = \sum_n \frac{\bar{\sigma}^n \hat{I}_n^{(i)}(\sigma)}{(k_\omega^2 - m_s^2)^{n+1}}, \quad (\text{C.29})$$

which gives rise to the same structure in Eq. (D.1) for the 3-particle contributions. The results for all relevant choices of the currents $\Gamma_{a,b}$ are collected in Appendix D.

¹⁸Note that the variable σ here is different from the 2-particle case, but since it becomes an integration variable in both cases, it will not matter.

C.3 Explicit derivation of Eq. (C.18)

We start considering (without justification) the integral:

$$\int_{\sigma_1}^{\sigma_2} d\sigma \frac{f(\sigma)}{(k_\omega^2 - m_s^2)^\ell} = (-1)^\ell \int_{\sigma_1}^{\sigma_2} d\sigma \frac{g(\sigma)}{(s - k^2)^\ell} . \quad (\text{C.30})$$

where $g(\sigma) = f(\sigma)/\bar{\sigma}^\ell$. The equality of the two integrals follows from Eq. (C.16). We want to derive a formula for the integral

$$\mathcal{I}_\ell(g; \sigma_1, \sigma_2) \equiv \int_{\sigma_1}^{\sigma_2} d\sigma \frac{g(\sigma)}{(s - k^2)^\ell} \quad (\text{C.31})$$

for any function $g(\sigma)$ and any integer $\ell \geq 1$, and any real numbers $0 < \sigma_1 < \sigma_2 < 1$.

We start by integrating by parts once:

$$\mathcal{I}_\ell(g; \sigma_1, \sigma_2) = \frac{1}{\ell - 1} \left\{ \frac{\eta(\sigma_1)g(\sigma_1)}{(s_1 - k^2)^{\ell-1}} - \frac{\eta(\sigma_2)g(\sigma_2)}{(s_2 - k^2)^{\ell-1}} \right\} + \frac{\mathcal{I}_{\ell-1}(\mathcal{D}_\eta[g], \sigma_1, \sigma_2)}{\ell - 1} \quad (\text{C.32})$$

where $s_i = s(\sigma_i)$. Then we infer the result of integrating by parts until the integrand has a single pole:

$$\mathcal{I}_\ell(g; \sigma_1, \sigma_2) = S_\ell(\sigma_1) - S_\ell(\sigma_2) + \frac{\mathcal{I}_1(\mathcal{D}_\eta^{\ell-1}[g]; \sigma_1, \sigma_2)}{(\ell - 1)!} \quad (\text{C.33})$$

with

$$S_\ell(\sigma_i) \equiv \sum_{n=1}^{\ell-1} \frac{(\ell - 1 - n)!}{(\ell - 1)!} \frac{\eta(\sigma_i)\mathcal{D}_\eta^{n-1}[g](\sigma_i)}{(s_i - k^2)^{\ell-n}} \quad (\text{C.34})$$

and where the notation is:

$$\mathcal{D}_\eta[g](x) = \frac{d}{d\sigma} [\eta(\sigma)g(\sigma)]_{\sigma=x} , \quad \mathcal{D}_\eta^2[g](x) = \frac{d}{d\sigma} \left[\eta(\sigma) \frac{d}{d\sigma} [\eta(\sigma)g(\sigma)] \right]_{\sigma=x} , \quad \dots \quad (\text{C.35})$$

Eq. (C.33) can be proven by induction easily.

Let us now consider $\mathcal{I}_\ell(g; 0, 1)$ and assume duality holds for $s > s_0$. The integral \mathcal{I}_ℓ in Eq. (C.33) can be written as an integral over $s \in (m_s^2, \infty)$, while $\eta(1) = 0$ (which implies that $S_\ell(1) = 0$), and the remaining surface term $S_\ell(0)$ has a singularity at $k^2 = m_s^2 \ll s_0$, not supposed to be contained in the OPE integral above s_0 . Therefore the duality subtraction should be applied only on the \mathcal{I}_1 term:

$$\mathcal{I}_\ell(g; 0, 1) \rightarrow S_\ell(0) + \frac{\mathcal{I}_1(\mathcal{D}_\eta^{\ell-1}[g]; 0, \sigma_0)}{(\ell - 1)!} . \quad (\text{C.36})$$

We can rewrite the r.h.s of the previous equation as:

$$S_\ell(0) + \frac{\mathcal{I}_1(\mathcal{D}_\eta^{\ell-1}[g]; 0, \sigma_0)}{(\ell - 1)!} = S_\ell(0) + [\mathcal{I}_\ell(g; 0, \sigma_0) - S_\ell(0) + S_\ell(\sigma_0)] = S_\ell(\sigma_0) + \mathcal{I}_\ell(g; 0, \sigma_0) \quad (\text{C.37})$$

which gives the prescription for the duality approximation:

$$\int_0^1 d\sigma \frac{\bar{\sigma}^\ell g(\sigma)}{(k_\omega^2 - m_s^2)^\ell} \rightarrow (-1)^\ell \left\{ \sum_{n=1}^{\ell-1} \frac{(\ell - n - 1)!}{(\ell - 1)!} \frac{\eta(\sigma_0)\mathcal{D}_\eta^{n-1}[g](\sigma_0)}{(s_0 - k^2)^{\ell-n}} + \int_0^{\sigma_0} d\sigma \frac{g(\sigma)}{(s - k^2)^\ell} \right\} . \quad (\text{C.38})$$

Applying the Borel transformation in the variable k^2 leads exactly to Eq. (C.18).

D OPE expressions

We present here the OPE expressions on the right-hand side of the sum rules, including two- and three-particle contributions up to twist-4, as discussed in Appendix B. The generic form for any form factor is written as:

$$\mathcal{P}_i^{(T),\text{OPE}}(q^2, \sigma_0, M^2) = \sum_{n \geq 0} \frac{f_B m_B}{(M^2)^n} \left\{ \int_0^{\sigma_0} d\sigma e^{-s(\sigma)/M^2} I_{i,n}^{(T)}(\sigma) + \sum_{\ell \geq 0} \eta(\sigma_0) \mathcal{D}_\eta^\ell [I_{i,n+\ell+1}^{(T)}](\sigma_0) e^{-s_0/M^2} \right\}, \quad (\text{D.1})$$

where the functions $I_n^{(T)}$ are a sum of two- and three-particle contributions:

$$I_{i,n}^{(T)}(\sigma) = I_{i,n}^{(2)(T)}(\sigma) + \int_0^{m_B \sigma} d\omega_1 \int_{m_B \sigma - \omega_1}^\infty \frac{d\omega_2}{\omega_2} I_{i,n}^{(3)(T)}(\sigma, \omega_1, \omega_2). \quad (\text{D.2})$$

The operator \mathcal{D}_η is defined in Eq. (C.19), and

$$\eta(\sigma) = \frac{\bar{\sigma}^2}{\bar{\sigma}^2 m_B^2 - (q^2 - m_s^2)}, \quad \hat{s}(\sigma) = \sigma - \frac{\sigma \hat{q}^2 - \hat{m}_s^2}{\bar{\sigma}},$$

$$\sigma(s) = \frac{1}{2} \left\{ 1 + \hat{s} - \hat{q}^2 - \sqrt{(1 - \hat{s} + \hat{q}^2)^2 - 4(\hat{q}^2 - \hat{m}_s^2)} \right\}, \quad (\text{D.3})$$

with $\hat{s} \equiv s/m_B^2$, $\hat{q}^2 \equiv q^2/m_B^2$ and $\hat{m}_s \equiv m_s/m_B$.

The full expressions for the coefficients $I_{i,n}^{(2)(T)}(\sigma)$ and $I_{i,n}^{(3)(T)}(\sigma, \omega_1, \omega_2)$ are given in electronic format as a supplementary file called ‘OPEcoefficients.m’ (see below for more details). For easy reference and comparison, we reproduce here only the results for the two-particle coefficients $I_{i,n}^{(2)(T)}(\sigma)$ for $q^2 = 0$ and in the limit $m_s \rightarrow 0$:

$$I_{\perp,0}^{(2)}(\sigma) = \frac{\phi_+}{\bar{\sigma}}, \quad I_{\parallel,0}^{(2)}(\sigma) = \frac{m_B^2 \phi_+}{2} + \frac{2g_+}{\bar{\sigma}^2}, \quad I_{-,0}^{(2)}(\sigma) = \frac{(\sigma - \bar{\sigma}) \phi_+}{\bar{\sigma}},$$

$$I_{t,0}^{(2)}(\sigma) = -\frac{m_b \sigma \bar{\Phi}_\pm}{\bar{\sigma}^2} - \frac{m_b m_B \sigma g_+}{\bar{\sigma}}, \quad I_{\perp,0}^{(2)T}(\sigma) = m_B \phi_+,$$

$$I_{\parallel,0}^{(2)T}(\sigma) = \frac{m_B^3 \bar{\sigma} \phi_+}{2} - \frac{2m_B g_+}{\bar{\sigma}} - \frac{2\bar{G}_\pm}{\bar{\sigma}^2}, \quad I_{-,0}^{(2)T}(\sigma) = -\frac{m_B(1+\sigma) \phi_+}{\bar{\sigma}} - \frac{2\sigma \bar{\Phi}_\pm}{\bar{\sigma}^2},$$

$$I_{\perp,1}^{(2)}(\sigma) = -\frac{4g_+}{\bar{\sigma}^2}, \quad I_{\parallel,1}^{(2)}(\sigma) = -\frac{2m_B^2 g_+}{\bar{\sigma}} - \frac{4m_B \bar{G}_\pm}{\bar{\sigma}^2}, \quad I_{-,1}^{(2)}(\sigma) = -\frac{2m_B \sigma \bar{\Phi}_\pm}{\bar{\sigma}} - \frac{4(\sigma - \bar{\sigma}) g_+}{\bar{\sigma}^2},$$

$$I_{t,1}^{(2)}(\sigma) = \frac{m_b m_B^2 \sigma \bar{\Phi}_\pm}{\bar{\sigma}} + \frac{4m_b m_B \sigma g_+}{\bar{\sigma}^2} + \frac{4m_b(1+\sigma) \bar{G}_\pm}{\bar{\sigma}^3}, \quad I_{\parallel,1}^{(2)T}(\sigma) = -2m_B^3 g_+ - \frac{2m_B^2 \bar{G}_\pm}{\bar{\sigma}},$$

$$I_{-,1}^{(2)T}(\sigma) = -\frac{2m_B^2 \sigma \bar{\Phi}_\pm}{\bar{\sigma}} + \frac{4m_B(1+\sigma) g_+}{\bar{\sigma}^2} + \frac{4(5\sigma - 1) \bar{G}_\pm}{\bar{\sigma}^3}, \quad I_{\perp,1}^{(2)T}(\sigma) = -\frac{4m_B g_+}{\bar{\sigma}} - \frac{4\bar{G}_\pm}{\bar{\sigma}^2},$$

$$I_{-,2}^{(2)}(\sigma) = \frac{8m_B \sigma \bar{G}_\pm}{\bar{\sigma}^2}, \quad I_{t,2}^{(2)}(\sigma) = -\frac{4m_b m_B^2 \sigma \bar{G}_\pm}{\bar{\sigma}^2}, \quad I_{-,2}^{(2)T}(\sigma) = \frac{8m_B^2 \sigma \bar{G}_\pm}{\bar{\sigma}^2}, \quad (\text{D.4})$$

where for brevity we have omitted the arguments of the LCDAs, $\phi_+ \equiv \phi_+(m_B\sigma)$, etc. These results can be easily extracted from the ancillary Mathematica package ‘`OPEcoefficients.m`’. For example, the expression for $I_{\parallel,1}^{(2)T}(\sigma)$ given in Eq. (D.4) is obtained by typing in a Mathematica notebook:

```
IparT[2,1]/.(("<<"OPEcoefficients.m")/.{ms -> 0,q2 -> 0}
```

The arguments in brackets are such that $I_{\perp,n}^{(k)} = \text{Iperp}[\mathbf{k}, \mathbf{n}]$, for example. For the three-particle contributions, one needs to take into account that $\bar{u} \equiv 1 - u$ and $u = (\sigma m_B - \omega_1)/\omega_2$. The syntax is otherwise obvious by looking at the given expressions.

E Results for OPE coefficients in different models

In this appendix we expand on the results of Section 5.4 and collect the results for the OPE coefficients $\kappa_i^{(T),\text{OPE}}$ and $\eta_i^{(T),\text{OPE}}$ in the three different models for the B -meson LCDAs presented in Appendix B.2. This is shown in Tables 9 and 10, which complement Table 4 by adding the corresponding results in Models IIA and IIB. The conclusion from the results presented here is the estimate of model-dependence quoted at the end of Section 5.4, which is obtained simply by taking the maximum spread of the central values in the three models for each parameter.

As mentioned in Section 5.4, the quoted parametric uncertainties in the OPE coefficients shown in Tables 4, 9 and 10 are strongly correlated. These correlations are described by one 42×42 correlation matrix for each of the three models. We do not find it illustrative to display in the text these correlation matrices. However, we wish to make available the correlation matrix for Model I in electronic format, since it is convenient for reproducing the results in Section 5.5 without the need to evaluate all the OPE functions. The corresponding file is a Mathematica package called ‘`CorrMatrixOPEparameters.m`’, which is available from the authors upon request. The order of the correlation coefficients in this matrix is given by:

$$\underbrace{\{\kappa_{\perp}^{\text{OPE}}, \eta_{\perp}^{\text{OPE}}, \kappa_{\parallel}^{\text{OPE}}, \eta_{\parallel}^{\text{OPE}}, \dots, \kappa_{-}^{T,\text{OPE}}, \eta_{-}^{T,\text{OPE}}\}}_{M^2=1}, \underbrace{\{\kappa_{\perp}^{\text{OPE}}, \eta_{\perp}^{\text{OPE}}, \dots\}}_{M^2=1.25}, \underbrace{\{\kappa_{\perp}^{\text{OPE}}, \eta_{\perp}^{\text{OPE}}, \dots\}}_{M^2=1.5}, \quad (\text{E.1})$$

where the order among the parameters gathered under each horizontal brace is given by $\{\xi_{\perp}, \xi_{\parallel}, \xi_{-}, \xi_t, \xi_{\perp}^T, \xi_{\parallel}^T, \xi_{-}^T\}$. For example, the element (7, 24) in this matrix contains the correlation coefficient:

$$\text{corr}\left(\kappa_t^{\text{OPE}}[M^2 = 1 \text{ GeV}], \eta_{\perp}^{T,\text{OPE}}[M^2 = 1.25 \text{ GeV}]\right) = 0.96. \quad (\text{E.2})$$

When using this correlation matrix one must take into account the degeneracies that exist among several of the form factor parameters.

<i>B</i> -LCDA Model	$M^2 = 1.00 \text{ GeV}^2$	$M^2 = 1.25 \text{ GeV}^2$	$M^2 = 1.50 \text{ GeV}^2$
Model MI	$\kappa_{\perp}^{\text{OPE}} = +0.007(4)$	$\kappa_{\perp}^{\text{OPE}} = +0.008(5)$	$\kappa_{\perp}^{\text{OPE}} = +0.009(5)$
	$\eta_{\perp}^{\text{OPE}} = -0.010(14)$	$\eta_{\perp}^{\text{OPE}} = -0.012(17)$	$\eta_{\perp}^{\text{OPE}} = -0.013(19)$
Model MIIA	$\kappa_{\perp}^{\text{OPE}} = +0.006(4)$	$\kappa_{\perp}^{\text{OPE}} = +0.008(4)$	$\kappa_{\perp}^{\text{OPE}} = +0.009(5)$
	$\eta_{\perp}^{\text{OPE}} = -0.024(19)$	$\eta_{\perp}^{\text{OPE}} = -0.029(23)$	$\eta_{\perp}^{\text{OPE}} = -0.034(26)$
Model MIIB	$\kappa_{\perp}^{\text{OPE}} = +0.007(4)$	$\kappa_{\perp}^{\text{OPE}} = +0.008(5)$	$\kappa_{\perp}^{\text{OPE}} = +0.009(5)$
	$\eta_{\perp}^{\text{OPE}} = -0.020(17)$	$\eta_{\perp}^{\text{OPE}} = -0.023(20)$	$\eta_{\perp}^{\text{OPE}} = -0.027(23)$
Model MI	$\kappa_{\parallel}^{\text{OPE}} = +0.100(58)$	$\kappa_{\parallel}^{\text{OPE}} = +0.120(69)$	$\kappa_{\parallel}^{\text{OPE}} = +0.137(78)$
	$\eta_{\parallel}^{\text{OPE}} = +0.246(85)$	$\eta_{\parallel}^{\text{OPE}} = +0.304(108)$	$\eta_{\parallel}^{\text{OPE}} = +0.355(128)$
Model MIIA	$\kappa_{\parallel}^{\text{OPE}} = +0.092(52)$	$\kappa_{\parallel}^{\text{OPE}} = +0.112(63)$	$\kappa_{\parallel}^{\text{OPE}} = +0.128(73)$
	$\eta_{\parallel}^{\text{OPE}} = +0.083(15)$	$\eta_{\parallel}^{\text{OPE}} = +0.102(18)$	$\eta_{\parallel}^{\text{OPE}} = +0.118(20)$
Model MIIB	$\kappa_{\parallel}^{\text{OPE}} = +0.098(55)$	$\kappa_{\parallel}^{\text{OPE}} = +0.118(66)$	$\kappa_{\parallel}^{\text{OPE}} = +0.135(76)$
	$\eta_{\parallel}^{\text{OPE}} = +0.146(39)$	$\eta_{\parallel}^{\text{OPE}} = +0.181(51)$	$\eta_{\parallel}^{\text{OPE}} = +0.212(62)$
Model MI	$\kappa_{-}^{\text{OPE}} = -0.004(3)$	$\kappa_{-}^{\text{OPE}} = -0.004(4)$	$\kappa_{-}^{\text{OPE}} = -0.005(5)$
	$\eta_{-}^{\text{OPE}} = -0.020(17)$	$\eta_{-}^{\text{OPE}} = -0.025(21)$	$\eta_{-}^{\text{OPE}} = -0.029(24)$
Model MIIA	$\kappa_{-}^{\text{OPE}} = -0.003(3)$	$\kappa_{-}^{\text{OPE}} = -0.003(4)$	$\kappa_{-}^{\text{OPE}} = -0.004(4)$
	$\eta_{-}^{\text{OPE}} = -0.018(18)$	$\eta_{-}^{\text{OPE}} = -0.021(22)$	$\eta_{-}^{\text{OPE}} = -0.024(26)$
Model MIIB	$\kappa_{-}^{\text{OPE}} = -0.003(3)$	$\kappa_{-}^{\text{OPE}} = -0.004(4)$	$\kappa_{-}^{\text{OPE}} = -0.004(4)$
	$\eta_{-}^{\text{OPE}} = -0.019(18)$	$\eta_{-}^{\text{OPE}} = -0.023(22)$	$\eta_{-}^{\text{OPE}} = -0.026(26)$
Model MI	$\kappa_t^{\text{OPE}} = -0.043(9)$	$\kappa_t^{\text{OPE}} = -0.052(11)$	$\kappa_t^{\text{OPE}} = -0.060(12)$
	$\eta_t^{\text{OPE}} = +0.210(30)$	$\eta_t^{\text{OPE}} = +0.249(34)$	$\eta_t^{\text{OPE}} = +0.282(37)$
Model MIIA	$\kappa_t^{\text{OPE}} = -0.045(10)$	$\kappa_t^{\text{OPE}} = -0.054(12)$	$\kappa_t^{\text{OPE}} = -0.062(14)$
	$\eta_t^{\text{OPE}} = +0.220(41)$	$\eta_t^{\text{OPE}} = +0.264(47)$	$\eta_t^{\text{OPE}} = +0.301(52)$
Model MIIB	$\kappa_t^{\text{OPE}} = -0.045(10)$	$\kappa_t^{\text{OPE}} = -0.055(12)$	$\kappa_t^{\text{OPE}} = -0.063(13)$
	$\eta_t^{\text{OPE}} = +0.216(35)$	$\eta_t^{\text{OPE}} = +0.257(39)$	$\eta_t^{\text{OPE}} = +0.291(42)$

Table 9: *Results for the OPE coefficients in the z -expansion of vector, axial-vector and timelike-helicity form factors in the three different models considered for B -meson LCDAs.*

B -LCDA Model	$M^2 = 1.00 \text{ GeV}^2$	$M^2 = 1.25 \text{ GeV}^2$	$M^2 = 1.50 \text{ GeV}^2$
Model MI	$\kappa_{\perp}^{T,\text{OPE}} = +0.036(21)$	$\kappa_{\perp}^{T,\text{OPE}} = +0.043(25)$	$\kappa_{\perp}^{T,\text{OPE}} = +0.050(29)$
	$\eta_{\perp}^{T,\text{OPE}} = -0.056(73)$	$\eta_{\perp}^{T,\text{OPE}} = -0.065(85)$	$\eta_{\perp}^{T,\text{OPE}} = -0.071(94)$
Model MIIA	$\kappa_{\perp}^{T,\text{OPE}} = +0.034(19)$	$\kappa_{\perp}^{T,\text{OPE}} = +0.041(23)$	$\kappa_{\perp}^{T,\text{OPE}} = +0.047(27)$
	$\eta_{\perp}^{T,\text{OPE}} = -0.122(95)$	$\eta_{\perp}^{T,\text{OPE}} = -0.148(115)$	$\eta_{\perp}^{T,\text{OPE}} = -0.171(133)$
Model MIIB	$\kappa_{\perp}^{T,\text{OPE}} = +0.036(20)$	$\kappa_{\perp}^{T,\text{OPE}} = +0.043(24)$	$\kappa_{\perp}^{T,\text{OPE}} = +0.049(28)$
	$\eta_{\perp}^{T,\text{OPE}} = -0.103(85)$	$\eta_{\perp}^{T,\text{OPE}} = -0.122(101)$	$\eta_{\perp}^{T,\text{OPE}} = -0.139(114)$
Model MI	$\kappa_{\parallel}^{T,\text{OPE}} = +0.492(290)$	$\kappa_{\parallel}^{T,\text{OPE}} = +0.589(346)$	$\kappa_{\parallel}^{T,\text{OPE}} = +0.671(393)$
	$\eta_{\parallel}^{T,\text{OPE}} = +1.347(458)$	$\eta_{\parallel}^{T,\text{OPE}} = +1.662(582)$	$\eta_{\parallel}^{T,\text{OPE}} = +1.939(693)$
Model MIIA	$\kappa_{\parallel}^{T,\text{OPE}} = +0.461(261)$	$\kappa_{\parallel}^{T,\text{OPE}} = +0.556(316)$	$\kappa_{\parallel}^{T,\text{OPE}} = +0.638(364)$
	$\eta_{\parallel}^{T,\text{OPE}} = +0.499(78)$	$\eta_{\parallel}^{T,\text{OPE}} = +0.614(96)$	$\eta_{\parallel}^{T,\text{OPE}} = +0.713(112)$
Model MIIB	$\kappa_{\parallel}^{T,\text{OPE}} = +0.488(276)$	$\kappa_{\parallel}^{T,\text{OPE}} = +0.586(331)$	$\kappa_{\parallel}^{T,\text{OPE}} = +0.671(379)$
	$\eta_{\parallel}^{T,\text{OPE}} = +0.828(230)$	$\eta_{\parallel}^{T,\text{OPE}} = +1.025(298)$	$\eta_{\parallel}^{T,\text{OPE}} = +1.200(360)$
Model MI	$\kappa_{-}^{T,\text{OPE}} = -0.021(19)$	$\kappa_{-}^{T,\text{OPE}} = -0.025(23)$	$\kappa_{-}^{T,\text{OPE}} = -0.028(26)$
	$\eta_{-}^{T,\text{OPE}} = -0.098(103)$	$\eta_{-}^{T,\text{OPE}} = -0.121(126)$	$\eta_{-}^{T,\text{OPE}} = -0.141(146)$
Model MIIA	$\kappa_{-}^{T,\text{OPE}} = -0.015(16)$	$\kappa_{-}^{T,\text{OPE}} = -0.018(20)$	$\kappa_{-}^{T,\text{OPE}} = -0.021(23)$
	$\eta_{-}^{T,\text{OPE}} = -0.087(108)$	$\eta_{-}^{T,\text{OPE}} = -0.104(135)$	$\eta_{-}^{T,\text{OPE}} = -0.118(160)$
Model MIIB	$\kappa_{-}^{T,\text{OPE}} = -0.018(18)$	$\kappa_{-}^{T,\text{OPE}} = -0.021(22)$	$\kappa_{-}^{T,\text{OPE}} = -0.025(25)$
	$\eta_{-}^{T,\text{OPE}} = -0.091(109)$	$\eta_{-}^{T,\text{OPE}} = -0.110(134)$	$\eta_{-}^{T,\text{OPE}} = -0.126(157)$

Table 10: Results for the OPE coefficients in the z -expansion of tensor form factors in the three different models considered for B -meson LCDAs.

F Beyond the narrow-width approximation

F.1 Breit-Wigner model with fixed widths

We consider the convolution of a Breit-Wigner function $D(s, \Gamma)$ with a smooth function $f(s)$

$$J = \int_{s_{\min}}^{s_{\max}} \frac{ds}{2\pi} D(s, \Gamma) f(s) , \quad D(s, \Gamma) = \frac{2m\Gamma}{(s - m^2)^2 + \Gamma^2 m^2} , \quad (\text{F.1})$$

which in the narrow-width limit $\Gamma \rightarrow 0$ becomes

$$J \rightarrow J_0 = \int_{s_{\min}}^{s_{\max}} ds \delta(s - m^2) f(s) = f(m^2) . \quad (\text{F.2})$$

We want to determine the $\mathcal{O}(\Gamma)$ correction to this limit, corresponding to $J - J_0$ at first order in Γ . To this end, we can use a similar approach as in Ref. [92], expressing the difference between the integral and its narrow-width limit as

$$J - J_0 = \int_{s_{\min}}^{s_{\max}} \frac{ds}{2\pi} D(s, \Gamma) [f(s) - f(m^2)] - \alpha J_0 , \quad (\text{F.3})$$

with

$$\begin{aligned} \alpha &= 1 - \int_{s_{\min}}^{s_{\max}} \frac{ds}{2\pi} D(s, \Gamma) = 1 + \frac{1}{\pi} \arctan \frac{m^2 - s_{\max}}{m\Gamma} - \frac{1}{\pi} \arctan \frac{m^2 - s_{\min}}{m\Gamma} \\ &= \frac{m\Gamma}{\pi} \frac{s_{\max} - s_{\min}}{(s_{\max} - m^2)(m^2 - s_{\min})} + \mathcal{O}(\Gamma^2) . \end{aligned} \quad (\text{F.4})$$

We then have

$$\frac{J - J_0}{J_0} = \int_{s_{\min}}^{s_{\max}} \frac{ds}{2\pi} D(s, \Gamma) \left[\frac{f(s)}{f(m^2)} - 1 \right] - \alpha = \int_{s_{\min}}^{s_{\max}} \frac{ds}{2\pi} D(s, \Gamma) [g(s) - g(m^2)] - \alpha , \quad (\text{F.5})$$

where

$$g(s) = \frac{f(s)}{f(m^2)} . \quad (\text{F.6})$$

Performing a Taylor expansion of the smooth function $g(s)$, we write

$$\frac{J - J_0}{J_0} = -\alpha + \int_{s_{\min}}^{s_{\max}} \frac{ds}{2\pi} D(s, \Gamma) \left[(s - m^2)g'(m^2) + \sum_{n \geq 2} \frac{(s - m^2)^n}{n!} g^{(n)}(m^2) \right] . \quad (\text{F.7})$$

Using the expression for α in Eq. (F.4), and integrating each of the remaining terms, we find

$$\begin{aligned} \frac{J - J_0}{J_0} &= -\frac{m\Gamma}{\pi} \frac{s_{\max} - s_{\min}}{(s_{\max} - m^2)(m^2 - s_{\min})} + \frac{2m\Gamma g'(m^2)}{4\pi} \log \frac{(s_{\max} - m^2)^2 + m^2\Gamma^2}{(s_{\min} - m^2)^2 + m^2\Gamma^2} \\ &\quad + \sum_{n \geq 2} \frac{1}{n!} g^{(n)}(m^2) K_n , \end{aligned} \quad (\text{F.8})$$

with K_n defined as

$$K_n = \int_{s_{\min}}^{s_{\max}} \frac{ds}{2\pi} D(s, \Gamma) (s - m^2)^n . \quad (\text{F.9})$$

We should take the expansion of the above expressions up to $\mathcal{O}(\Gamma^2)$. In particular,

$$K_n = \frac{1}{(2\pi)} \frac{2m\Gamma}{n-1} [(s_{\max} - m^2)^{n-1} - (s_{\min} - m^2)^{n-1}] + \mathcal{O}(\Gamma) . \quad (\text{F.10})$$

We now define the intermediate function

$$G(s) = \sum_{n \geq 2} g^{(n)}(m^2) \frac{1}{n!} \frac{1}{n-1} (s - m^2)^{n-1} \quad (\text{F.11})$$

such that

$$G'(s) = \sum_{n \geq 2} g^{(n)}(m^2) \frac{1}{n!} (s - m^2)^{n-2} = \frac{1}{(s - m^2)^2} [g(s) - g(m^2) - g'(m^2)(s - m^2)] , \quad (\text{F.12})$$

$$G(s) = \int_{m^2}^s d\tau \frac{1}{(\tau - m^2)^2} [g(\tau) - g(m^2) - g'(m^2)(\tau - m^2)] . \quad (\text{F.13})$$

This leads to

$$\begin{aligned} \frac{J - J_0}{J_0} &= -\frac{m\Gamma}{\pi} \frac{s_{\max} - s_{\min}}{(s_{\max} - m^2)(m^2 - s_{\min})} + \frac{2m\Gamma g'(m^2)}{2\pi} \log \frac{s_{\max} - m^2}{m^2 - s_{\min}} \\ &\quad + \frac{2m\Gamma}{2\pi} \sum_{n \geq 2} \frac{1}{(n-1)n!} g^{(n)}(m^2) [(s_{\max} - m^2)^{n-1} - (s_{\min} - m^2)^{n-1}] + \mathcal{O}(\Gamma^2) \\ &= -\frac{m\Gamma}{\pi} \frac{s_{\max} - s_{\min}}{(s_{\max} - m^2)(m^2 - s_{\min})} + \frac{2m\Gamma g'(m^2)}{2\pi} \log \frac{s_{\max} - m^2}{m^2 - s_{\min}} \\ &\quad + \frac{2m\Gamma}{2\pi} [G(s_{\max}) - G(s_{\min})] + \mathcal{O}(\Gamma^2) , \end{aligned} \quad (\text{F.14})$$

and therefore

$$\begin{aligned} \frac{J - J_0}{J_0} &= \frac{m\Gamma}{\pi f(m^2)} \left[-f(m^2) \frac{s_{\max} - s_{\min}}{(s_{\max} - m^2)(m^2 - s_{\min})} \right. \\ &\quad \left. + f'(m^2) \log \frac{s_{\max} - m^2}{m^2 - s_{\min}} + F(s_{\max}, m) - F(s_{\min}, m) \right] + \mathcal{O}(\Gamma^2) , \end{aligned} \quad (\text{F.15})$$

with the following definition of $F(s, m)$

$$F(s, m) = \int_{m^2}^s d\tau \frac{1}{(\tau - m^2)^2} [f(\tau) - f(m^2) - f'(m^2)(\tau - m^2)] . \quad (\text{F.16})$$

The validity of this formula can be checked for polynomial expressions without difficulty, and it provides the relative error due to the narrow-width approximation.

F.2 The case of s -dependent widths

We can adapt the formalism to a Breit-Wigner resonance with a s -dependent width

$$J = \int_{s_{\min}}^{s_{\max}} ds \tilde{D}(s, \Gamma) \Phi(s) , \quad \tilde{D}(s, \Gamma) = \frac{1}{\pi} \frac{\sqrt{s} \Gamma(s)}{(s - m^2)^2 + \Gamma(s)^2 s} , \quad (\text{F.17})$$

where $\Gamma(s)$ is a function of the form

$$\Gamma(s) = \Gamma \times \gamma(s) , \quad \Gamma = \Gamma(m^2) , \quad \gamma(m^2) = 1 . \quad (\text{F.18})$$

We can recover the structure in Eq. (F.1) by defining

$$f(s) = \Phi(m^2) \phi(s) \rho(s, \Gamma) , \quad \phi(s) = \frac{\Phi(s)}{\Phi(m^2)} , \quad \rho(s, \Gamma) = \gamma(s) \frac{\sqrt{s}}{m} \frac{(s - m^2)^2 + \Gamma^2 m^2}{(s - m^2)^2 + \Gamma^2 \gamma(s)^2 s} . \quad (\text{F.19})$$

Now $f(s)$ depends also on Γ , but this dependence starts only at $\mathcal{O}(\Gamma^2)$:

$$\rho(s, \Gamma) = \rho(s) + \mathcal{O}(\Gamma^2/m^2) , \quad \rho(s) = \gamma(s) \frac{\sqrt{s}}{m} . \quad (\text{F.20})$$

These functions fulfill the relations

$$\rho(m^2) = 1 , \quad \rho'(m^2) = \frac{1}{2m^2} + \gamma'(m^2) , \quad \phi(m^2) = 1 , \quad f(m^2) = \Phi(m^2) . \quad (\text{F.21})$$

We can now apply the previous analysis, with $J_0 = \Phi(m^2)$ and

$$\begin{aligned} \frac{J - J_0}{J_0} = \frac{\Gamma}{m \pi} \left[- \frac{m^2 (s_{\max} - s_{\min})}{(s_{\max} - m^2)(m^2 - s_{\min})} + m^2 [\phi'(m^2) + \rho'(m^2, \Gamma)] \log \frac{s_{\max} - m^2}{m^2 - s_{\min}} \right. \\ \left. + \tilde{F}(s_{\max}, m, 0) - \tilde{F}(s_{\min}, m, 0) \right] + \mathcal{O}(\Gamma^2) , \end{aligned} \quad (\text{F.22})$$

with the definition of $\tilde{F}(s, m, \Gamma)$

$$\tilde{F}(s, m, \Gamma) = \int_1^{s/m^2} d\tau \frac{1}{(\tau - 1)^2} [\phi(m^2 \tau) \rho(m^2 \tau) - 1 - (\tau - 1) m^2 [\phi'(m^2) + \rho'(m^2)]] . \quad (\text{F.23})$$

These are the final formulas used in Section 4.2 to calculate the $\mathcal{O}(\Gamma)$ corrections to the narrow-width limit.

G Kinematics for $B \rightarrow K \pi \ell \ell$

We consider the decay $\bar{B}^0 \rightarrow K^-(k_1) \pi^+(k_2) \ell^-(q_1) \ell^+(q_2)$. We follow the ‘‘theory’’ conventions for $B \rightarrow K^*(\rightarrow K \pi) \ell \ell$ as defined in Ref. [72] (in agreement with Ref. [69]) to define the three

angles θ_K , θ_ℓ and ϕ . In particular, the definition of θ_K agrees with that in Section 2. In the B -meson rest frame we obtain, for the 4-vectors of interest for the leptonic side:

$$q^\mu = \begin{pmatrix} \frac{m_B^2 - k^2 + q^2}{2m_B} \\ 0 \\ 0 \\ \frac{\sqrt{\lambda}}{2m_B} \end{pmatrix}, \quad \bar{q}^\mu = \begin{pmatrix} -\frac{\sqrt{\lambda_q \lambda}}{2m_B q^2} \cos \theta_\ell \\ \sqrt{\frac{\lambda_q}{q^2}} \sin \theta_\ell \cos \phi \\ \sqrt{\frac{\lambda_q}{q^2}} \sin \theta_\ell \sin \phi \\ -\frac{\sqrt{\lambda_q}}{2m_B q^2} (m_B^2 - k^2 + q^2) \cos \theta_\ell \end{pmatrix}, \quad (\text{G.1})$$

and on the hadronic side:

$$k^\mu = \begin{pmatrix} \frac{m_B^2 + k^2 - q^2}{2m_B} \\ 0 \\ 0 \\ -\frac{\sqrt{\lambda}}{2m_B} \end{pmatrix}, \quad \bar{k}^\mu = \begin{pmatrix} \frac{\sqrt{\lambda_{K\pi\lambda}}}{2m_B k^2} \cos \theta_K \\ -\sqrt{\frac{\lambda_{K\pi}}{k^2}} \sin \theta_K \\ 0 \\ -\frac{\sqrt{\lambda_{K\pi}}}{2m_B k^2} (m_B^2 + k^2 - q^2) \cos \theta_K \end{pmatrix}, \quad (\text{G.2})$$

which leads to the following basis structures in the Lorentz decomposition of form factors and transversity amplitudes:

$$k_t^\mu = \begin{pmatrix} \frac{m_B^2 - k^2 + q^2}{2m_B \sqrt{q^2}} \\ 0 \\ 0 \\ \frac{\sqrt{\lambda}}{2m_B \sqrt{q^2}} \end{pmatrix}, \quad k_0^\mu = \begin{pmatrix} -\frac{\sqrt{\lambda}}{2m_B \sqrt{q^2}} \\ 0 \\ 0 \\ -\frac{m_B^2 - k^2 + q^2}{2m_B \sqrt{q^2}} \end{pmatrix}, \quad k_\perp^\mu = \begin{pmatrix} 0 \\ 0 \\ i \frac{\lambda_{K\pi}}{k^2} \sin \theta_K \\ 0 \end{pmatrix}, \quad k_\parallel^\mu = \begin{pmatrix} 0 \\ -\frac{\lambda_{K\pi}}{k^2} \sin \theta_K \\ 0 \\ 0 \end{pmatrix}. \quad (\text{G.3})$$

References

- [1] S. Descotes-Genon, L. Hofer, J. Matias and J. Virto, “Global analysis of $b \rightarrow s\ell\ell$ anomalies,” JHEP **1606**, 092 (2016) [arXiv:1510.04239 [hep-ph]].
- [2] S. Bifani, S. Descotes-Genon, A. Romero Vidal and M. H. Schune, “Review of Lepton Universality tests in B decays,” J. Phys. G **46** (2019) no.2, 023001 [arXiv:1809.06229 [hep-ex]].
- [3] S. Aoki *et al.*, “Review of lattice results concerning low-energy particle physics,” Eur. Phys. J. C **77**, no. 2, 112 (2017) [arXiv:1607.00299 [hep-lat]].
- [4] I.I. Balitsky, V.M. Braun and A.V. Kolesnichenko, “ $\Sigma^+ \rightarrow p\gamma$ Decay in QCD,” Sov. J. Nucl. Phys. **44** (1986) 1028.
- [5] I.I. Balitsky, V.M. Braun and A.V. Kolesnichenko, “Radiative Decay $\Sigma^+ \rightarrow p\gamma$ in Quantum Chromodynamics,” Nucl. Phys. B **312** (1989) 509.
- [6] V.L. Chernyak and I.R. Zhitnitsky, “B meson exclusive decays into baryons,” Nucl. Phys. B **345** (1990) 137.
- [7] V. M. Belyaev, A. Khodjamirian and R. Ruckl, “QCD calculation of the $B \rightarrow \pi, K$ form factors,” Z. Phys. C **60**, 349 (1993) [hep-ph/9305348].
- [8] G. Duplancic, A. Khodjamirian, T. Mannel, B. Melic and N. Offen, “Light-cone sum rules for $B \rightarrow \pi$ form factors revisited,” JHEP **0804**, 014 (2008) [arXiv:0801.1796 [hep-ph]].
- [9] P. Ball and V. M. Braun, “Exclusive semileptonic and rare B meson decays in QCD,” Phys. Rev. D **58**, 094016 (1998) [hep-ph/9805422].
- [10] P. Ball and R. Zwicky, “ $B_{d,s} \rightarrow \rho, \omega, K^*, \phi$ decay form-factors from light-cone sum rules revisited,” Phys. Rev. D **71**, 014029 (2005) [hep-ph/0412079].
- [11] A. Khodjamirian, T. Mannel and N. Offen, “B-meson distribution amplitude from the $B \rightarrow \pi$ form-factor,” Phys. Lett. B **620** (2005) 52 [hep-ph/0504091].
- [12] A. Khodjamirian, T. Mannel and N. Offen, “Form-factors from light-cone sum rules with B-meson distribution amplitudes,” Phys. Rev. D **75**, 054013 (2007) [hep-ph/0611193].
- [13] Y. M. Wang and Y. L. Shen, “QCD corrections to $B \rightarrow \pi$ form factors from light-cone sum rules,” Nucl. Phys. B **898**, 563 (2015) [arXiv:1506.00667 [hep-ph]].
- [14] C. D. L, Y. L. Shen, Y. M. Wang and Y. B. Wei, “QCD calculations of $B \rightarrow \pi, K$ form factors with higher-twist corrections,” JHEP **1901** (2019) 024 [arXiv:1810.00819 [hep-ph]].

- [15] N. Gubernari, A. Kokulu and D. van Dyk, “ $B \rightarrow P$ and $B \rightarrow V$ Form Factors from B -Meson Light-Cone Sum Rules beyond Leading Twist,” JHEP **1901** (2019) 150 [arXiv:1811.00983 [hep-ph]].
- [16] J. Gao, C. D. Lü, Y. L. Shen, Y. M. Wang and Y. B. Wei, “Precision calculations of $B \rightarrow V$ form factors in QCD,” arXiv:1907.11092 [hep-ph].
- [17] R. R. Horgan, Z. Liu, S. Meinel and M. Wingate, “Lattice QCD calculation of form factors describing the rare decays $B \rightarrow K^* \ell^+ \ell^-$ and $B_s \rightarrow \phi \ell^+ \ell^-$,” Phys. Rev. D **89**, no. 9, 094501 (2014) [arXiv:1310.3722 [hep-lat]].
- [18] A. Bharucha, D. M. Straub and R. Zwicky, “ $B \rightarrow V \ell^+ \ell^-$ in the Standard Model from light-cone sum rules,” JHEP **1608**, 098 (2016) [arXiv:1503.05534 [hep-ph]].
- [19] S. Cheng, A. Khodjamirian and J. Virto, “ $B \rightarrow \pi\pi$ Form Factors from Light-Cone Sum Rules with B -meson Distribution Amplitudes,” JHEP **1705**, 157 (2017) [arXiv:1701.01633 [hep-ph]].
- [20] S. Faller, T. Feldmann, A. Khodjamirian, T. Mannel and D. van Dyk, “Disentangling the Decay Observables in $B^- \rightarrow \pi^+ \pi^- \ell^- \bar{\nu}_\ell$,” Phys. Rev. D **89**, no. 1, 014015 (2014) [arXiv:1310.6660 [hep-ph]].
- [21] P. Böer, T. Feldmann and D. van Dyk, “QCD Factorization Theorem for $B \rightarrow \pi\pi\ell\nu$ Decays at Large Dipion Masses,” JHEP **1702**, 133 (2017) [arXiv:1608.07127 [hep-ph]].
- [22] C. Hambrock and A. Khodjamirian, “Form factors in $\bar{B}^0 \rightarrow \pi\pi\ell\bar{\nu}_\ell$ from QCD light-cone sum rules,” Nucl. Phys. B **905**, 373 (2016) [arXiv:1511.02509 [hep-ph]].
- [23] S. Cheng, A. Khodjamirian and J. Virto, “Timelike-helicity $B \rightarrow \pi\pi$ form factor from light-cone sum rules with dipion distribution amplitudes,” Phys. Rev. D **96**, no. 5, 051901 (2017), [arXiv:1709.00173 [hep-ph]].
- [24] V. M. Braun, Y. Ji and A. N. Manashov, “Higher-twist B-meson Distribution Amplitudes in HQET,” JHEP **1705**, 022 (2017) [arXiv:1703.02446 [hep-ph]].
- [25] A. Khodjamirian, T. Mannel, A. A. Pivovarov and Y.-M. Wang, “Charm-loop effect in $B \rightarrow K^{(*)} \ell^+ \ell^-$ and $B \rightarrow K^* \gamma$,” JHEP **1009**, 089 (2010) [arXiv:1006.4945 [hep-ph]].
- [26] D. Das, G. Hiller, M. Jung and A. Shires, “The $\bar{B} \rightarrow \bar{K} \pi \ell \ell$ and $\bar{B}_s \rightarrow \bar{K} K \ell \ell$ distributions at low hadronic recoil,” JHEP **1409**, 109 (2014) [arXiv:1406.6681 [hep-ph]].
- [27] D. Das, G. Hiller and M. Jung, “ $B \rightarrow K \pi \ell \ell$ in and outside the K^* window,” arXiv:1506.06699 [hep-ph].

- [28] B. Grinstein and D. Pirjol, “Factorization in $B \rightarrow K\pi\ell^+\ell^-$ decays,” Phys. Rev. D **73**, 094027 (2006) [hep-ph/0505155].
- [29] M. Beneke, G. Buchalla, M. Neubert and C. T. Sachrajda, “QCD factorization for $B \rightarrow \pi\pi$ decays: Strong phases and CP violation in the heavy quark limit,” Phys. Rev. Lett. **83**, 1914 (1999) [hep-ph/9905312].
- [30] C. W. Bauer, D. Pirjol, I. Z. Rothstein and I. W. Stewart, “ $B \rightarrow M_1M_2$: Factorization, charming penguins, strong phases, and polarization,” Phys. Rev. D **70**, 054015 (2004) [hep-ph/0401188].
- [31] S. Kränkl, T. Mannel and J. Virto, “Three-body non-leptonic B decays and QCD factorization,” Nucl. Phys. B **899**, 247 (2015) [arXiv:1505.04111 [hep-ph]].
- [32] J. Virto, “Charmless Non-Leptonic Multi-Body B decays,” PoS FPCP **2016**, 007 (2017) [arXiv:1609.07430 [hep-ph]].
- [33] R. Klein, T. Mannel, J. Virto and K. K. Vos, “CP Violation in Multibody B Decays from QCD Factorization,” JHEP **1710**, 117 (2017) [arXiv:1708.02047 [hep-ph]].
- [34] T. Feldmann, B. Müller and D. van Dyk, “Analyzing $b \rightarrow u$ transitions in semileptonic $\bar{B}_s \rightarrow K^{*+}(\rightarrow K\pi)\ell^-\bar{\nu}_\ell$ decays,” Phys. Rev. D **92**, no. 3, 034013 (2015) [arXiv:1503.09063 [hep-ph]].
- [35] S. Descotes-Genon, A. Khodjamirian, J. Virto and K. K. Vos, in preparation.
- [36] D. Epifanov *et al.* [Belle Collaboration], “Study of $\tau^- \rightarrow K_S\pi^-\nu_\tau$ decay at Belle,” Phys. Lett. B **654**, 65 (2007) [arXiv:0706.2231 [hep-ex]].
- [37] M. Tanabashi et al. (Particle Data Group), “Review of Particle Physics,” Phys. Rev. D **98**, 030001 (2018).
- [38] C. Bourrely, I. Caprini and L. Lellouch, “Model-independent description of $B \rightarrow \pi\ell\nu$ decays and a determination of $|V_{ub}|$,” Phys. Rev. D **79**, 013008 (2009), Erratum: [Phys. Rev. D **82**, 099902 (2010)], [arXiv:0807.2722 [hep-ph]].
- [39] P. Gelhausen, A. Khodjamirian, A. A. Pivovarov and D. Rosenthal, “Decay constants of heavy-light vector mesons from QCD sum rules,” Phys. Rev. D **88**, 014015 (2013) Erratum: [Phys. Rev. D **89**, 099901 (2014)] Erratum: [Phys. Rev. D **91**, 099901 (2015)] [arXiv:1305.5432 [hep-ph]].
- [40] S. Aoki *et al.* [Flavour Lattice Averaging Group], arXiv:1902.08191 [hep-lat]. See latest update in: http://flag.unibe.ch/Media?action=AttachFile&do=get&target=FLAG_webupdate.pdf.

- [41] R. J. Dowdall *et al.* [HPQCD Collaboration], “B-Meson Decay Constants from Improved Lattice Nonrelativistic QCD with Physical u, d, s, and c Quarks,” *Phys. Rev. Lett.* **110** (2013) no.22, 222003 [arXiv:1302.2644 [hep-lat]].
- [42] A. Bussone *et al.* [ETM Collaboration], “Mass of the b quark and B -meson decay constants from $N_f=2+1+1$ twisted-mass lattice QCD,” *Phys. Rev. D* **93** (2016) no.11, 114505 [arXiv:1603.04306 [hep-lat]].
- [43] A. Bazavov *et al.*, “*B*- and *D*-meson leptonic decay constants from four-flavor lattice QCD,” *Phys. Rev. D* **98** (2018) no.7, 074512 [arXiv:1712.09262 [hep-lat]].
- [44] C. Hughes, C. T. H. Davies and C. J. Monahan, “New methods for B meson decay constants and form factors from lattice NRQCD,” *Phys. Rev. D* **97** (2018) no.5, 054509 [arXiv:1711.09981 [hep-lat]].
- [45] V. M. Braun, D. Y. Ivanov and G. P. Korchemsky, “The B meson distribution amplitude in QCD,” *Phys. Rev. D* **69**, 034014 (2004) [hep-ph/0309330].
- [46] A. Heller *et al.* [Belle Collaboration], “Search for $B^+ \rightarrow \ell^+ \nu_\ell \gamma$ decays with hadronic tagging using the full Belle data sample,” *Phys. Rev. D* **91**, no. 11, 112009 (2015) [arXiv:1504.05831 [hep-ex]]
- [47] M. Beneke and J. Rohrwild, “*B*-meson distribution amplitude from $B \rightarrow \gamma \ell \nu$,” *Eur. Phys. J. C* **71**, 1818 (2011), [arXiv:1110.3228 [hep-ph]].
- [48] V. M. Braun and A. Khodjamirian, “Soft contribution to $B \rightarrow \gamma \ell \nu_\ell$ and the *B*-meson distribution amplitude,” *Phys. Lett. B* **718**, 1014 (2013), [arXiv:1210.4453 [hep-ph]].
- [49] M. Beneke, “Soft-collinear factorization in *B* decays,” *Nucl. Part. Phys. Proc.* **261-262**, 311 (2015), [arXiv:1501.07374 [hep-ph]].
- [50] M. Beneke, T. Huber and X. Q. Li, “NNLO vertex corrections to non-leptonic B decays: Tree amplitudes,” *Nucl. Phys. B* **832**, 109 (2010) [arXiv:0911.3655 [hep-ph]].
- [51] Y. M. Wang and Y. L. Shen, “QCD corrections to $B \rightarrow \pi$ form factors from light-cone sum rules,” *Nucl. Phys. B* **898**, 563 (2015), [arXiv:1506.00667 [hep-ph]].
- [52] A. Khodjamirian, T. Mannel, N. Offen and Y.-M. Wang, “ $B \rightarrow \pi \ell \nu_\ell$ Width and $|V_{ub}|$ from QCD Light-Cone Sum Rules,” *Phys. Rev. D* **83**, 094031 (2011), [arXiv:1103.2655 [hep-ph]].
- [53] A. Pich, “Precision Tau Physics,” *Prog. Part. Nucl. Phys.* **75**, 41 (2014) [arXiv:1310.7922 [hep-ph]].

- [54] R. Escribano, S. González-Solís, M. Jamin and P. Roig, “Combined analysis of the decays $\tau^- \rightarrow K_S \pi^- \nu_\tau$ and $\tau^- \rightarrow K^- \eta \nu_\tau$,” JHEP **1409**, 042 (2014) [arXiv:1407.6590 [hep-ph]].
- [55] J. Erler, “Electroweak radiative corrections to semileptonic tau decays,” Rev. Mex. Fis. **50**, 200 (2004) [hep-ph/0211345].
- [56] S. Descotes-Genon, A. Falkowski, M. Fedele, M. González-Alonso and J. Virto, “The CKM parameters in the SMEFT,” JHEP **1905**, 172 (2019) [arXiv:1812.08163 [hep-ph]].
- [57] P. Ball and R. Zwicky, “SU(3) breaking of leading-twist K and K^* distribution amplitudes: A Reprise,” Phys. Lett. B **633**, 289 (2006) [hep-ph/0510338].
- [58] M. A. Shifman, A. I. Vainshtein and V. I. Zakharov, “QCD and Resonance Physics. Theoretical Foundations,” Nucl. Phys. B **147**, 385 (1979).
- [59] M. A. Shifman, A. I. Vainshtein and V. I. Zakharov, “QCD and Resonance Physics: Applications,” Nucl. Phys. B **147** (1979) 448.
- [60] H. Leutwyler, “The ratios of the light quark masses,” Phys. Lett. B **378** (1996) 313, [hep-ph/9602366].
- [61] B. L. Ioffe, “Condensates in quantum chromodynamics,” Phys. Atom. Nucl. **66** (2003) 30, Yad. Fiz. **66** (2003) 32, [hep-ph/0207191].
- [62] T. Feldmann, B. O. Lange and Y. M. Wang, “B -meson light-cone distribution amplitude: Perturbative constraints and asymptotic behavior in dual space,” Phys. Rev. D **89**, no. 11, 114001 (2014) [arXiv:1404.1343 [hep-ph]].
- [63] A. Khodjamirian, “Form-factors of $\gamma^* \rho \rightarrow \pi$ and $\gamma^* \gamma \rightarrow \pi^0$ transitions and light cone sum rules,” Eur. Phys. J. C **6** (1999) 477 [hep-ph/9712451].
- [64] B. Capdevila, A. Crivellin, S. Descotes-Genon, J. Matias and J. Virto, “Patterns of New Physics in $b \rightarrow s \ell^+ \ell^-$ transitions in the light of recent data,” JHEP **1801** (2018) 093 [arXiv:1704.05340 [hep-ph]].
- [65] M. Alguer, B. Capdevila, A. Crivellin, S. Descotes-Genon, P. Masjuan, J. Matias and J. Virto, “Emerging patterns of New Physics with and without Lepton Flavour Universal contributions,” arXiv:1903.09578 [hep-ph].
- [66] S. Descotes-Genon, J. Matias, M. Ramon and J. Virto, “Implications from clean observables for the binned analysis of $B \rightarrow K * \mu^+ \mu^-$ at large recoil,” JHEP **1301**, 048 (2013) [arXiv:1207.2753 [hep-ph]].

- [67] S.Descotes-Genon, T.Hurth, J.Matias, J.Virto, “Optimizing the basis of $B \rightarrow K^* \ell \ell$ observables in the full kinematic range,” JHEP **1305**, 137 (2013) [arXiv:1303.5794 [hep-ph]].
- [68] R. Aaij *et al.* [LHCb Collaboration], “Differential branching fraction and angular moments analysis of the decay $B^0 \rightarrow K^+ \pi^- \mu^+ \mu^-$ in the $K_{0,2}^*(1430)^0$ region,” JHEP **1612** (2016) 065 [arXiv:1609.04736 [hep-ex]].
- [69] W. Altmannshofer, P. Ball, A. Bharucha, A. J. Buras, D. M. Straub and M. Wick, “Symmetries and Asymmetries of $B \rightarrow K^* \mu^+ \mu^-$ Decays in the Standard Model and Beyond,” JHEP **0901** (2009) 019 [arXiv:0811.1214 [hep-ph]].
- [70] C. Bobeth, M. Chrzaszcz, D. van Dyk and J. Virto, “Long-distance effects in $B \rightarrow K^* \ell \ell$ from analyticity,” Eur. Phys. J. C **78** (2018) no.6, 451 [arXiv:1707.07305 [hep-ph]].
- [71] R. Aaij *et al.* [LHCb Collaboration], “Differential branching fraction and angular analysis of the decay $B^0 \rightarrow K^{*0} \mu^+ \mu^-$,” JHEP **1308**, 131 (2013) [arXiv:1304.6325 [hep-ex]].
- [72] J. Gratrex, M. Hopfer and R. Zwicky, “Generalised helicity formalism, higher moments and the $B \rightarrow K_{J_K}(\rightarrow K\pi)\bar{\ell}_1 \ell_2$ angular distributions,” Phys. Rev. D **93** (2016) no.5, 054008 [arXiv:1506.03970 [hep-ph]].
- [73] B. Dey, “Angular analyses of exclusive $\bar{B} \rightarrow X \ell_1 \ell_2$ with complex helicity amplitudes,” Phys. Rev. D **92**, 033013 (2015) [arXiv:1505.02873 [hep-ex]].
- [74] R. Aaij *et al.* [LHCb Collaboration], “Angular analysis of the $B^0 \rightarrow K^{*0} \mu^+ \mu^-$ decay using 3 fb^{-1} of integrated luminosity,” JHEP **1602** (2016) 104 [arXiv:1512.04442 [hep-ex]].
- [75] H. H. Asatryan, H. M. Asatrian, C. Greub and M. Walker, “Calculation of two loop virtual corrections to $b \rightarrow s \ell^+ \ell^-$ in the standard model,” Phys. Rev. D **65**, 074004 (2002) [hep-ph/0109140].
- [76] H. M. Asatrian, C. Greub, J. Virto, “Exact NLO Matching and Analyticity in $b \rightarrow s \ell \ell$,” arXiv:1912.09099 [hep-ph].
- [77] M. Beneke, T. Feldmann and D. Seidel, “Systematic approach to exclusive $B \rightarrow V \ell^+ \ell^-$, $V \gamma$ decays,” Nucl. Phys. B **612**, 25 (2001) [hep-ph/0106067].
- [78] J. Matias, F. Mescia, M. Ramon, J. Virto, “Complete Anatomy of $\bar{B}_d \rightarrow \bar{K}^{*0}(\rightarrow K\pi)\ell^+ \ell^-$ and its angular distribution,” JHEP **1204**, 104 (2012) [arXiv:1202.4266 [hep-ph]].
- [79] A. Agadjanov, V. Bernard, U. G. Meiner and A. Rusetsky, “The $B \rightarrow K^*$ form factors on the lattice,” Nucl. Phys. B **910** (2016) 387 [arXiv:1605.03386 [hep-lat]].

- [80] M. Beneke and T. Feldmann, “Symmetry breaking corrections to heavy to light B meson form-factors at large recoil,” Nucl. Phys. B **592**, 3 (2001), [hep-ph/0008255].
- [81] A. G. Grozin and M. Neubert, “Asymptotics of heavy meson form-factors,” Phys. Rev. D **55**, 272 (1997) [hep-ph/9607366].
- [82] S. Descotes-Genon and C. T. Sachrajda, “Factorization, the light cone distribution amplitude of the B meson and the radiative decay $B \rightarrow \gamma \ell \nu_\ell$,” Nucl. Phys. B **650** (2003) 356 [hep-ph/0209216].
- [83] S. Descotes-Genon and N. Offen, “Three-particle contributions to the renormalisation of B-meson light-cone distribution amplitudes,” JHEP **0905** (2009) 091 [arXiv:0903.0790 [hep-ph]].
- [84] H. Kawamura and K. Tanaka, “Evolution equation for the B-meson distribution amplitude in the heavy-quark effective theory in coordinate space,” Phys. Rev. D **81** (2010) 114009 [arXiv:1002.1177 [hep-ph]].
- [85] M. Knodlseder and N. Offen, “Renormalisation of heavy-light light ray operators,” JHEP **1110** (2011) 069 [arXiv:1105.4569 [hep-ph]].
- [86] G. Bell, T. Feldmann, Y. M. Wang and M. W. Y. Yip, “Light-Cone Distribution Amplitudes for Heavy-Quark Hadrons,” JHEP **1311**, 191 (2013) [arXiv:1308.6114 [hep-ph]].
- [87] M. Beneke, V. M. Braun, Y. Ji and Y. B. Wei, “Radiative leptonic decay $B \rightarrow \gamma \ell \nu_\ell$ with subleading power corrections,” JHEP **1807** (2018) 154 [arXiv:1804.04962 [hep-ph]].
- [88] Y. M. Wang, “Factorization and dispersion relations for radiative leptonic B decay,” JHEP **1609**, 159 (2016) [arXiv:1606.03080 [hep-ph]].
- [89] Y. M. Wang and Y. L. Shen, “Subleading-power corrections to the radiative leptonic $B \rightarrow \gamma \ell \nu$ decay in QCD,” JHEP **1805**, 184 (2018) [arXiv:1803.06667 [hep-ph]].
- [90] T. Nishikawa and K. Tanaka, “QCD Sum Rules for Quark-Gluon Three-Body Components in the B Meson,” Nucl. Phys. B **879**, 110 (2014) [arXiv:1109.6786 [hep-ph]].
- [91] I. I. Balitsky and V. M. Braun, “Evolution Equations for QCD String Operators,” Nucl. Phys. B **311**, 541 (1989).
- [92] C. F. Uhlemann and N. Kauer, “Narrow-width approximation accuracy,” Nucl. Phys. B **814** (2009) 195 [arXiv:0807.4112 [hep-ph]].